ABSTRACT

Title of dissertation: DISTINCT MOLECULAR AND MORPHOLOGICAL SUBCIRCUITS OF THE SUBPLATE NEURONS

Sarada Viswanathan, Doctor of Philosophy, 2014

Dissertation directed by: Dr. Patrick. O. Kanold, Associate Professor
Department of Biology, University of Maryland
Dr. Loren. L. Looger, Group Leader,
Howard Hughes Medical Institute, Janelia Farm Research Campus

Subplate neurons (SPNs) are a population of neurons in the mammalian cerebral cortex that exist predominantly in the prenatal and early postnatal period. Loss of SPNs prevents functional maturation of the cerebral cortex. SPNs receive subcortical input from the thalamus and relay this information to the developing cortical plate and thereby can influence cortical activity in a feed-forward manner. Little is known about potential feedback projections from the cortical plate to SPNs. SPNs are also a heterogeneous population in

terms of molecular and morphological identity. And the functional role of the different subpopulations of SPNs remains poorly defined. This is mainly due to the lack of tools- *i.e.* transgenic lines and reporters to target and manipulate the SPNs at different stages of development. Hence the functional significance of this molecular diversity remains unexplored. In this study, we used a combination of genetic, molecular, anatomical and physiological approaches to address these questions and also to identify and characterize transgenic mouse lines to manipulate the SPN. We identified and characterized a set of reporters and transgenic lines expressing Cre recombinase or green fluorescent protein with different levels of specificity in the subplate (SP). Using these transgenic driver lines and specific antibodies, we find that defined SPNs project to the main thalamo-recipient layers – L4 and L1 – and the spatial pattern of SPN projections to layer 4 is related to the spatial pattern of thalamo-cortical projections. However different subclasses have distinct patterns of projections with respect to the thalamic afferents. While certain subclasses have been shown to project locally, we observe that certain cell types of SPN also extend long-range projections to different thalamic nuclei. Thus molecularly defined SPN cell types are differentially integrated into the thalamo-cortical and intra-cortical connectivity. We also find a laminar difference in intra-cortical connectivity

of the SPN. The first class of SPNs receives inputs from only deep cortical layers, while the second class of SPNs receives inputs from deep as well as superficial layers (including layer 4) and are located more superficially. These superficial cortical inputs to SPNs emerge in the second postnatal week in the mouse. Taken together, we demonstrate the presence of distinct laminar and molecular circuits in the developing subplate and characterize yet another aspect of heterogeneity of this population.

DISTINCT LAMINAR AND MOLECULAR SUBCIRCUITS OF THE SUBPLATE NEURONS

by

Sarada Viswanathan

Dissertation submitted to the Faculty of the Graduate School of the University of Maryland, College Park in partial fulfillment of the requirements for the degree of Doctor of Philosophy

2014

Advisory committee:

Dr. Patrick O Kanold, Chair

Dr. Loren L Looger

Dr. Catherine E Carr

Dr. Dan A Butts

Dr. Matthew R Roesh

Preface

Data on the characterization of the spaghetti monster probes summarized in Figure 3.2 was obtained in collaboration with Dr. Megan E Williams, University of Utah.

Dedication:

To my wonderful family, friends and mentors. I especially dedicate this work to my boy Charan, my source of energy, enthusiasm and inspiration.

Acknowledgements:

I would like to thank my advisors – Dr. Patrick O. Kanold and Dr. Loren L. Looger for their constant support, encouragement, constructive criticism and endless patience through this journey. Thank you for teaching me what it means to be a good scientist. As with all graduate students, I have had my phases of ups and downs and without your constant support through all that, I could not have reached this stage. Thanks to Loren for initiating this effort and empowering me with the confidence to take up this challenge and to Patrick for being a true 'entropy generator'.

I would like to particularly thank my committee member, Dr. Catherine E. Carr. Dr. Carr, thanks for all the encouragement that you have given me during my time in the program. Your office/lab was always open to me for any kind of question – academic to scientific and I am fortunate and proud to be associated with you.

Dr. Daniel Butts, I would like to thank you for all the sound advice, especially when I needed it the most. That's something I could not have done without. Thank you also for your patience through the Computational Neuroscience class and for putting up with this 'MATLAB Mindbender'. I would like to thank Dr. Hye-Kyoung Lee for the initial inputs and Dr.

Mathew R. Roesch for taking time to read my work and to be a part of my committee.

I am fortunate to be a part of two labs – The Looger Lab at Howard Hughes Medical Institute, Janelia Farm Research Campus (JFRC) and the Kanold Lab at the University of Maryland, College Park (UMD). Although I spent relatively less time of my graduate school career at UMD, I will have very fond memories of the Kanold Lab. Aminah, you have been an amazing friend and thank you for everything. Dan, you have been a real help throughout my graduate school life. Always ready to help and always ready with advice even when you had a lot of things going on. A big thanks to all the members – past and present – of the Kanold Lab for making this a great place to work.

Thanks to Dr. Michele Brooks, Ms. Gwen Warman, and the past members of the BISI office for helping me in every possible way to deal with the administrative aspects of the program.

I would like to extend a big thanks to the Looger Lab for all their support. In spite of (most all of us) having a traditional biochemistry background, they took special efforts to understand the nuances of mouse neuroanatomy and development, and provided valuable inputs to my research. I would like to extend a special thanks to Dr. Jonathan Marvin, Dr. Eric Schreiter and Mrs.

Margaret Jefferies. I would also like to thank Dr. Karel Svoboda, Dr. Vivek Jayaraman, Dr. Gilbert “Lee” Henry, and Dr. Nick Betley for their sound advice at every stage.

I am blessed with a wonderful family and could not have achieved any of this without the unconditional support from my husband, son and my parents. Charan, you are very smart and have been a wonderful boy and thank you for letting Amma devote a lot of time to my studies. I am very proud of you. Thanks to my Amma for listening to my ramblings every morning.

My work presented here is a reflection of positive reinforcement, encouragement, and support also from a big family of friends whom I would like to thank.

TABLE OF CONTENTS

CHAPTER 2: CHARACTERIZATION OF TRANSGENIC LINES

List Of Figures:

Appendix Figures:

List of Tables:

List of abbreviations:

A1	Primary Auditory cortex
AAV	Adeno-Associated Virus
ABA	Allen Brain Atlas
AMPA	α-Amino-3-hydroxy-5-methyl-4-isoxazolepropionic acid
ASD	Autism Spectrum Disorder
BAC	Bacterial artificial chromosome
CCK	Cholecystokinin
ChR2	Channelrhodopsin-2
cp	Critical period
CP	Cortical Plate
Cplx3	Complexin-3
CTGF	Connective Tissue Growth Factor
Dlx	Distal-less homeobox
DNA	Deoxyribonucleic Acid
Drd1a	Dopamine receptor D1A
ECM	Extra-cellular Matrix
FP	Fluorescent Protein
GABA	γ-Aminobutyric acid
GFP	Green Fluorescent Protein
HA	Human influenza hemagglutinin
Kcc2	Neuronal K+/Cl- co-transporter
Lenti	Lentivirus

LGN	lateral geniculate nucleus
M1	primary motor cortex
MGB	medial geniculate body
Moxd1	Monooxygenase DBH-like 1
MRI	Magnetic resonance imaging
NFH	NeuroFilament Heavy chain
NMDA	N-methyl-D-aspartate
nNos	Neuronal nitric oxide synthase
NpHR	Halorhodopsin
Npy	Neuropeptide Y
ODC	Ocular Dominance Column
PBS	Phosphate Buffered Saline
PFA	Paraformaldehyde
PVL	Periventricular leukomalacia
RNA	Ribonucleic Acid
S1	Primary Whisker Somatosensory Cortex
sfGFP	Superfolder GFP
SP	Subplate
SPN	subplate neuron
SST	Somatostatin
SVZ	Subventricular zone
Tbr1	T-box, brain 1 transcription factor
TC	Thalamo-cortical

TMEM163	Transmembrane protein 163
Vpm	Ventral posteromedial nucleus of the thalamus
YFP	Yellow Fluorescent Protein

1.0 Introduction:

The brain is an amazing organ, performing numerous complicated computations and information processing events that are essential for proper function of the entire body (Lichtman and Denk 2011). The brain is composed of specialized cells called neurons that form connections with one another called synapses. In higher animals such as mammals, single neurons may synapse onto many thousands of other partner neurons and thus form a network of connections. This network of connections forms the basis of the function of the brain.

Synaptic connectivity is studied at different scales (Sporns, Tononi et al. 2005) — the microscale, formed by individual neurons synapsing with one another (Sporns, Tononi et al. 2005), the mesoscale, where populations of neurons are arranged into functional groups such as columns (Mountcastle 1997), and the macroscale (Craddock, Jbabdi et al. 2013), wherein different anatomical regions are connected to one another. Since different brain regions specialize in diverse functions, macroscale connections between brain regions are critical to the proper functioning of the entire nervous system.

An essential feature of the brain is that connections are not necessarily inherently hard-wired. They are established during development and refined over the lifetime of the animal. The cerebral cortex is the region of the brain most commonly associated with computation and higher-level reasoning (Raizada and Grossberg 2003), whereas the thalamus performs critical relay functions between sensory organs and high-level regions such as cortex (Macchi, Bentivoglio et al. 1996). Hence proper connections between thalamus and cortex (thalamo-cortical, or TC, connections) are essential for information processing. TC connectivity is typically first established in the embryonic stage and

refined over a developmental window called the 'critical period' (critical in that disruption of these processes during this time leads to irreversible damage to the animal's brain) (Hubel and Wiesel 1970, Hensch 2004). A transient population of neurons in the cerebral cortex called the subplate neurons (SPNs) is instrumental in the establishment of this connectivity.

SPNs are a heterogeneous population of neurons located in the cortical white matter (Kanold and Luhmann 2010), just below the deepest cortical layer ('layer 6'). They are transient in nature: they are present from the embryonic stage through the critical period. At the end of the critical period, a large fraction of these neurons are eliminated by programmed cell death, or apoptosis (Valverde, Lopez-Mascaraque et al. 1995), while some of them persist into the adult, as interstitial neurons, layer 6b in mouse, *etc*. (Hoerder-Suabedissen, Oeschger et al. 2013).

SPNs are generated in the sub-ventricular zone (SVZ) and comprise one of the earliest neuronal populations in the cortical plate (CP). As such, they possess mature morphological and synaptic properties, when the rest of the cortical plate is still immature. By virtue of their location, early origin and maturation, they participate in some of the earliest circuitry in the developing cortex. They are also engaged in early spontaneous network activity, via electric coupling during early development (Hanganu, Kilb et al. 2002) and act as an obligate relay in the TC circuitry (Kanold and Shatz 2006). SPNs form the 'teacher circuit' involved in the establishment and refinement of TC connections (Kanold and Luhmann 2010). Ablation studies show that the absence of SPNs results in severe deficits in connectivity (Kanold and Shatz 2006, Tolner, Sheikh et

al. 2012). Taken together, these results show that SNPs are tightly embedded in intra-cortical and sub-cortical circuitry during the critical period.

SPNs are present in all placental mammals (Molnar, Metin et al. 2006); however their presence in marsupials is debatable (Harman, Eastough et al. 1995). The size of the subplate (SP) increases with complexity of the organism, indicating an important role in higher order connectivity (Kanold and Luhmann 2010). While the remnant SPNs (*i.e.* those surviving after the critical period) exhibit mature synaptic properties, the precise role of this population of neurons and synapses remains unknown.

The population of SPNs is heterogeneous in both gene expression and neuronal morphology (Kanold and Luhmann 2010, Hoerder-Suabedissen and Molnar 2012). SPNs express a range of partly overlapping molecular markers, many of them transcription factors and growth factors, some of which are molecular markers of autism and schizophrenia (Hoerder-Suabedissen, Oeschger et al. 2013). Another interesting feature of SPNs is some of the SPNs are highly coupled *via* gap junctions (Kanold and Luhmann 2010). This gap junction coupling might be involved in amplification of network activity (Luhmann, Kilb et al. 2009, Dupont, Hanganu et al. 2006).

1.1 Discovery and preliminary developmental characterization of the SP:

The sequence of developmental events in the central nervous system (CNS) was first formally documented by the Boulder Committee (Bystron, Blakemore et al. 1970) in 1970. However the existence of SP was not documented in the original Boulder Committee report (1970)(Bystron, Blakemore et al. 2008). It was later described, for the first time (Molliver, Kostovic et al. 1973), in gyrencephalic mammals (*i.e.* those with

highly convoluted brain surfaces), which are characterized by extensive white matter and a long gestation period. The transient subplate zone was first reported in humans (Kostovic and Rakic 1990, Kostovic, Judas et al. 2011) as a layer appearing during early gestation. This transient zone is rich in fibers and present between the intermediate zone and developing cortical plate (Molliver, Kostovic et al. 1973, Kostovic and Rakic 1990). Their existence in other species was subsequently documented in cats (Luskin and Shatz 1985), rats (Rickmann, Chronwall et al. 1977) and fetal macaque monkeys (Rakic 1976). Prior to a systematic description, their presence was noted in the form of interstitial neurons in adult human brains (Kostovic and Rakic 1980), believed to be the remnants of the fetal subplate neurons (Kostovic, Judas et al. 2011, Suarez-Sola, Gonzalez-Delgado et al. 2009, Judas, Sedmak et al. 2010). In rodents, 'Layer 7' was proposed to be a distinct layer in the cerebral cortex (Reep and Goodwin 1988), originating from the primordial plexiform layer. Tracing studies in rats showed that this layer engages in cortical connectivity and is overlaid by a cell-sparse zone traversed by cortico-cortical axons.

1.2 Gross morphological characterization of the SP:

The size of the subplate (SP) zone relative to the cortical plate varies between species (Aboitiz and Montiel 2007). The ratio of SP to CP is higher in primates as compared to rodents (Kostovic and Rakic 1990). The size of the subplate in primates increases during corticogenesis (Kostovic and Rakic 1990, Bystron, Blakemore et al. 2008), mainly due to the accumulation of axons and dendrites (Kostovic and Goldman-Rakic 1983, Kostovic and Rakic 1990). Although the subplate zones of humans and non-human primates and other experimental organisms share many common features, their

developmental history is different (Judas, Sedmak et al. 2010) — the main difference lies in the fact that the subplate zone in primates increases in size even during cortical neurogenesis (Kostovic and Rakic 1980, Kostovic and Rakic 1990, Smart, Dehay et al. 2002, Bystron, Blakemore et al. 2008), which is not seen in rodents.

1.3 Subplate Neurons Vs Subplate Zone – an important distinction:

The terms 'Subplate zone' and 'Subplate neurons' are often used interchangeably. However, there is an important distinction between the two terms. The subplate zone is a transient zone appearing in the early fetal period composed of early generated neurons (SPNs), migratory neurons, axons (Kostovic and Rakic 1990), neuropil (Kostovic and Goldman-Rakic 1983) and synapses (Kostovic and Jovanov-Milosevic 2008, Judas, Sedmak et al. 2010), all embedded in an extracellular matrix (ECM) (Kostovic and Jovanov-Milosevic 2008).The ECM is rich in axon guidance cues (Sheppard, Hamilton et al. 1991) and acts as a permissive matrix for traversing axon fibers. While the subplate zone is a transient developmental structure, a significant number of SPNs survive into adulthood long after the SP zone has dissolved and persist in white matter as interstitial neurons (Torres-Reveron and Friedlander 2007). The extent of remnant SPNs varies with species, but they have been shown to retain functional properties (Torres-Reveron and Friedlander 2007).

1.4 Cellular composition of the subplate zone:

It should first be noted that despite the clear developmental and gross anatomical conservation of the subplate zone, the precise micro-anatomical structure and molecular

composition of the SP varies between species. For instance, in a recent study (Miller, Ding et al. 2014), the authors have shown a cyto-architectural difference between the human and mouse subplate. For the remainder of this chapter (and for the experimental chapters that follow), discussion is largely restricted to the rodent (*i.e.* mouse) SP, with properties conserved in higher animals (notably humans) pointed out where information is available.

The ventricular zone is composed of proliferative cells that undergo rapid cell division to give rise to the sub-ventricular zone (Bystron, Blakemore et al. 2008). Subsequent cell division gives rise to a set of post-mitotic neurons that form the 'preplate'. The preplate is split into the marginal zone and subplate by migrating neurons that form the cortical plate (Marin-Padilla 1971, Bystron, Blakemore et al. 2008). The neurons in the subplate zone comprise the pioneer neurons expressing *transcription factor T-box, brain, 1* (*Tbr1*), and are generated in the ventricular zone. In addition to this the zone is also occupied by glutamatergic neurons that are migratory in nature, and GABAergic neurons generated in the ganglionic eminence expressing the *Distal-less homeobox* (*Dlx*) transcription factor. Pioneer neurons extend neurites into the cortical plate and axons into the internal capsule, while the GABAergic neurons migrate radially and tangentially through the subplate (Hevner and Zecevic 2006).

Rodent subplate neurons reside in two zones: a densely packed zone beneath the cortical plate and a loosely packed layer in the white matter (Luskin and Shatz 1985, Wahle and Meyer 1987). Kostovic and Rakic made similar observations in humans and primates (Kostovic and Rakic 1980). In a comparative study in visual, somatosensory and motor cortices, they observed two types of cells: 'type 1' cells are polymorphic,

superficial and seen more in the neonatal stage and infancy, and 'type 2' cells are typically fusiform and found deep in white matter and seen more in the adult stage. The type 2 cells, most likely, comprise the persisting SPN population.

1.5 Diversity of subplate neurons:

One of the most interesting features of SPNs is their diversity with respect to both neuronal morphology and molecular markers. A primary guiding principle of the work done in this thesis has been the systematic description of such morphological and molecular diversity, with an attempt to (1) make a catalog of 'cell types' in the mouse SP according to each definition, and (2) discover relationships between morphology (and related parameters such as projection targets) and molecular expression (with an eye towards aspects of neuronal function).

1.5a Morphological diversity:

SPNs are characterized by profound variability in morphology. Being early born, they exhibit mature morphological properties during a relatively immature phase of development. Neuronal morphology consists largely of a description of the cell body (shape and orientation), size and spread of the dendritic arbor, and length and target of axonal projections. Although a complete description of SPN morphological diversity is lacking as yet, several general observations have been made. In primates, two subtypes have been described - 'fusiform' and 'polymorphic' subtypes. Fusiform cells are embedded in the white matter while polymorphic cells are more superficial, at the interface of the cortical plate and the white matter. In general, SPNs show extensive

ramification of dendritic processes throughout the cortical plate, and through their extensive somato-dendritic arborizations, they are capable of integrating responses over their many cortical and sub-cortical inputs (Kostovic and Rakic 1980, Friauf, McConnell et al. 1990, Hanganu, Kilb et al. 2002). Some polymorphic cells extend dendrites towards the white matter (inverted pyramid) while others resemble displaced pyramidal neurons (Kostovic and Rakic 1980). Many SPN dendrites are spiny, indicating the excitatory (*i.e.* glutamatergic) nature of their inputs. As for axonal variation, Wahle *et al.* described the morphology of GABAergic neurons in the white matter of kitten and found two populations distinguished by axonal length, branching and bending (Wahle and Meyer 1987).

Some studies have attempted to correlate morphological subclasses with physiological properties (Hanganu, Kilb et al. 2002) and axonal projections (Hoerder-Suabedissen and Molnar 2012). While there is a correlation between projection targets and neuronal geometry (Hoerder-Suabedissen and Molnar 2012), the intrinsic physiological properties remain largely similar between the two groups (Hanganu, Kilb et al. 2002).

1.5b Molecular diversity:

In addition to morphological diversity, SPNs also express a wide range of molecular markers. Different molecular markers expressed by SPNs have been documented in early literature. Examples include calbindin (ferrets- (Ghosh, Antonini et al. 1990, Ghosh, Antonini et al. 1990)), CTGF (rats– (Heuer, Christ et al. 2003)), fibronectin (cats- (Chun and Shatz 1989)), p75 neurotrophin receptor (rats- (McQuillen,

DeFreitas et al. 2002)), Nurr1 (rats- (Arimatsu, Ishida et al. 2003)), neuronal nitric oxide synthase nNos1 (ferrets- (Finney and Shatz 1998)), estrogen receptor (mice- (Osheroff and Hatten 2009)), and progesterone receptor (rats- (Lopez and Wagner 2009)). Recent advances in molecular profiling have revealed an extensive diversity in gene expression in the subplate (mice- (Hoerder-Suabedissen, Wang et al. 2009)); in a microarray screen, they identified several novel markers of subplate and validated already known markers, including complexin 3 (Cplx3), CTGF (connective tissue growth factor), monooxygenase DBH-like 1 (MoxD1), and transmembrane protein 163 (TMEM163). The most recent work by this group has classified the spatio-temporal pattern of different molecular subtypes of SPNs and associated several subplate-enriched genes with neurodevelopmental disorders (Hoerder-Suabedissen, Oeschger et al. 2013).

In this recent work, systematic molecular profiling followed by immunohistochemistry and *in situ* hybridization further segregated genes expressed in the SP as SP-specific or merely SP-enriched. An interesting observation regarding gene expression in the subplate is the co-expression of SP-specific genes in different layers of cortex. It has been observed that genes enriched in the SP are frequently also expressed at a lower level in layers 5 and 2/3 (Hoerder-Suabedissen, Oeschger et al. 2013). An example of a gene showing this pattern of expression is Cplx3, which shows SP-specific expression in addition to expression in a small fraction of layer 5 cells. Another interesting aspect of SP gene expression is that genes expressed at one developmental time point in a SP-specific fashion can lose or gain specificity over development. Examples of this type of gene expression include Sema5b and Drd1a, which show SP specificity, but only at postnatal ages.

Thus, to summarize, SPNs are an essential component of the thalamo-cortical pathway in the developing nervous system. This transient population is seen in most mammals and is likely to play an important role in the establishment of circuitry. SPNs are incredibly diverse, from the view of both cellular morphology and molecular expression. In this thesis, I attempt to shed light on these two manifestations of cell type difference, and to find correlations between the two, in an attempt to better understand the role of these transient cell populations in cortical development.

1.6 Functional relevance of Subplate Neurons:

1.6.1 Spontaneous network activity and establishment of early circuitry:

Subplate neurons, apart from being the earliest born neurons in the cortical plate, are also the earliest to attain mature synaptic properties. They express Map2 and neurotransmitters/neuromodulators such as GABA, cholecystokinin (CCK), neuropeptide Y (Npy) or somatostatin (SST), long before cortical neurons do (Chun, Nakamura et al. 1987, Chun and Shatz 1989, Chun and Shatz 1989). The earliest evidence for their involvement in connectivity came from the discovery of functional synapses in the subplate before their presence in the cortical plate (Molliver, Kostovic et al. 1973, Kostovic and Rakic 1980, Chun and Shatz 1988). Herrmann *et al.* demonstrated, through tracer studies in ferrets, that some of these synapses were from thalamus (Herrmann, Antonini et al. 1994). Interestingly, a recent molecular profiling study observed that semaphorin5a (Sema5a), an axon guidance molecule, is enriched in the subplate and is probably involved in early synaptogenesis.

SPNs play an instrumental role in the establishment and refinement of early cortical connections. Spontaneous network activity is a hallmark of developing neural circuits. While spontaneous activity has different roles in different system, in the neocortex it contributes to the development of circuitry (Yuste, Nelson et al. 1995). More recently, it has been shown that focal ablation of SP soon after birth eliminates spontaneous network activity in the cortex (Tolner, Sheikh et al. 2012).

1.6.2 Establishment and refinement of thalamo-cortical circuitry:

SPNs act as an obligate relay in thalamo-cortical connectivity. Early studies in experimental animals showed that the subplate is a 'waiting compartment' for incoming thalamic fibers (Rakic 1976). Ablating SPNs at the onset of this 'waiting period' resulted in the anomalous growth of thalamic axons in the cortical plate, which shows that they also play an important role in target selection by thalamic afferents (Ghosh and Shatz 1993). Apart from being an obligate relay in the early TC connectivity, they are also important for the functional maturation of thalamo-cortical circuits. Axons from the thalamic lateral geniculate nucleus (LGN) of the thalamus form patterned structures in L4 visual cortex of cats called ocular dominance columns (ODCs)(Hubel and Wiesel 1977). Ablation of SPNs results in failure of proper ODC formation (Ghosh, Antonini et al. 1990, Kanold and Shatz 2006). Similar results were seen in somatosensory whisker ('barrel') cortex (Tolner, Sheikh et al. 2012), where whisker barrels failed to form following SP ablation. Thus SNPs, and especially their L4 thalamo-cortical synapses, are involved in many of the early events during cortical development.

1.6.3 Maturation of Inhibition

Another important function of SPNs lies in the maturation of inhibition, which, in turn, controls synaptic plasticity during the critical period (Hensch 2004). Maturation of inhibition involves developmental changes in GABA receptor subunit composition (Golshani, Truong et al. 1997, Chen, Yang et al. 2001). Another key event is the developmental upregulation of the chloride ion transporter KCC2, which results in shift of GABA from depolarizing to hyperpolarizing (Ganguly, Schinder et al. 2001). Ablation of subplate neurons results in receptor subunit composition remaining in its developmental state (α2, α3) and failure of upregulation of KCC2, as a result of which GABA remains depolarizing (Kanold and Shatz 2006). Glutamatergic inputs are required for this upregulation, and during development SPNs are the main source of glutamatergic inputs in the cortex.

1.7 Disease association:

The function of SPNs is thus two-fold. During early development, they play a role in axon guidance and target selection for appropriate establishment of thalamo-cortical connections. They also initiate and maintain some of the early network activities that form the blueprint of connectivity. During later development, they have a distinct role in maturation, refinement and plasticity of this circuitry, particularly through maturation of inhibitory connections. Given the large-scale involvement of SPNs with cortical development and function, it is thus unsurprising that they are of particular importance in both the healthy and diseased state.

Over the past few years, a growing body of evidence has pointed towards the

relevance of subplate neurons to various neurological disorders. Their role has been implicated in cases of neurodevelopmental deficits like cerebral palsy and periventricular leukomalacia (PVL) (Volpe 2009). A strong correlation is also emerging between SPN abnormalities and neuropsychiatric disorders like autism (Hoerder-Suabedissen, Oeschger et al. 2013, McFadden and Minshew 2013, Avino and Hutsler 2010, Xu, Knutsen et al. 2010) and schizophrenia (Kostovic, Judas et al. 2011).

1.7.1 Autism:

Autistic spectral disorder (ASD) ('autism') is a family of neurodevelopmental disorders characterized by impaired social and communicative skills, along with repetitive and stereotyped behavior (NIMH). While the symptoms are well defined, the cellular and molecular basis for this disorder is not clear. Deficits in cortical migration have long been acknowledged as a possible cause for ASD (Piven, Berthier et al. 1990). A recent study conducted on eight individuals with ASD found abnormal cortical – white matter boundaries, which might have resulted from SPNs that failed to undergo apoptosis or that experienced neonatal injury (Avino and Hutsler 2010, Hutsler and Avino 2013).

1.7.2 Schizophrenia:

Schizophrenia is another neurological disorder with psychotic manifestations and cognitive impairments. Abnormal cortical circuitry has been postulated to be the underlying neurological basis of this disease (Friston and Frith 1995, Bunney and Bunney 2000). This abnormality in cortical wiring might be due to remnant SPNs. Kostovik *et al.* (Kostovic, Judas et al. 2011) further propose that inhibitory neurons in the SP might also

have a ‘gating’ function regulating overall connectivity, by virtue of their modulated inhibition either allowing or disallowing excitatory signals to propagate through the cortex. In injuries resulting in lesions to the SP, this gating function is altered, resulting in wiring abnormalities. Thus SPNs are a putative candidate for the neurological basis of schizophrenia. Further evidence comes from recent studies where abnormal cortical folding resulting from differential cortical growth and SP remodeling has been implicated in schizophrenia (Xu, Knutsen et al. 2010, Lewis and Levitt 2002).

The genetic basis of the contribution of SPNs to both autism and schizophrenia has been investigated in a recent gene expression profiling study that showed that mouse SP is enriched for genes associated with these neuropsychiatric disorders (Hoerder-Suabedissen, Oeschger et al. 2013).

1.7.3 Neonatal injury and neurodevelopment disorders:

Subplate neurons are highly prone to injury (especially hypoxic ischemic injury) and are most vulnerable at a time when injuries result in neurodevelopmental impairment, making them likely candidates for involvement in proper development (McQuillen, Sheldon et al. 2003). SPNs are vulnerable to both hypoxia and anoxia, and this vulnerability has been shown to be due to excitotoxicity. The cortical abnormalities resulting from hypoxic ischemia mirror the effects seen in common neurodevelopment disorders. Molecular resonance imaging (MRI) studies have shown that the subplate region in humans is a primary target for hypoxic ischemic insults (Ferriero and Miller 2010) and such injuries are also associated with cerebral palsy (Hankins and Speer 2003) and epilepsy (Freeman and Nelson 1988). In humans, subplate neurons are four times as

thick as the cortical plate at gestation week 24 (McQuillen, Sheldon et al. 2003)— a period that coincides with maximum susceptibility to PVL, a type of brain injury affecting infants (Volpe 2009). Thus subplate neurons may be the key factor in several developmental impairments seen in brain injury.

1.7.4 Epilepsy:

Epilepsy, resulting in recurrent seizures, is one of the most common neurological disorders (Rakhade and Jensen 2009). The highest incidence of epilepsy is during early development (Volpe: Neurology of the Newborn, 5th ed) resulting from insults like hypoxic ischemia. Subplate neurons are possible cellular targets of such insults resulting in epileptic seizures. These neurons express high levels of AMPA- and NMDA-type glutamate receptors during development (Hanganu, Kilb et al. 2002), and are particularly susceptible to excitotoxicity. Since they foster inhibition in the developing cortical system (Kanold and Shatz 2006), loss of SPNs results in imbalance between excitation and inhibition, which can result in seizures. Lein *et al.* have shown via kainate-mediated excitotoxicity that SP ablation results in seizures in cats (Lein, Hohn et al. 2000).

1.7.5 Effects of substance abuse on SPNs:

Subplate neurons express receptors for a wide range of neurotransmitters and hormones, including GABA, serotonin and progesterone. Hence exposure to drugs (either in the womb or through breast milk) could affect their activity and as such, result in abnormal development. Thus subplate neurons may be a central component in developmental impairments seen in brain injuries resulting from maternal substance

abuse.

Recent advances in sequencing technology have led to remarkable progress in associating genes expressed in the subplate with certain neuropsychiatric disorders, mainly autism and schizophrenia (Hoerder-Suabedissen and Molnar 2013). Genes whose expression is enriched in the SP as compared to the cortical plate (including *Atp6a2, Cadps2, Cdh10, Cdh18, Cdh9, Gabra5, Nrxn1, Plp1, Prss12, Sema5a,* and *Tppp*) were associated with autism. Similarly, other SP-enriched genes (including *Apoe, Dbi, Ddr, Drd1a, Fn1, Gad1, Insig2, Notch2, Nr4a2,* and Slca2) were associated with schizophrenia. This close association between molecular subtypes and neuro-pathological deficits further emphasizes the importance of studying SPNs at a molecular level.

1.8 Current SPN research largely falls into two classes:

The field of SPN research is largely dichotomous. On the one hand, a wealth of research in different model organisms has provided detailed insight into the physiological properties of SPNs and their role in connectivity. On the other hand, cutting-edge molecular techniques have made immense contributions to our understanding of the diversity of molecular subclasses of SPNs and the spatio-temporal gene expression of SPNs. However the precise role of the different subclasses of SPNs still remains largely unanswered. It is not known if different subclasses are integrated differently into the circuitry, so as to subserve different functions. Overall, neurons in the neocortex exhibit an amazing range of molecular diversity (Druga 2009), which makes the problems of classification difficult. Given this great diversity of SPNs, and their critical involvement in health and disease, it would be highly informative to see if there is any correlation

between the molecular phenotype and neuronal geometry. As a general rule, neurons belonging to a particular molecular class typically express a distinct set of molecular markers and have distinct morphology. This has indeed been found to hold true for SPNs, although descriptions of SPNs in both respects fall well short of complete.

A key to studying a neuronal population is the ability to target it for imaging, genetic manipulation or other interventions. Specifically, transgenic driver lines expressing a reporter and / or Cre recombinase in the SP are invaluable tools for studying these populations at a molecular level. Since SPNs are not a single homogeneous population, in addition to the availability of good Cre lines, multiple reporters are essential to mapping the connectivity of the different subpopulations.

The primary focus of my thesis, and my contribution to the study of cortical development, has been to develop and characterize a set of reagents and protocols for the study of SP neuroanatomy and molecular expression, in order to try to understand the underlying basis for the diversity of this population and its myriad contributions to brain function and psychiatric disease. A breakdown of the research program into a set of experiments, each published as a paper in a peer-reviewed scientific journal, follows.

1.9 Research outline:

1. **Characterization of transgenic lines to study this population at a molecular level:**

Targeting and manipulating a neuronal population, especially during development, requires the availability of transgenic lines with precise spatio-temporal expression of either a reporter and/or a Cre recombinase. There is a profound lack of transgenic lines

that target this population. As a first step, in Chapter 2, I characterize existing lines and postulate best candidates for the development of future lines. In particular I study:

a) Expression pattern

b) Specificity

c) Temporal characteristics

d) Subpopulations labeled.

This set of information lays the groundwork for the molecular neuroanatomical studies and enables studies like targeted activation, inactivation and ablation of SPNs to elucidate the functional significance of the different subclasses.

2. **Development of a set of reporters to enable the study of different subclasses of SPNs:**

The success of any tracing study depends largely on the quality of the reporters used. Genetic tracing has largely relied on fluorescent proteins such as green fluorescent protein (GFP). While GFP performs well as a reporter in genetic tracing experiments, options for multiple tracing suffer from serious drawbacks. Since SPNs are a mixed neuronal population, their genetic study inherently requires multiple tracers. In an effort to facilitate the connectivity of different cell types, in chapter 3, I describe the development of a 'toolbox' of tracers for multi-color light and electron microscopic studies. In addition to facilitating the SPN studies proposed here, these tools are of general interest to neuroscience and other fields.

3. Study of the molecular neuroanatomy of SPNs to integrate different subtypes into connectivity:

A main question underlying SP neurobiology is whether or not there is a specific functional significance of the diversity of this neuronal population. Do the different subpopulations engage in different aspects of connectivity and function? While it is known that SPNs provide instructional roles to the developing cortical plate, especially L4, the main thalamo-recipient layer, the precise connectivity remains unknown. Using the whisker barrel field of primary somatosensory cortex as a model, in chapter 4, I anatomically investigate how one particular subclass of SPNs is integrated into this complex circuitry.

4. Understanding the neuronal architecture of molecular subtypes of SPNs:

SPNs exhibit diverse morphology. However, the molecular correlates of these anatomical subtypes have not been studied in detail. As an example, inhibitory neurons of the neocortex expressing certain molecular markers exhibit a certain geometry (Druga 2009). A similar correlation is as yet undescribed for the different cell types of SPNs. In chapter 5, I document my observations about one specific subclass: the CTGF-positive SPNs.

Chapter 2: Characterization of Potential Transgenic Lines labeling SPN

2.0 Introduction:

The ability to target and manipulate specific sets of neurons is invaluable to studying the functional role that they play in behavior. Common techniques for achieving the delivery of particular transgenes for the labeling (Figure 2.1) or manipulation of cells include electroporating the DNA into the ventricle of developing embryos at different gestational stages (*in utero* electroporation, IUE) (Shimogori and Ogawa 2008) or performing postnatal stereotaxic delivery *via* viral vectors (Kaspar, Vissel et al. 2002, Taymans, Vandenberghe et al. 2007). A more difficult, yet ultimately more reliable, method is transgenesis, wherein a reporter or effector gene is stably integrated into the genome. This ensures more reliable cell-type specific expression (Gerfen, Paletzki et al. 2013) and maintains relatively constant levels of transgene throughout the life of the animal (and transgenes can come on early, allowing the study of development, which can be difficult with other methods).

In case of SPN, since a large part of functional activity takes place during early developmental stages, the transgenic strategy allows manipulation at the embryonic and early developmental with a level of target specificity not possible with postnatal viral delivery or embryonic DNA electroporation.

The use of Cre recombinase (Gong, Doughty et al. 2007, Gerfen, Paletzki et al. 2013), (Kuhlman and Huang 2008) enables the cell type-specific expression of a variety of payloads, including those for labeling the neuronal population and tracing axonal projections, and manipulation of targeted cells with Channelrhodopsin-2 (ChR2), a light-gated activator (Petreanu, Huber et al. 2007) or light- gated silencers including NpHR

(Zhang, Wang et al. 2007), (Gradinaru, Thompson et al. 2008), or Archaeorhodopsin (Arch) (Chow, Han et al. 2010). Recent advances in protein engineering also enable researchers to monitor the activity of a specific set of neurons by tracking calcium activity (*e.g.* with GCaMP (Chen, Wardill et al. 2013)) or directly observing synaptic glutamate transmission (*e.g.* with iGluSnFR (Marvin, Borghuis et al. 2013)). However such studies have not been attempted in SPN mainly due to the inability to target these neurons with spatiotemporal specificity, which in turn is primarily due to the lack of well characterized transgenic lines that express Cre recombinase ('Cre driver lines') or specific reporters like eGFP, in a large population of SPN with high specificity.

As such, I adopted a two-fold approach to address this issue. As a first step, I set out to characterize the existing Cre lines created by public databases like GENSAT (http://www.gensat.org/index.html) and the Allen Brain Atlas (http://www.brain-map.org/) that can help enable genetic labeling and targeting of SPN. In this study, I have made an attempt to characterize the transgenic lines in relation to the specificity of expression within the cortex and extra-cortical expression. This will enable future studies to select appropriate driver lines to express transgenes and perform precise manipulation (Figure 2.2). Alongside this, I created and characterized novel transgenic lines using SPN-specific genes (see Chapter 1).

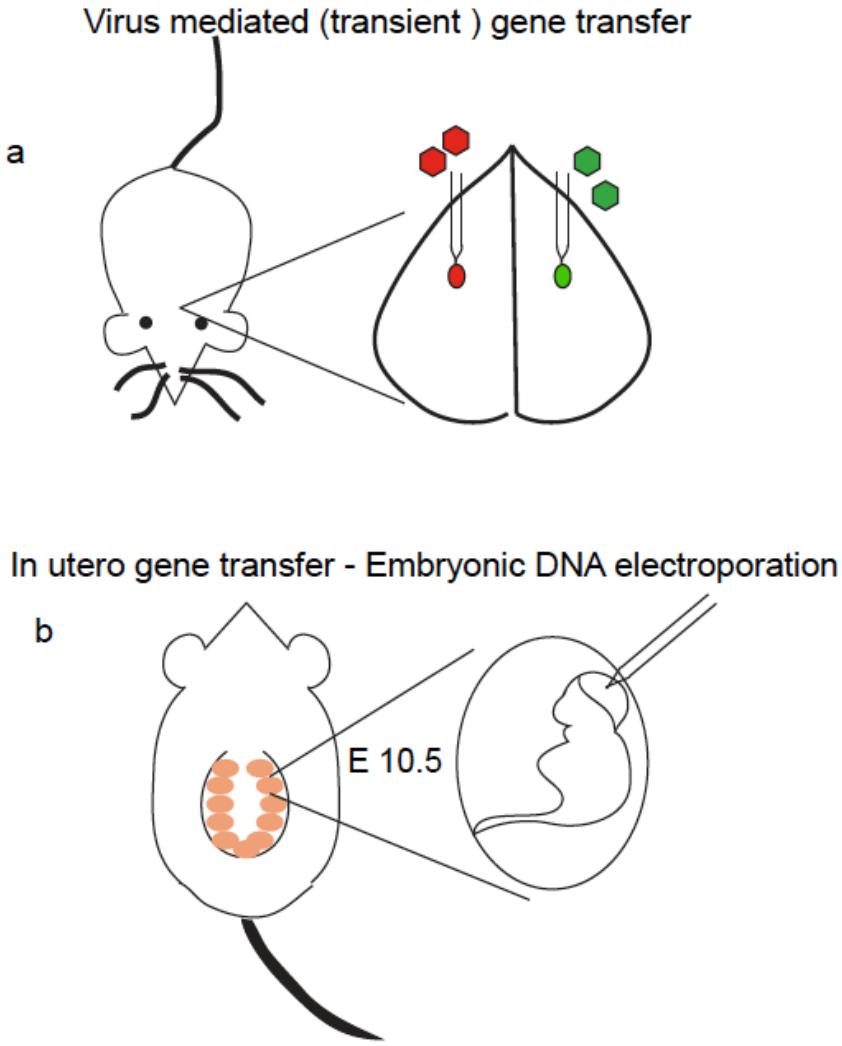

Figure 2.1:Strategies of transgene expression: Cartoon shows commonly used strategies for gene transfer in mouse brain. Panel (a) shows a cartoon describing postnatal gene transfer in mouse brain using AAV vectors encoding the gene of interest. Depending on the promoter used, specific celltypes can be targeted using this strategy. Precise stereotaxic targeting enables targeting particular brain regions. Panel (b) shows a cartoon describing embryonic gene transfer in mouse brain. In this process, DNA encoding the gene of interest is electroporated into developing embryos. Electroporation on specific gestation days, will enable targeting particular layers.

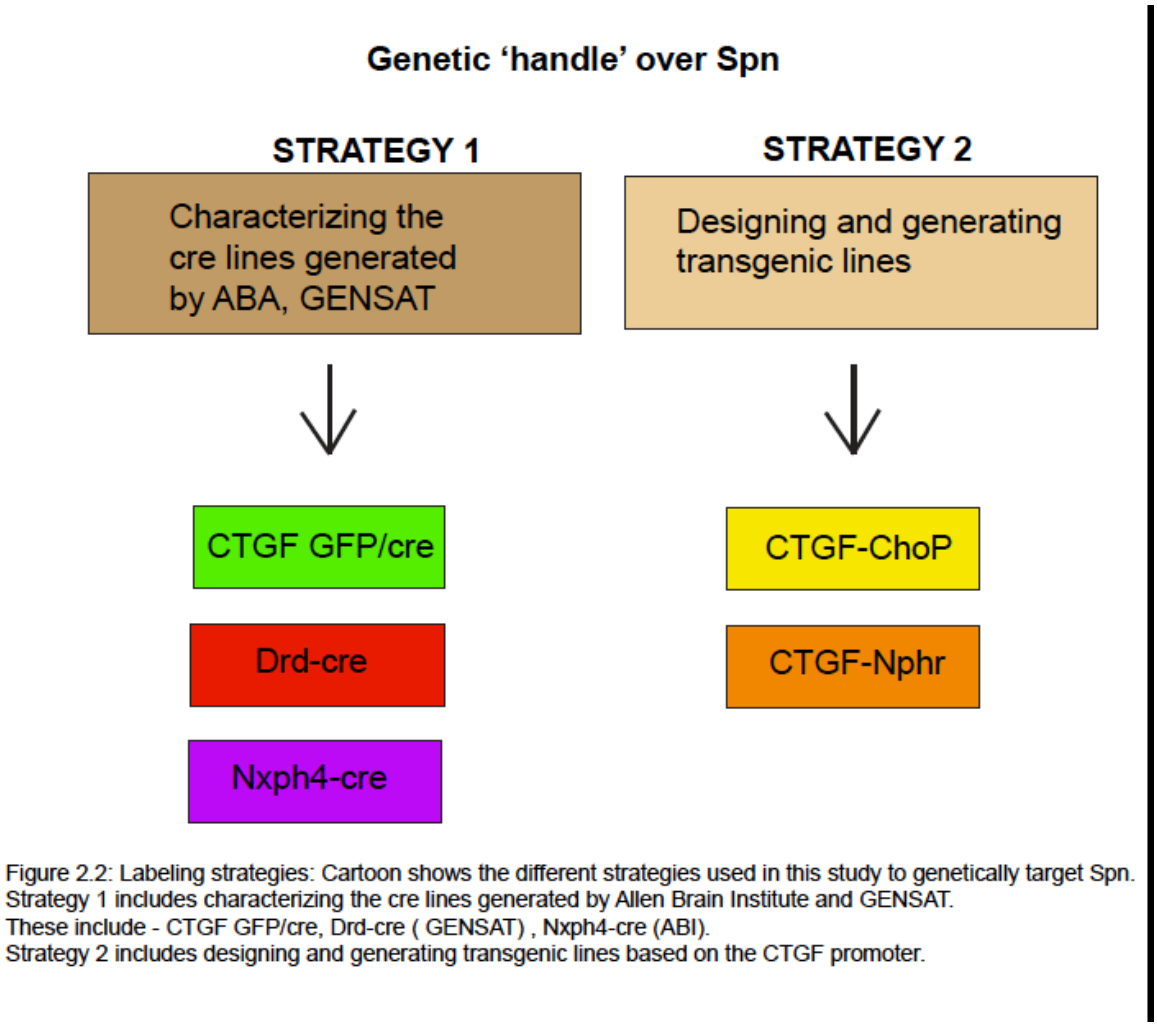

Figure 2.2: Labeling strategies: Cartoon shows the different strategies used in this study to genetically target Spn. Strategy 1 includes characterizing the cre lines generated by Allen Brain Institute and GENSAT. These include - CTGF GFP/cre, Drd-cre (GENSAT) , Nxph4-cre (ABI). Strategy 2 includes designing and generating transgenic lines based on the CTGF promoter.

2.1 Specific Aims:

a) Characterization of transgenic lines, generated by GENSAT and Allen Institute that label SPN. This includes reporter gene-expressing lines – CTGF-GFP and Cre recombinase expressing lines – CTGF-Cre, Drd-Cre, Nxph4-Cre.

b) Design, generation and characterization of transgenic lines that enable targeting and manipulation of SPN. This includes CTGF-channelrhodopsin (activation) and CTGF-NpHR halorhodopsin (silencing).

2.2 Gene expression within the SP: SPN are a molecularly diverse population (Allendoerfer and Shatz 1994, Kanold and Luhmann 2010). While this makes it interesting from a functional aspect, selecting a gene to generate a pan-SPN driver line is challenging. Microarray analysis of genes expressed in the SP from the somatosensory and visual cortices has provided valuable insights into the gene expression patterns within the SP at different stages of development (Hoerder-Suabedissen, Wang et al. 2009, Hoerder-Suabedissen, Oeschger et al. 2013) (Figure 2.3a). This rich diversity in gene expression provided us with several options for transgenesis to target this population:

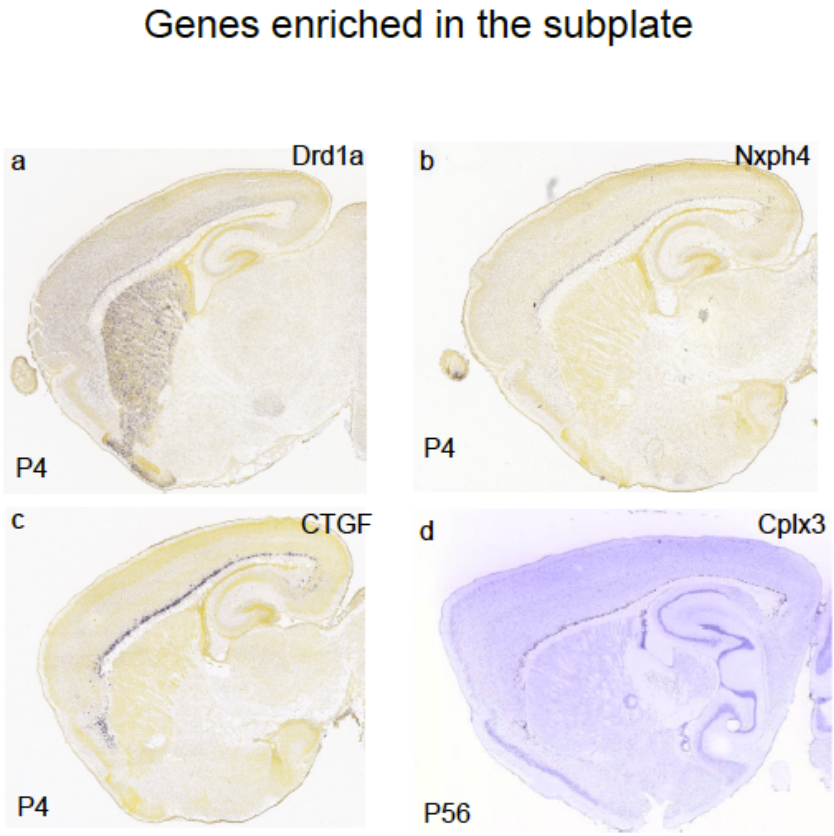

Figure 2.3b: Genes enriched in the subplate :Figure shows images of Insitu Hybridization from Allen Brain Atlas. All the panels show saggital sections of mouse brain at P4 (except panel d which is at P56). Panel a – d show mRNA expression in the neortex and subcortical areas detected by in situ hybridization for specific genes. A- CTGF, b- Drd1a, c-Nxph4, d- Cplx3. Note that in neocortex, the gene expression is enriched in the subplate.

Table 2.1 lists genes that are potential candidates for transgenic strategies.

Gene	**Symbol**	**Expression**	**Onset**
Complexin3	Cplx3	SP specific Some expression is seen in L5 during development	Postnatal
Connective Tissue Growth Factor	CTGF	SP specific	Embryonic
Neurexophilin	Nxph4	SP specific	Embryonic
Dopamine receptor D1a	Drd1a	SP specific Some expression is seen in L6	Postnatal

- Table 2.2 lists the transgenic lines characterized in this study

Gene	**Insert**	**Type**	**Expression**	**Availability**	**Possible applications**
CTGF	eGFP	Bac (RP24-96J1)	Sparse	Cryopreserved	Sparse labeling
CTGF	Cre	Bac (RP24-96J1)	Non Specific	Cryopreserved	Not applicable
Drd1a	Cre	Bac	Specific to SP with some upper cortical expression in S1	Cryopreserved	1.Sparse labeling 2.Targeted activation, silencing

2.3 Results:

We characterize the following transgenic lines in mice aged between P7 –P9 in coronal sections:

2.3.1 CTGF-GFP:

CTGF (Connective Tissue Growth factor) belongs to a family of secreted extra-cellular matrix (ECM) proteins that play a vital role in cellular proliferation, migration (Shimo, Nakanishi et al. 1999), angiogenesis (Shimo, Nakanishi et al. 2001), mitosis and differentiation (Lee, Shah et al. 2010). CTGF has been shown to express selectively in deep cortical layer (Layer VII) in rats (Heuer, Christ et al. 2003). The SP-specific expression of CTGF was further validated in a microarray screen by Saubadeisen et al. (Hoerder-Suabedissen, Wang et al. 2009). CTGF mRNA is expressed throughout the rostral-caudal (RC) gradient of the SP (ABA). While this gene has an embryonic onset of expression, the levels are up-regulated in the post-natal stage (Heuer, Christ et al. 2003, Hoerder-Suabedissen, Wang et al. 2009). CTGF mRNA is expressed throughout the SP zone in the RC gradient as seen in ABA (Figure 2.3 panel c) making it an ideal target for transgenesis. The Tg(Ctgf-EGFP)156Gsat transgenic mouse was generated as a part of the GENSAT Project at Rockefeller University (https://www.mmrrc.org/catalog/sds.php?mmrrc_id=11899). The transgenic line was generated by the insertion of multiple copies of Bacterial Artificial Chromosome (BAC) RP24-96J1 wherein eGFP is inserted into the coding locus of CTGF. Mice harboring the transgene express eGFP from the CTGF promoter (Figure 2.4).

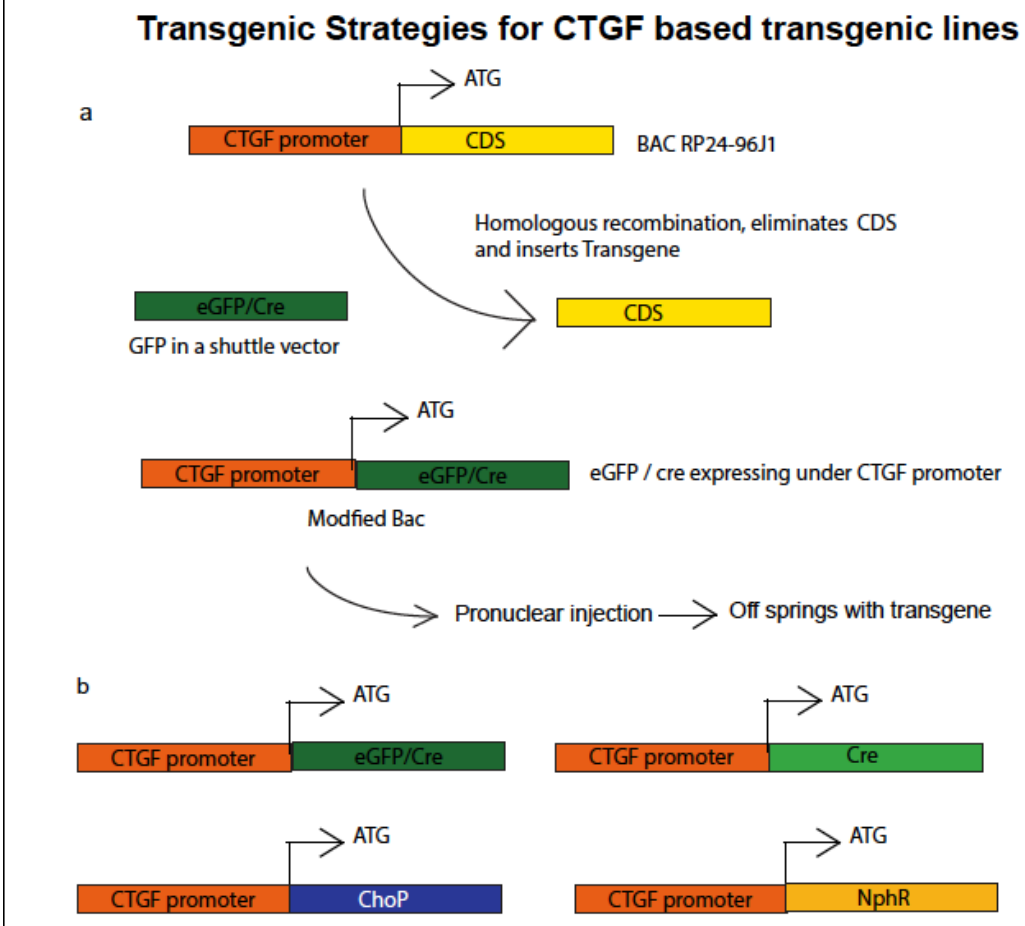

Figure 2.4:Transgenic Strategy_CTGF: Figure shows the scheme used to generate the transgenic lines: Panel (a) shows the strategy for all the CTGF promoter based transgenic lines. BacRP24-96J1 harbors the CTGF promoter and coding sequence (CDS) along with the surrounding genomic elements. A shuttle vector with the transgene – eGFP, cre recombinase, chop, NpHr- with regions of homology between the CTGf coding sites, facilitates homologous recombination that eliminates the CTGF CDS and replaces it with the transgene after the start codon. The resulting modified Bac is then injected into the pronucleus of fertilized oocyte and transferred into the oviduct of fertilized female mice. Panel (b) shows the bac modifications for different transgenics.

2.3.1.1 Gene expression in CTGF eGFP transgenic line:

Reporter expression in the neocortex:

GFP expression in the transgenic line has also been characterized by Molnar et al. (Saubadesiien, personal communication). In our hands, the GFP expression is strong and within the cortical plate, expression is largely restricted to the subplate. eGFP expression within the SP is sparse and seen in a small subset of CTGF-positive SPN. eGFP-

expressing neurons are seen in rostral regions including Vibrissal Motor Cortex M1 and Primary Somatosensory Cortex S1. Very few neurons are seen in areas caudal to S1 (Figure 2.5). SPN residing in differ laminas within the SP receive different patterns of synaptic inputs. In our preparations, neurons expressing eGFP are present in different SP laminas (Figure 2.6). Figure 2.6a (white arrow) shows a representative image of a CTGF positive SPN residing in the upper and lower (blue arrow) SP.

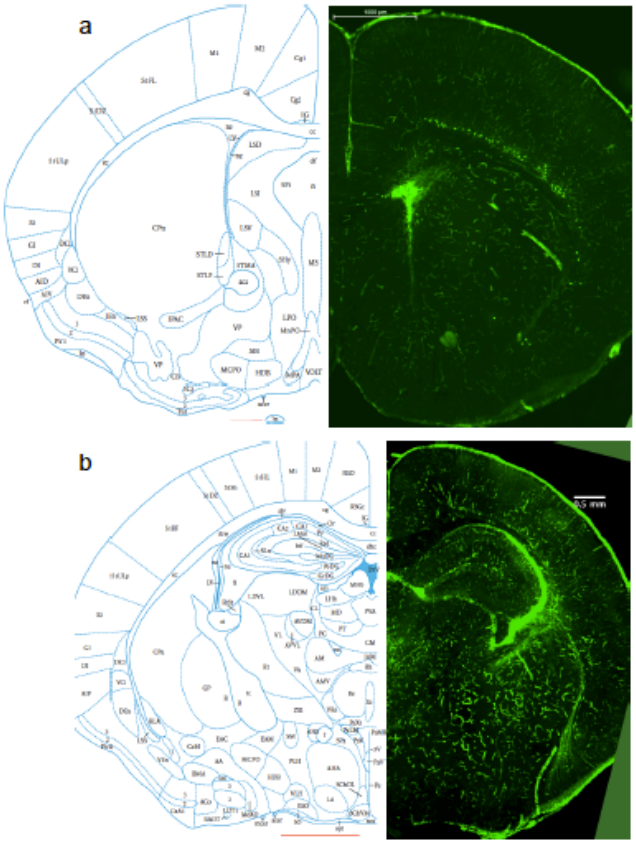

Figure 2.5: Transgene expression _CTGF GFP transgenic line. Figure shows images of coronal sections -CTGF GFP mouse brain at P9. GFP expression is seen in the cortical plate and in. Each panel shows images from rostral brain region to the caudal areas (right) in the left is the representative image of an atlas at P9 (Atlas of the Developing Mouse Brain at E17.5, P0 and P6, 1st Edition). Scale bars on the atlas image (red) – 1mm and scale bar on the image (white) – 500µm.
Panel a shows a representative image of brain areas including Vibrissal motor cortex (M1) , M2. Panel b, shows a similar image showing M2, M1 and regions of the somatosensory cortex (S1) including S1FL, S1DZ, S1J, S1DZO, S1BF.
Note the strong eGFP expression seen in blood vessel, pia, and Choroid plexus in addition to neurons.
Within the cortical plate, eGFP expression is restricted to the Sp.

Diverse morphologies of CTGF positive Spn

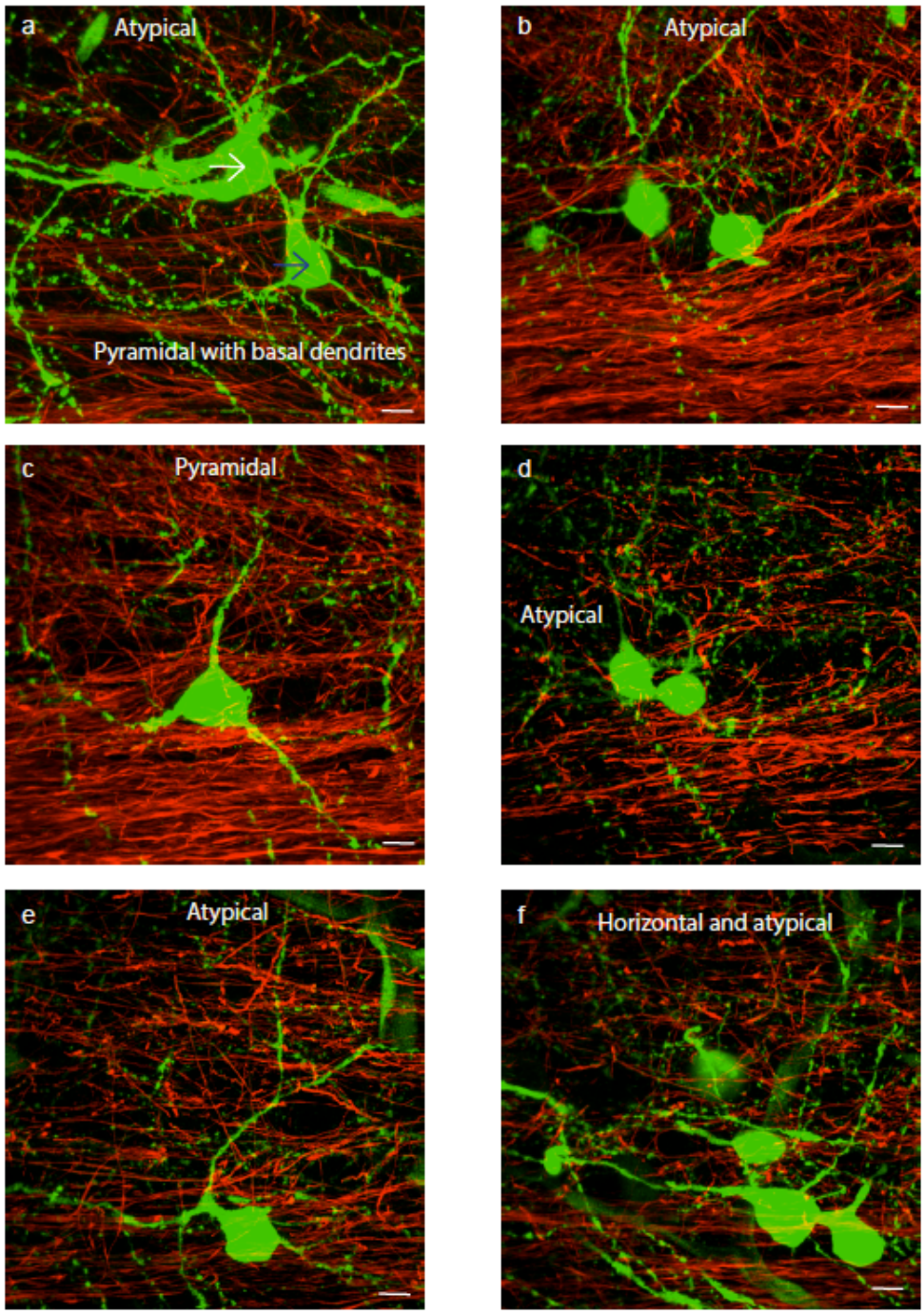

CTGF positive Spn have exhibit morphologies. They are oriented in different directions and occupy different SP lamina. Their dendrites have a beaded appearance.
Scale bar - 20 microns.

SPN are heterogeneous with respect to neuronal geometry. Although we have not done a thorough quantification, the GFP positive neurons in this line appear to exhibit a range of morphology (Figure 2.6) A systematic morphometric analysis will further validate this observation. The different morphological classes that we observed in this transgenic line include pyramidal, horizontal and multipolar. (For definitions of the different geometry and criteria of classification, please refer to chapter 6 under appendix). The morphology and dendritic patterns of this subclass has been described in Chapter 6 appendix in detail. Presence in different laminas and different morphological subclasses imply that these neurons likely integrate synaptic inputs from different areas.

Profuse neuropil density, including axons and dendrites, is seen within the Subplate (Figure 2.6), indicating that they are involved in intra-SP connectivity. Within the cortical plate, neuropil density, including axons and dendrites, is seen in all layers especially in L1 and L4 (Figure 2.7). This implies that CTGF positive neurons are integrated in intra-cortical connections. In order to conclusively determine the identity of the neuropil, we co-labeled with Neurofilament H (NFH) (Roy, Coffee et al. 2000) and found that some of the neuropil density in L4 is from GFP positive axons (Figure 2.7). This could imply that CTGF positive SPN is probably providing synaptic inputs to L4. Axonal projections as determined by NFH co-labeling are seen within the cortical plate, especially in L4 but not in upper layers (Figure 2.7).

CTGF neurites in L4 neurites

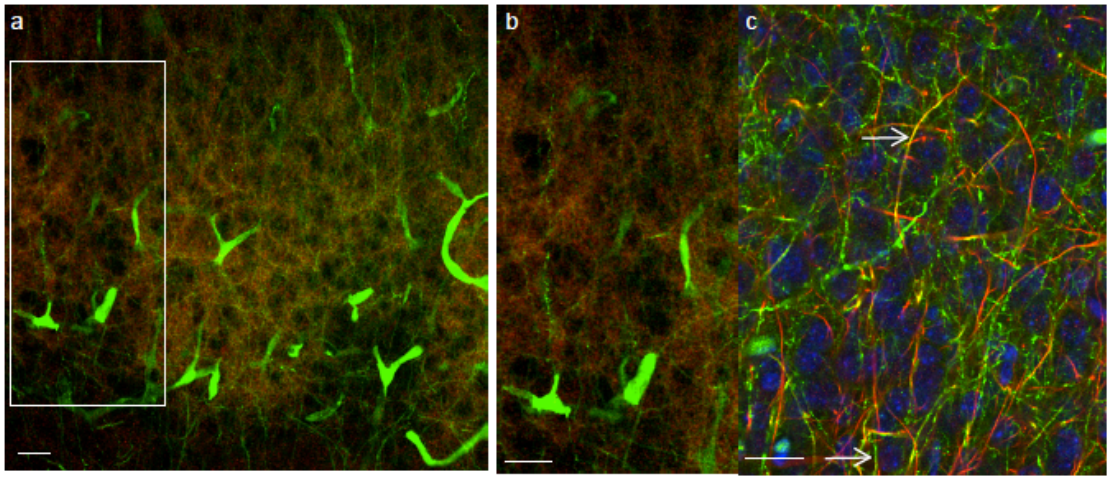

Figure shows neurites in upper cortical layers in a coronal section of a CTGF GFP mouse.
Panel a shows a representative field of view in the barrel field.In this ection, CTGF psoitive neurites are labeled by GFP (signal amplified by anti GFP) and Vglut2 labeling thalamic afferents forming the barrel field(red).
Panel b shows a zoomed view of the region enclosed by the white box.Note the spiny dendrites in the barrel field
Panel c shows a similar field of view with CTGF positive axons in green and NFH labeling axons (red).
to mark GFP positive axons. (white arrowheads)

2.3.1.2 CTGF/Cplx3 co-localization: Saubadeissen et al. observed that 2/3rds of GFP positive cells in the CTGF GFP line are Cplx3 positive. In this study, we observed similar localization patterns at P9 **(Figure 2.8).** This implies that CTGF and Cplx3 form a partly overlapping population SPN.

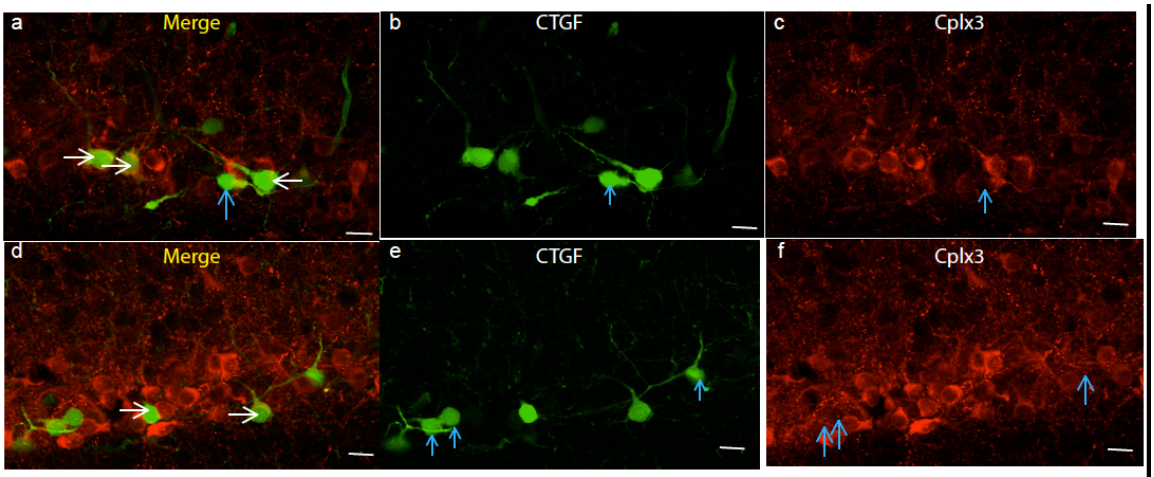

Figure 2.8 CTGF Cplx3 co localization:
Figure shows images of CTGF positive GFP expressing Spn from the CTGF GFP transgenic line. The GFP is enhanced with anti GFP antibody (green) and in all the images Cplx3 positive Spn are labeled with a specific antibody (red). Panels a-c show one field of view while panels d-f show another field of view. In panel a and d show the Spn co expressing CTGF and Cplx3 (white arrowhead) and ones expressing CTGF alone. The panels b and e show only the GFP positive neurons in the field and c and f show only Cplx3 positive neurons. Blue arrows in both panels point to the CTGF expressing neurons (b and e) and the absence of those neurons (c and f).

2.3.1.3 Arrangement of axons within L4:

SPN play an instructive role in the developing TC system especially during the critical period (Kanold and Luhmann 2010). L4 is the primary thalamo-recipient cortical layer (Nahmani and Erisir 2005); previous studies have noted that SP neurites have a characteristic pattern of arrangement in L4 with respect to their thalamic afferents (Pinon, Jethwa et al. 2009). Hence we investigated the pattern of the GFP positive neurites in L4.

Thalamic afferents within L4 of vibrissal somatosensory cortex (also known as 'barrel cortex'), are clustered into a patterned arrangement called barrels (Agmon, Yang et al. 1995) that are separated by inter-barrel spaces called septa. Afferents from the Vpm (Ventral posterior medial nucleus of the thalamus) representing a single whisker projects to a single barrel in L4. Barrels in l4 are occupied by both excitatory and inhibitory neurons. The excitatory neurons– the spiny stellate cells and the pyramidal neurons- far outnumber the inhibitory neurons (Sun, Huguenard et al. 2006).

In the thalamo-cortical information pathway, afferents from the Vpm (Ventral posterior medial nucleus of the thalamus) representing a single whisker projects to a single barrel in L4. Excitatory neurons from a single barrel in L4 project to L2/3 in the same column. Weak trans columnar activation is also seen in adjacent columns.

In a parallel pathway, the septal region between adjacent barrels receives inputs from different whiskers from the posterior medial nucleus (Petersen 2007). The barrel and septa however encode distinct information about the whisker movement (Alloway 2008) – barrel related circuits encode the spatiotemporal information about whisker movement while septal circuits encode the kinetics and frequency of whisker movement (Alloway 2008).

Since barrels and septa serve different functions in information processing (Alloway 2008) (Agmon, Yang et al. 1995) we sought to study the spatial distribution of neurites with respect to thalamic afferents clustered as barrels and septa, and see if axons from different cell types had different patterns of arrangement with respect to the thalamic afferents arranged as barrel and septa.

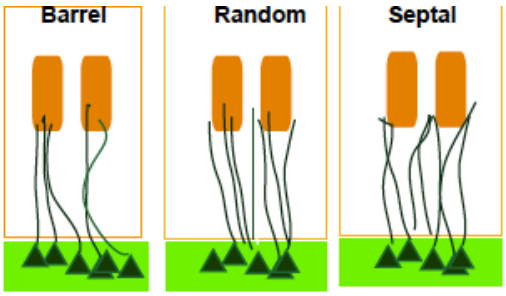

Figure 2.9_ Possible arrangements of CTGF positive neurites :
Cartoon shows the three possible arrangements of GFP positive neurites in L4 with respect to the barrel cytoarchitecture. The neurites could be entirely within the barrels (left), randomly oriented (centre) or clustered between two barrels also known as septa (right).

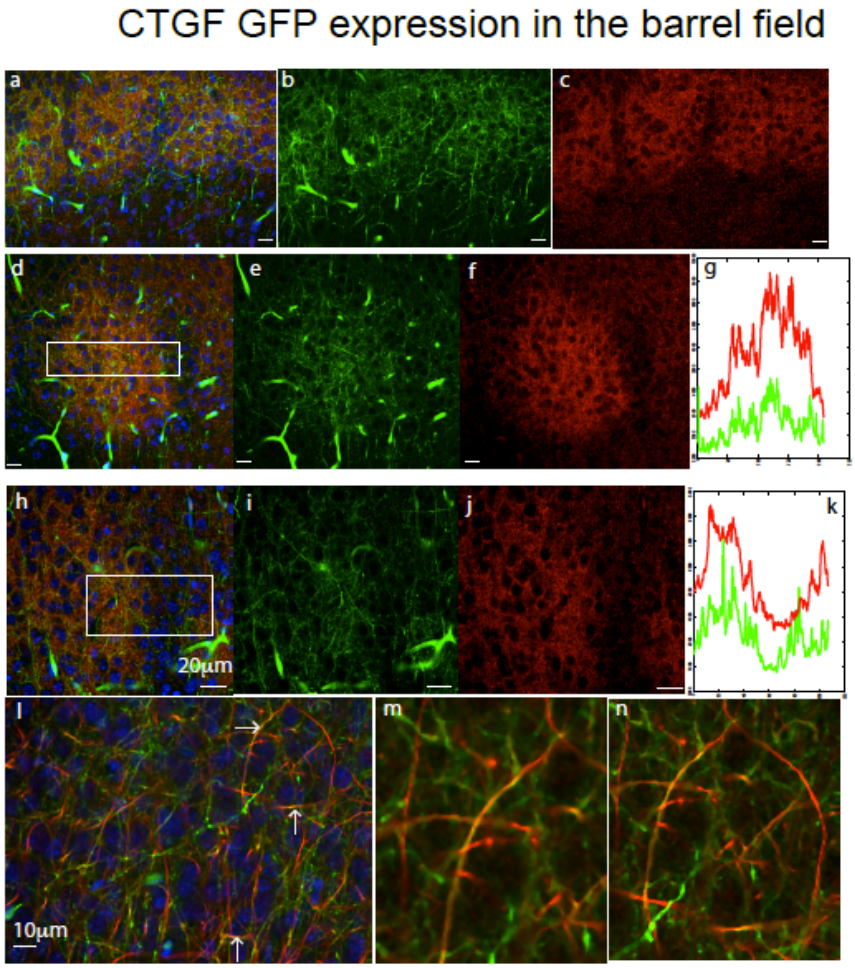

Figure 2.10_CTGF _ neurites in the thalamorecepient layers:
Figure shows the distribution of GFP positive neurons in coronal sections of CTGF GFP transgenic line at P9. In all the figures, GFP positive neurites are in green, thalamic afferents labeled with Vglut 2 (red) and nucleus counterstained with DAPI. Panel a-c show GFP positive neurites in the barrel field. Panel a is a merged image showing thalamic afferents (red), GFP positive neurites (green) and DAPI labeling the neurons in the barrel field. Panel b and c show GFP positive neurites (b) and thalamic afferents alone (c) in the same field. Note that almost entire GFP positive neuropil is localized within the barrels. Panel d –f is a view of a single barrel with surrounding septal compartment in the field of view. Panel d is a merged image while e and f show GFP and thalamic afferents respectively. Once again note the high density of GFP neuropil within the barrel hollow. Panel g shows the quantification of pixel intensities of Vglut 2 (ref) and GFP (green) in the boxed region in panel d. This clearly shows that most of the GFP density is in the same region as the Vglut density. Panel h – j show a similar field of view in a septal region. With panel h being a merged view of GFP (i) and Vglut 2 (red) densities. Panel k shows the quantification of pixel intensities of Vglut 2 and GFP(green) in the boxed region in panel h. This further shows that most of the GFP density is in the same region as the Vglut2 density. Panels l-n show GFP positive neurons colabeled with NFH (red). Arrowheads in panel l point to the neurites co-expressing GFP and NFH indicating that they are axons. Panels m and n show a higher magnification image of two such neurites.

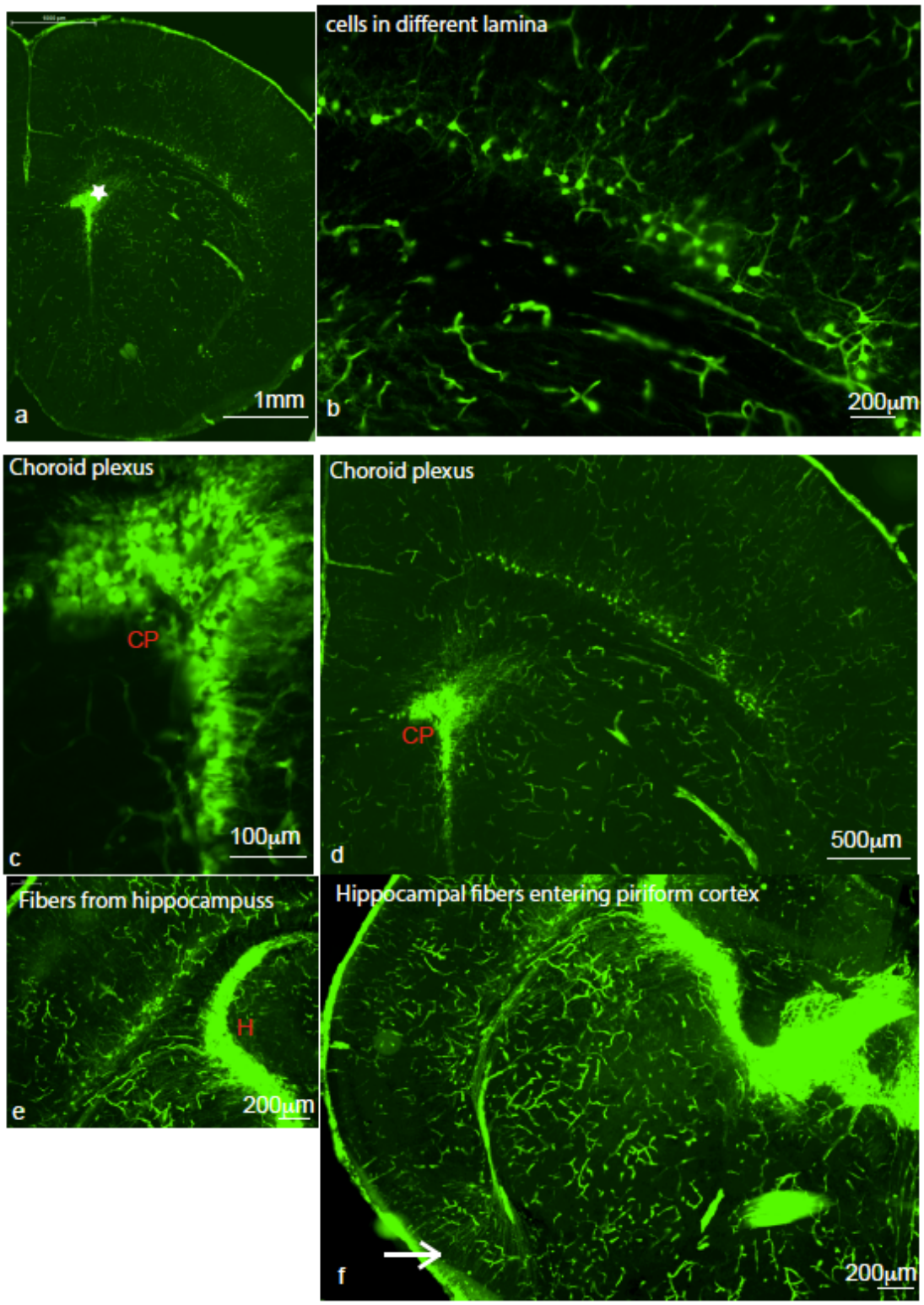

Figure 2.10/11: CTGF-GFP expression pattern: figure shows a coronal section from a CTGF GFP transgenic line. GFP signal is enhanced with anti-GFP antibody. Panel

a shows labeled SPNs in rostral areas mainly M1 and S1. Also seen is the GFP label in the blood vessels. Also seen is dense GFP label in Choroid plexus (*). Panel b is a higher magnification image zooming in on the labeled cells. Notice the different morphology and the different SP lamina occupied by the GFP positive cells. Notice the GFP label in minute blood vessels. Panel c shows the GFP label in choroid plexus (CP) panel d shows a zoomed out view showing the GFP label in the choroid plexus in the context of the SP label. Panel e shows label in the base of the hippocampus (H). Note the fibers rising from the base of the hippocampus into the internal capsule into the cortical plate. Panel f shows fibers from base of the hippocampus into the piriform cortex. Note the fan-like pattern (arrowhead) in the piriform cortex formed by the fibers rising up.

Axons in L4 could have three possible patterns of projections with respect to the thalamic afferents: inter-barrel, intra-barrel or a non-specific /random arrangement of axons in the barrel field (Figure 2.9). In order to determine the location of neurites from SPN with respect to the whisker pattern, we labeled thalamic afferents by localizing the vesicular glutamate transporter 2 protein (VGLUT2) (Methods). Most of the GFP positive axons are within the barrel hollow (Figure 2.10). While we do observe neuropil in the septa, the density is much higher within the barrel hollow (Figure 2.10). Since the GFP labels both axons and dendrites, we co-labeled the GFP positive neurites with NFH-200 to selectively label the axonal population (Figure 2.10), and found a high degree of co-localization (Fig 2.10 l,m,n).

2.3.1.4 Extra-cortical expression:

In addition to the CP, GFP expression is seen in hippocampus. Labeled fibers arise from hippocampus and enter the piriform cortex (Figure 2.11) where they spread out into a fan-like structure. In addition to the neocortex, we observed labeled neurons in different thalamic nuclei in this labeled line. Labeled neurons are seen in the ventrobasal complex (VB) and some association nuclei (Figure 2.12).

While the CTGF gene is specific to the SP in the neocortex, it also labels connective tissue (hence its name), and thus strong expression is seen in blood vessels and the choroid plexus (Figure 2.11 c,d). Strong eGFP expression is seen in the vasculature, which sometimes obscures the fine neuropil density. A majority (2/3rds) of GFP expressing cells (14 out of 25 neurons) from 2 animals express Cplx3.

The CTGF-GFP line thus faithfully labels a sparse population of SPN that exhibit different morphologies. However, the GFP positive neurons might be a distinct subpopulation of the CTGF positive cells, as GFP is expressed in many more SP neurons. This might be a position effect of the BAC integration event, or due to some regulatory elements in the BAC itself.

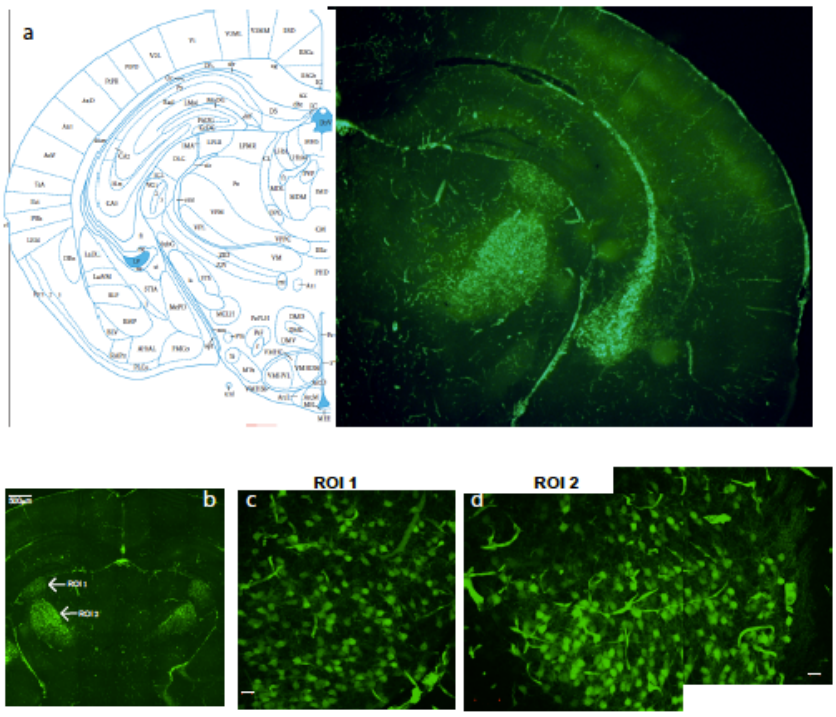

Figure shows the GFP expression in different thalamic nuclei.
Panel a shows a low power image of a coronal section with thalamic nuclei in the field of view (right) and an atlas image of the corresponding section (left).
Panel b shows the two region (ROI 1 and 2 - white arrowhead) with GFP expressing cells.
Roi 1 correspnds to dorsal lateral geniculate nucleus (DLG) while ROI 2 corresponds roughly to ()Vpm.
Panels c and d show a high power image of ROIs 1 and 2 respectively. Note the eGFP expressing neurons,

2.3.1.5 Barrel-specific arrangement of neurites and non – specific expression:

Barrel cyto-architecture in cortex is formed by the clustering of thalamic afferents in L4 (Agmon and Connors 1991). Vpm is the main thalamic nuclei that send axonal projections to barrels (Petersen 2007). Since eGFP positive cells were also observed in the Vpm, it is likely that the GFP positive axons are from the thalamus. However since SPN are known to project to L4 (Pinon, Jethwa et al. 2009) during the critical period, it is likely that some of the axons are from the subplate. This confounding issue can be resolved by segregating thalamic afferents from the SP afferents. This can be accomplished by:

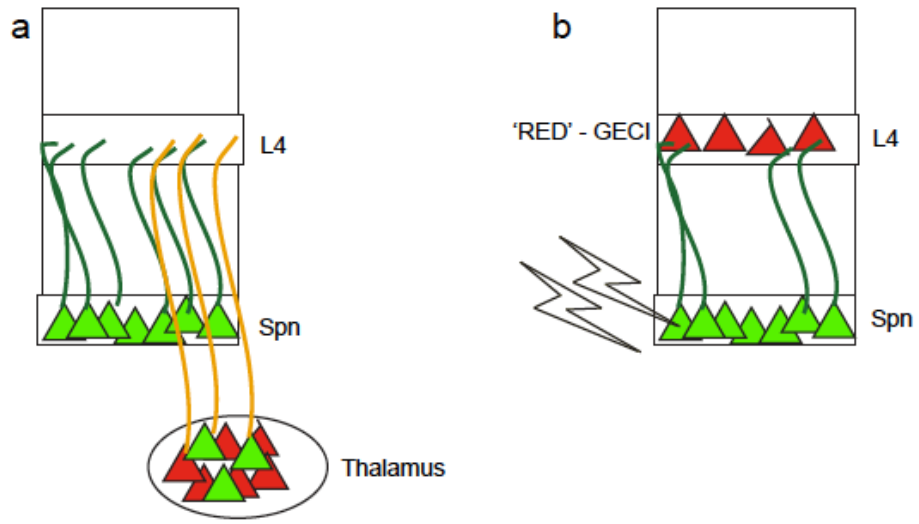

Figure 2.13 Triple transgenic strategy:
Figure shows a cartoon of some possible transgenic strategies that will enable us to distinguish between GFP positive neurons from SPn from those from thalamic 'contaminants'. Panel 1 demonstrates an anatomical strategy wherein thalamic neurons are labeled red. Hence axons from thalamus that also express GFP will be yellow in color. (RFP+ GFP), while those from SP will be green. Thus if the axons in L4 are green, then they are most likely from spn. If they are yellow or red are from thalamus. Panel 2 demonstrates and functional imaging s trategy wherein a red Calcium indicator RGECO or a RCamp is expressed in L4. 2P glutamate uncaging on GFP expressing Spn and imaging calcium activity in L4 will allow us to functionally look at projections from Spn in L4.

Triple transgenic tracing: Creating a triple transgenic line that expresses a fluorescent protein, spectrally well separated from eGFP, in thalamic neurons in addition to GFP in the SP. In theory, this is possible by crossing a transgenic line expressing Cre recombinase in specific thalamic nuclei (*e.g.* Vpm) with a Cre reporter – tdTomato and crossing this line with CTGF-eGFP mice (Figure 2.13). The resulting triple transgenic will enable us to segregate the two populations and see if SPN provide feed-forward projections specifically to the barrel hollow. However, while some driver lines do exist in the GENSAT collection that express Cre recombinase in the thalamus, there is also expression seen in the cortical plate, which might confound interpretation of the results.

Targeted stimulation of SP and imaging calcium activity in barrels: Another approach would be to express a calcium indicator in layer 4 and selectively stimulate the SP and observe calcium activity in L4. Specific stains like Cytochrome oxidase can selectively

label barrels *post hoc*, and the location of the activity can be determined. However the current state-of-the-art transgenic reporter line (Ai38, which expresses GCaMP3 (Tian, Hires et al. 2009), (Zariwala, Borghuis et al. 2012)is not sensitive enough to report sparse signals (data not shown). As such next generation reporter lines encoding the GCaMP6 variants (Chen, Wardill et al. 2013) are required to perform these analyses. These mice are under construction but will not be available for many months.

2.3.2 Drd1a-Cre:

Catecholamine neurotransmitters like dopamine play an essential role in the normal functioning of the brain (Fernstrom and Fernstrom 2007, Schultz 2007). Such functions include motor control (Klemm 1989), reward (Wise and Rompre 1989) and cognition (Nieoullon 2002). The effects of dopamine in the nervous system are mediated by dopamine receptors that fall into two major classes – D1 and D2. While both receptor classes are transmembrane proteins belonging to the G-protein coupled receptor (GPCR) family (Beaulieu, Del'guidice et al. 2011, Hasbi, O'Dowd et al. 2011), they are distinct in their mode of action. Dopamine receptor dysfunction has been implicated in neuropsychiatric disorders like schizophrenia. While the gain-of-function effects (hallucinations) are likely mediated by excessive dopaminergic signaling in subcortical areas through the D2 receptor (Seeman and Kapur 2000), the loss-of-function effects (cognitive deficits) are most likely mediated by dysfunctional D1 signaling in pre-frontal cortex (Goldman-Rakic, Castner et al. 2004).

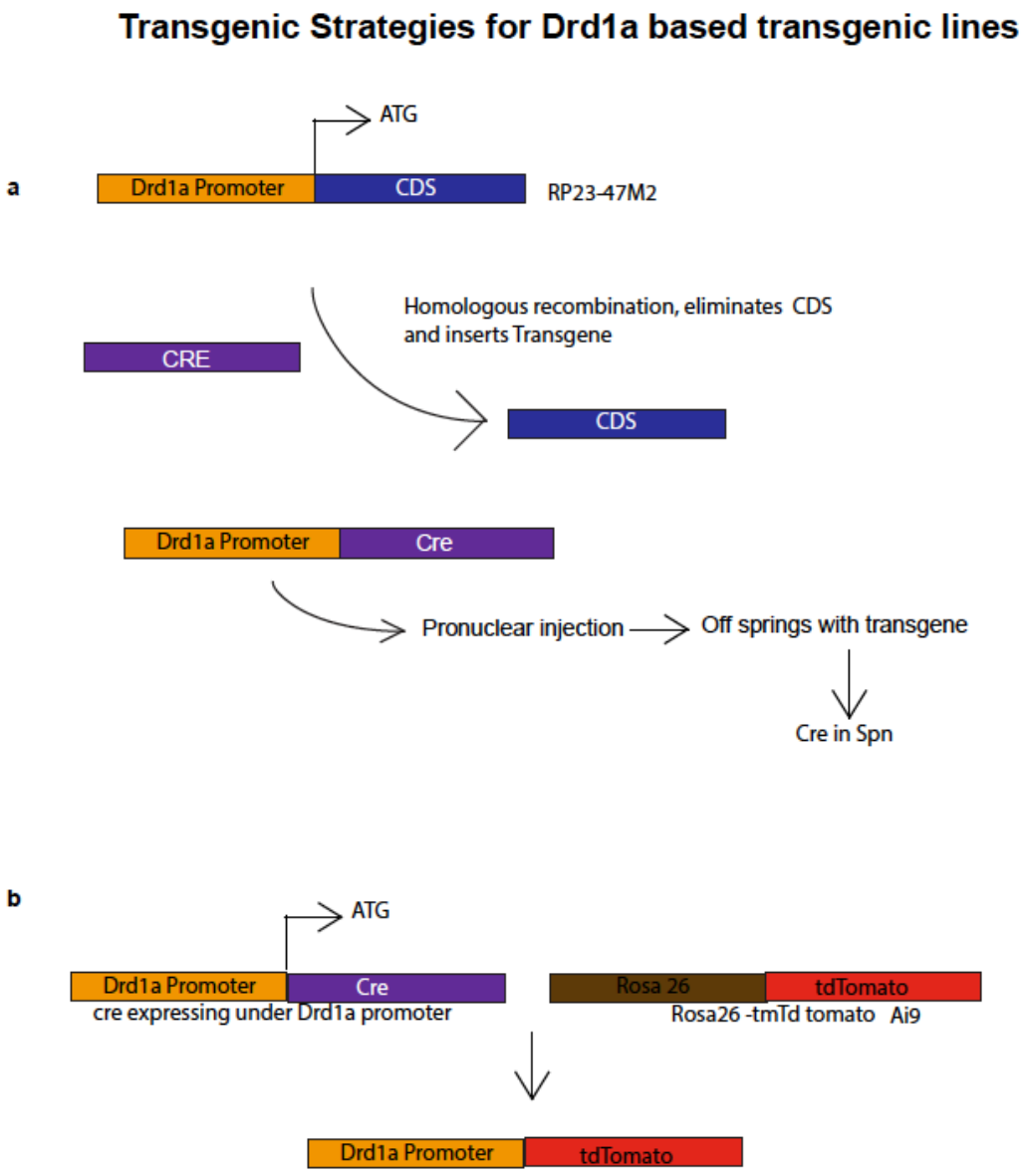

Figure 2.14: shows the transgenic stratgeies used to generate the Drd cre transgenic lines.
Panel a shows the generation of the cre encoding bac construct .
Panel b shows the cross used to generate Drd RFP lines.

Within the cerebral cortex, dopamine receptor D1 expression is enriched in the SP (Anna et al. '13 and ABA). This gene, according to Anna et al., has a post-natal SP specific expression and is hence a good target to study post-natal SPN. The BAC transgenic line Drd1a-Cre-FK164Gsat was also generated as a part of the GENSAT

project. This line was created by inserting multiple copies of BAC RP23-47M2 into the mouse genome. The BAC is modified by inserting Cre recombinase into the coding region of dopamine receptor D1 (after the start codon) (Figure 2.14).

2.3.2.1 Cre expression in the cortex:

Upon crossing with a reporter line, Ai9 (Madisen, Zwingman et al. 2010), the RFP protein fills somato-dendritic compartments and fine axonal branches, thereby allowing us to study the connectivity of this population of SPN. Figure 2.15 shows Drd RFP expression relative to Cplx3 in M1, S1 and A1. RFP expression is strong and robust in the SP zone and extends beyond the subplate into the deep cortical layers in M1 (Figure 2.15 a,b, c) and partly in S1 (Figure 2.15 d,e,f). Upper cortical expression, primarily in L6, is seen in S2 and part of S1BF (Figure 2.15 g,h,i). Qualitatively, the Cre expression becomes increasingly SP restricted in caudal S1BF. In further caudal areas, expression becomes sparse and SP restricted in A1. This suggests an areal difference in Cre expression in this transgenic line. Such areal differences, however, are not seen in the mRNA expression (ABA *in situ* data). In rostral cortical areas, like M1, this transgenic mouse line might be a good genetic tool where additional specificity can be achieved through optogenetic methods.

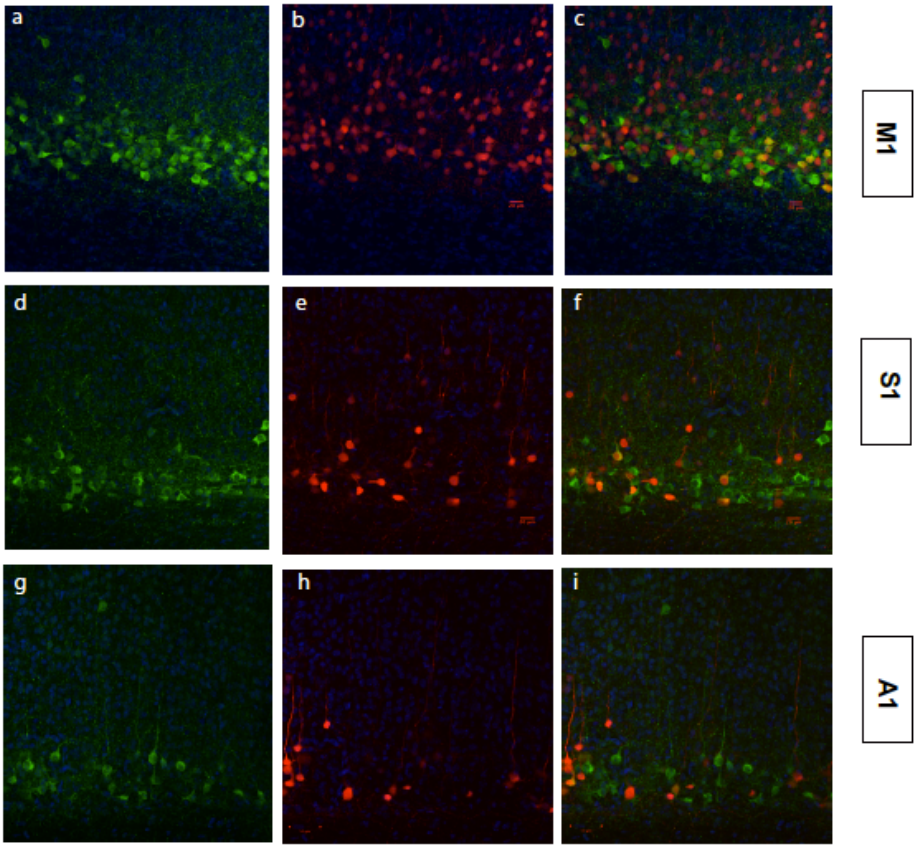

Figure 2.15: Shows the expression of Drd1a (red) with respect to Cplx3 (green) in three different cortical area
Panels a-c show expression in M1, d-f in S1, g-i in A1.
Panels a,d,g - show Cplx3 expression in the three cortical modalities,
Panels b,e,h - show Drd1a expression in the three cortical modalities,
Panels c,f,i - show a merge of Drd and cplx3 exxpression.
note that Drd is expressed well into the lower layers of the cortical plate in M1 (panels ba nd c and becomes restricted to the same lamina as Cplx3 in caudal areas like S1 (panels e and f) and A1 (Panels h and i)

2.3.2.2 Sharp rostral-caudal gradient of Cre expression:

The expression of Cre recombinase, as visualized by the fluorescent reporter expression, has a sharp gradient of expression in the rostral-caudal axis. While extra-SP expression is seen in the deep cortical layers, the expression becomes increasingly SP specific in the barrel cortex. Figure 2.17 shows that in the center of the barrel cortex,

extra SP-expression shows a remarkable down regulation, and expression is almost entirely restricted to the SP. This further shows that this line could be a SP specific driver line for SPN in S1BF.

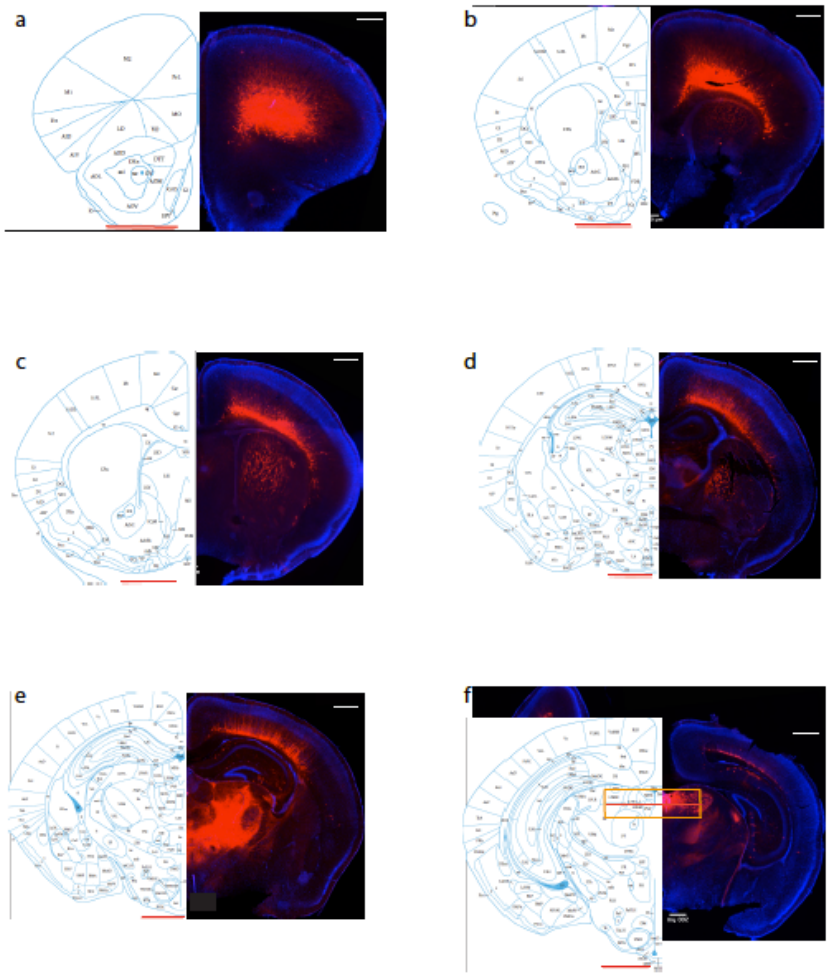

Figure shows images of coronal sections of mouse brain at P9. Drd1a cre mice are crossed / bred with a tarsngenic line expressing td tomato in a cre dependent manner (Ai9) . The resultant double transgenics express RFP in brain regions expressing cre recombinase. Each panel shows images from rostral brain region to the caudal areas (right) in the left is the representative image of an atlas at P9 (Atlas of the Developing Mouse Brain at E17.5, P0 and P6, 1st Edition). Scale bars on the alas image (red) – 1mm and sacle bar on the image (white) – 500µm. Panel a shows a representative image of brain areas including Vibrissal motor cortex (M1) , M2. Note the strong label in M1 and M2 from SP extending into the deep cortical layer. Panel b, c , d show a similar image showing M2, M1 and r egions of the somatosensory cortex (S1) including S1FL, S1DZ, S1J, S1DZO, S1BF. Also seen in Cpu. Note the labels cells in M1 and S1. Expression in the upper cortical layers is reduced in the Somatosensory cortex and the expression is increasingly SP specific. Also note axons traversing through the CPU. Panels e and f show expression in the caudal areas like V1 and A1. And thalamic nuclei. Note the dense label from axon terminals in thalamic nuclei – Vpm, Po. Some labeled cells are also seen in thalamic nuclei.

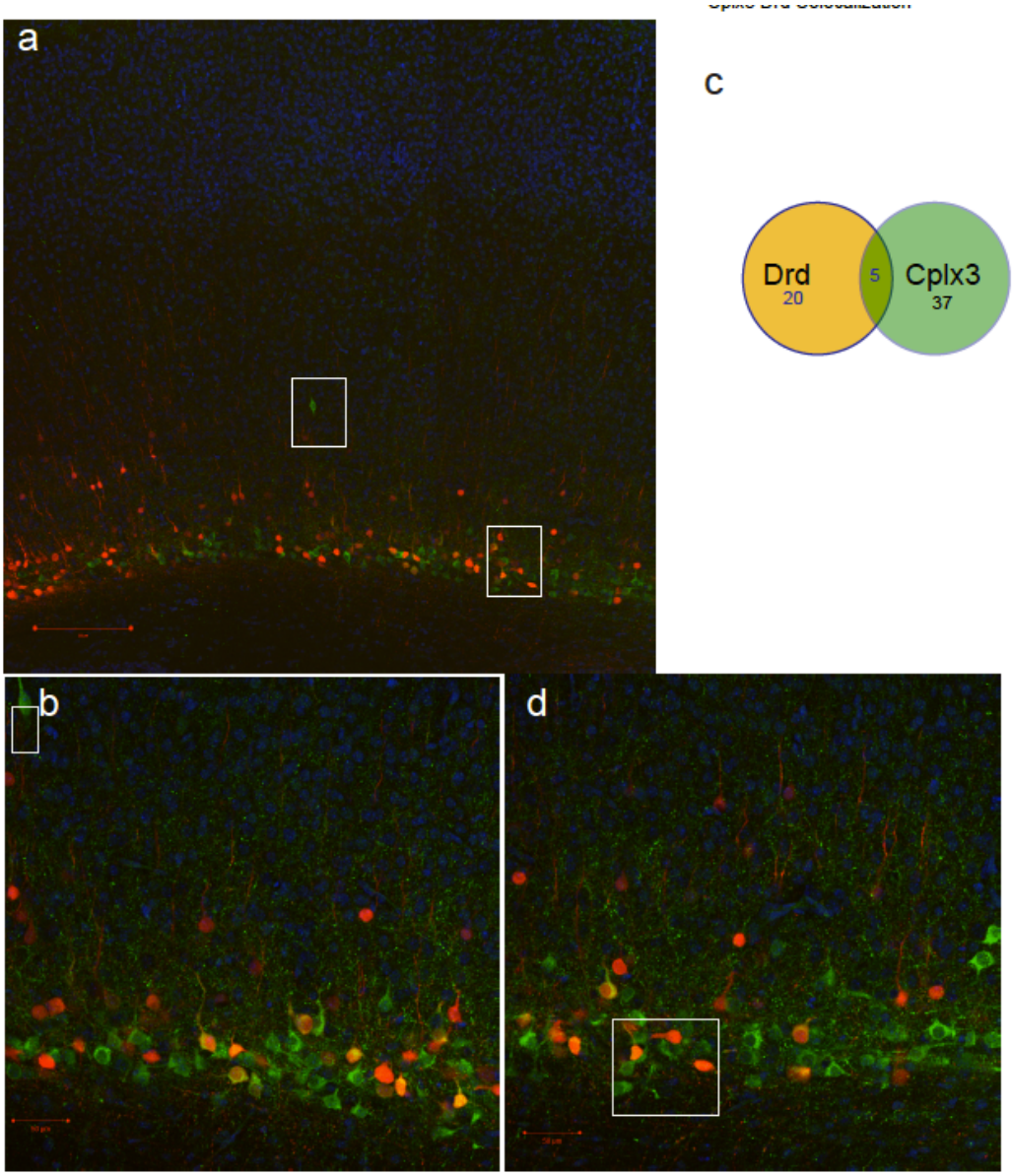

Figure 2.19 shows the colocalization of Cplx3 and Drd1a in S1. Panel a shows a tiled image of the S1BF region. Notice that Drd expresion becomes increasingly SP restricted in the rostral areas. Panel b shows the rostral part of S1BF . Note the neuron in the white box in the tile image corresponds to the boxed one in panel b. Panel d shows a more caudal area . Note the white boxed region to the right in panel a corresponds to the white box in panel d . Note that the Drd expression is increasingly SP restricted in the R-C axis.Panel c shows the extent of colocalization between Drd and Cplx3 in S1BF.

2.3.2.3 Morphology of neurons in CP:

SPN present themselves in diverse geometries. Drd1a positive neurons within the SP also present a heterogeneous morphology (Figure 2.17 and 2.18). We observe neurons that appear pyramidal, horizontal and atypical as seen with the CTGF positive SPN. Within the SP lamina, cells were seen in both superficial and deep cortical layers. Hence Drd positive SPN within the SP also form a mixed population like CTGF. And this line could be useful to perform SP specific studies in the barrel cortex.

2.3.2.4 Drd/Cplx3 co-localization:

Cplx3 gene expression is restricted to the SP except for the few genes in L5. In order to determine how much of the Drd expression is within the SP, we counted the number of Drd-expressing neurons in compartments marked by Cplx3. We localized our study to S1, as this is the region where Drd1a expression is mostly SP restricted (Figure 2.18).

2.3.2.5 Neuropil in cortex:

Extensive neuropil density is seen in different layers of the neocortex. At P7, we observe neuropil density within the SP and extending into the cortical plate, especially in deep cortical layers and in layer 4/5 boundary. Some density is also observed in upper layers. While some of these are clearly dendrites as determined by the thickness and presence of spines (Figure 2.19), some of them appear to be axon terminals as determined by the punctate appearance of the terminals.

Fig: Neurites in the cortical plate

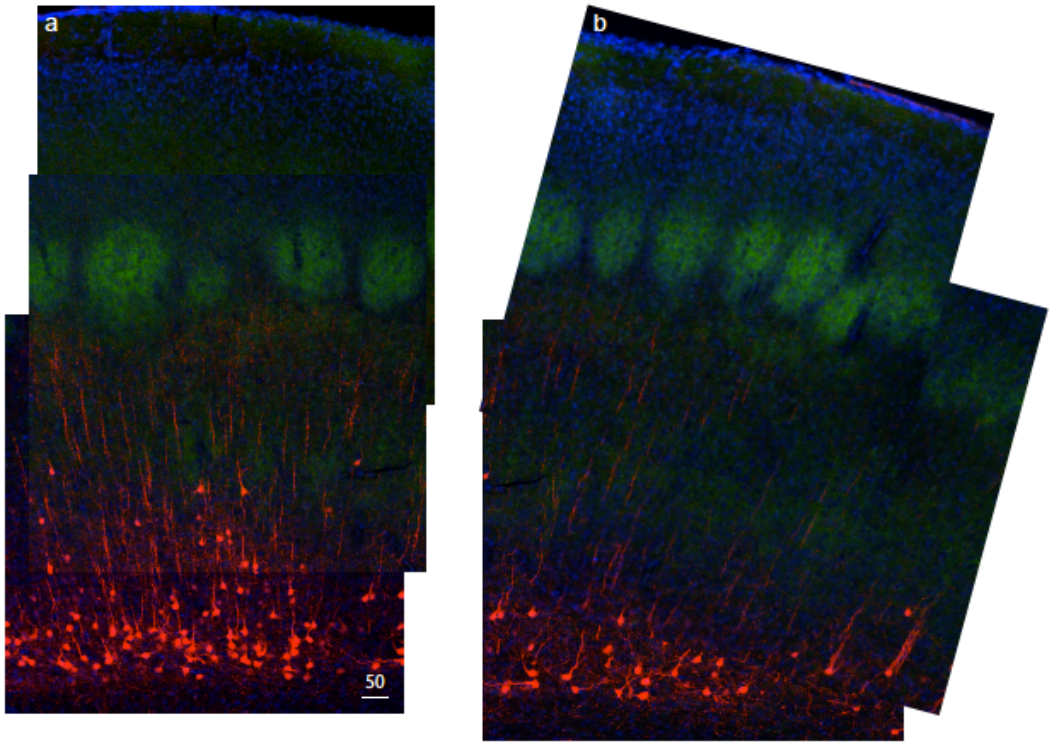

Figure shows a tiled image of S1Bf region of a coronal section from a transgenic line expressing RFP in Drd1a positive Spn.

Panel a shows a tiled representation of a rostral part of S1BF. Panel b shows a caudal region. Note th eneuropil density at the bottom of the barrel field. Also note that this density is below the barrels.

2.3.2.6 Pattern of arrangement:

As with CTGF, we wanted to see if the Drd positive SPN had a characteristic pattern of projections in the cortical plate. A patterned arrangement of the SPN could imply an instructive role in the patterned cyto-architecture like the barrels. In layer IV, the possible arrangements include: within the barrel hollow, between the barrel hollows, and random orientations.

2.3.2.7 Barrel related arrangement of neurites and non – specific pattern with respect to the thalamic afferents in L4 (Figure 2.9 b). As before, in order to determine the layers

that the Drd1a positive SPNs project to, we localized neuropil density with respect to thalamic afferents using VGLUT2 immunoreactivity.

2.3.2.8 Drd neurites in L4

L4 is one of the main thalamo-recipient layers in the neocortex (Bannister 2005), and SPN are essential for the maturation of TC projections to L4 (Kanold, Kara et al. 2003). Since we observed neuropil density in L4, Drd positive neurites were examined in relation to the barrel cyto-architecture to see if they were within the barrel hollow or within the septa. At P9, we observed that Drd positive SPN neurites, as seen by RFP fluorescence, were excluded from the barrel hollow and most of the neurites were primarily localized at the L4/5 boundary (Figure 2.20). It is important to note that the neuropil density was at the L4/5 boundary and not in L4. While some of the neuropil density was clearly from dendrites (as seen by the presence of spines) some of them were axons. This pattern is similar to what is seen with Cplx3 and distinct from that seen with CTGF positive SPN, which extend neurites mostly within the barrel hollow. However, an important distinction between Cplx3 and Drd1a distribution is that while the former is entirely indicative of the projections from the SPN, the latter includes axons and dendrites.

2.3.2.9 Drd neurites in L1

Upon localizing with respect to VGLUT2 –immunoreactive cells, we observed Drd1a positive neurites in layer 1 in the different cortical areas studied. High-

magnification images revealed punctate Drd1a positive neurites and varicosities along with VGLUT2+ terminals in L1. These results are consistent with prior physiological and anatomical studies showing SPN projections to layer 1 (Clancy and Cauller 1999). Since this is one of the main feedback layers in the neocortex, presence of axon terminals in this layer indicates a role of SPN in the feed-forward cortical circuit.

2.3.2.10 Technical limitations - Extra-cortical expression:

A major technical limitation of this observation is that in the Drd1a line, in addition to the expression in the neocortex, there is expression in some thalamic nuclei as well, primarily Po (Figure 2.16f). Although the main thalamo-cortical afferents originate from those nuclei, Po extends projections primarily to the septal compartment in L4 (Alloway 2008), while we see most of the neuropil density from this cross in the L4/5 boundary. Hence while some of the neuropil density could also be from these thalamic nuclei, the pattern of distribution with resect to the thalamic afferents (barrels) is not likely to be affected by this extra cortical expression.

2.3.3 NxpH4-Cre

This is an inducible Cre Nxph4-2A-CreER2. This has been developed by the Allen Brain Institute and has been recently procured by the lab. Preliminary analysis on an adult brain sample shows that Cre expression is almost exclusively restricted to the subplate. However, some labeled somata are also observed in thalamic nuclei. The inducible Cre might provide a temporal handle over expression. Although we have no data from this line yet, recent studies (Hoerder-Suabedissen, Oeschger et al. 2013, Miller,

Ding et al. 2014), have shown that Nxph4 is a SP marker that is enriched in the postnatal SP and hence selective modulation of the SP at different stages of development might provide insight into its precise role during the critical period. However Cre induction in neonatal animals might be a challenge. *In utero* administration of tamoxifen has recently been shown to have adverse side effects during development (Hilakivi-Clarke, Cho et al. 2000, Eberling, Wu et al. 2004). Postnatal administration might exceed the critical period time window for expression.

2.3.4 Other transgenic lines from GENSAT:

CTGF-Cre:

This line was also generated a part of the GENSAT project. The design scheme is similar to that of CTGF GFP. However the Cre recombinase shows broad expression both within the SP and in the upper cortical layers. We did not characterize this line further because of this non-specific expression.

2.3.5 Transgenic lines generated in this study:

While the GFP labeled line enables anatomical study of the CTGF positive SP neurons, we tried to generate lines that would enable functional manipulation of the CTGF positive SPN. To achieve this, we created lines that would express Channelrhodopsin (ChR2) (activation) or Halorhodopsin (NpHR) (inactivation) under the CTGF promoter. Our goal was to create a genetic toolbox that would enable functional and anatomical studies of one of the major subpopulation of SPN. We cloned ChR2-Venus and NpHR-

YFP into the coding sequence of CTGF in the BAC RP24-96J1 (Figure 2.4b,c,d) and inserted multiple copies into the genome.

2.3.6 Gene expression: The expression pattern of the effectors ChR2 and NpHR in different founder lines was very interesting. While almost all the ChR2 founders had a very sparse expression like CTGF GFP, NpHR founders had a broad non-specific expression similar to the CTGF Cre line (Figure 2.22). Functionally, these lines failed to produce optogenetic activation and inactivation. This was most likely because a single copy ChR2 or NpHR, which have very low conductance, was not sufficient modulate the activity. So while these transgenic lines were not successful for further research, it is clear that there is probably some regulatory element associated either with the genomic segment in the BAC or with the integration site that results in either a sparse but specific (CTGF-GFP and CTGF–ChR2) or a dense but non specific expression (CTGF-Cre and CTGF-NpHR). This information will be useful in the generation of future transgenic lines.

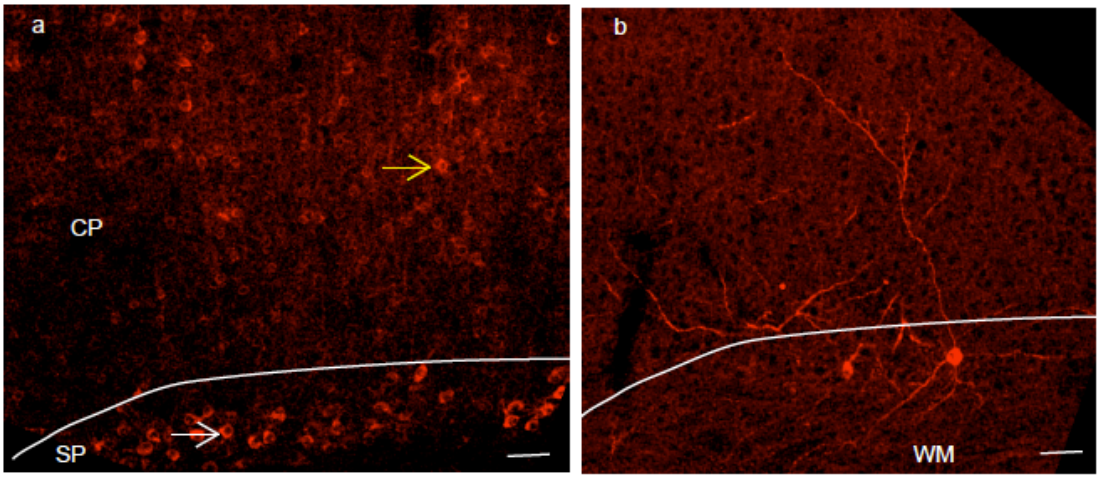

Figure shows representative images of two optogenic lines driven by the CTGF promoter. Coronal sections expressing the transgeneare stained with anti GFP antobody detected with a secondary antibody conjugated to AF 594. The red label, both cases represent transgene expression.Panel a shows the exoression from the line expressing Nphr from the CTGF promoter. White arrowhead point to the expression witin the subplate while yellow arrowhead pointto expression in the extra SP cortical layers.

Panel b shows an image from the ChoP expressing mice. Coronal sections expressing the transgeneare stained with anti GFP antobody detected with a secondary antibody conjugated to AF 594. The red label, both cases represent transgene expression.Note the sparse but SP restricted exression in the ChoP line. No neurons were observed in the cortical plate.

2.3.7 Possibilities for future knock-in transgenics or promoter encoded expression:

Cell type-specific promoters have been used to gain access to particular cell types (Chhatwal, Hammack et al. 2007). While in certain cases, the *cis*-regulatory elements extend many kilobases (kb) into the genome, sometimes they span just few kb and can thus be packaged into viral vectors like adeno-associated virus (AAV) or lentivirus and used for cell type specific gene expression (Nathanson, Jappelli et al. 2009). Given the existence of such short sequences, viral vector-encoded promoter with a reporter gene could be delivered *in utero* to attain SP-specific gene expression (Rahim, Wong et al. 2012). This approach avoids *in utero* manipulation at early gestational age, which is technically challenging. These methods could be used in conjugation with Drd-Cre and

CTGF-GFP transgenic lines to gain combinatorial specificity. Thus I tried to see if any of the SP markers had upstream sequences short enough to be potential targets for such an approach.

The criteria for such a regulatory element upstream of a gene include:

a) SP specific or SP enriched expression with no or limited expression in other subcortical areas, specifically in thalamic nuclei and brainstem. Such a pattern of expression will eliminate the thalamic 'contamination' seen with other transgenic lines.
b) Distance between upstream gene (with respect to the direction of gene expression). The two commonly used viral vectors include AAV vector has a payload limit of ~ 4.5 kb (Hirsch, Agbandje-McKenna et al. 2010, Wu, Yang et al. 2010) and lentivirus can accommodate a payload of ~9kb. So ideally a flanking region less than these limits could be ideal.
c) Flanking genes should ideally be transcribed in the same direction as this gene. If not, the upstream region might also encompass the regulatory element(s) for the flaking gene resulting in anomalous gene expression.

Our approach includes:

a) Picking candidates from recent expression profiling data (Hoerder-Suabedissen and Molnar 2013) that have postnatal specificity of expression in the subplate.
b) UCSC genome browser (http://genome.ucsc.edu/) gives gene location in the genomic context. We used it to look at the position of the gene of interest, flanking regions and genes and expression patterns. Table 2.3 summarizes the genomic context of SP specific

genes. Cplx3 and Nxph4 seem putative candidates for upstream regulatory element targeting.

Table 2.3: Genomic context of SP specific genes

Gene	Upstream	Downstream	Transcription
Cplx3	800	3767	all genes in the same orientation
Abhd4	5425	88971	Upstream gene opposite orientation
Nxph4	8317	1599	all genes in the same orientation

2.4 Discussion:

Most of the current knowledge of the SP circuitry comes from physiological techniques like Laser Scanning Photostimulation (LSPS). LSPS is a technique based on the photolysis of caged glutamate that allows the precise mapping of the position and strength of inputs to a single postsynaptic neuron. However, this technique does suffer from certain limitations. For instance, it is not feasible to map the pre-synaptic inputs to a defined cell population. This can be overcome with the help of a transgenic line wherein a transgene expression enables labeling and manipulating a specific neuronal population to gain insight into the function of this group of neurons. Some of the common methods of transgene expression include a) delivery of the gene of interest under specific promoters using viral vectors, b) *in utero* electroporation, and c) transgenic mouse lines wherein germline transmission of the gene is achieved via a BAC transgenic or by 'knocking' the gene into the genome under the endogenous promoter.

In a developing system like the SPN, viral vector-mediated expression is not a practical strategy because the time for adequate expression (~2 weeks) will exceed the critical period even if injection is performed right after birth. The promoter size of most SP-specific genes far exceeds the payload of viral vectors.

Since SPN are early born, *in utero* electroporation is generally performed around E10.5 to target this population. While this procedure has been performed in different laboratories at this gestational stage, it is challenging. Also since different subpopulations of SP are born on different days within a time window of E10.5 – E12 (Molnar '13 early born), achieving a uniform SP expression via this technique is not possible. Hence transgenic lines with germline transmission offer the most efficient approach to gain genetic access into the SPN.

In this study, we characterized two transgenic lines that offer different levels of specificity and expression. For a sparse but highly specific expression, CTGF-GFP is the choice while Drd-Cre offers the advantage of more dense expression but at the cost of specificity especially in the rostral areas of the neocortex. Since the transgenic line expresses Cre recombinase, it allows the expression of a reporter (*e.g.* fluorescent proteins), activator (*e.g.* ChR2), silencer (*e.g.* NpHR), or activity indicator (*e.g.* GCaMP). Potential issues resulting from extra SP expression in the upper cortical layers (mainly L6) can be overcome by targeted activation /inactivation (optogenetics) or by focusing the region of interest within the SP (GCaMP).

2.4.1 Possible integration of SPN in intra-cortical and thalamo-cortical circuitry:

Layer 1, in addition to receiving apical dendrites from different cortical layers, is the point of convergence of several connections, including intra-areal connections (Ma, Yao et al. 2013) and thalamo-cortical afferents (O'Leary, Schlaggar et al. 1994). Hence if part of the neuropil density in L1 from a Drd1a positive SPN consists of axon terminals then it is most likely indicative of a role in synaptic integration.

Layer 4 is the main thalamo-recipient layer and the presence of CTGF positive axons in this layer might be indicative of an instructional role. There are two distinct possibilities with this type of neurite arrangement:

a) A fraction (~2/3) of CTGF-GFP positive SPN are also Cplx3 positive. Maybe those are the Cplx3 positive SPN also projecting to the barrel hollow.
b) In case of CTGF- GFP positive neuropil in the barrel hollow, we see entire axons, not just axon terminals, within the barrel hollow. So maybe this is indeed reflective of the pattern of SPN axons within the barrel field – all axons traverse through the barrel hollow and then turn and make terminations capable of forming synapses at the walls of the barrel hollow. Since Cplx3 is localized exclusively in the terminals (Zanazzi and Matthews 2010), we observed density from Cplx3 positive SPN in the barrel-septal boundary.

And since barrels and septal circuits encode different aspects of the circuitry, this could imply their differential integration in the cortical circuitry. Further, the differential orientation might be an example of different subpopulations of SPN segregating into different functional subclasses. However, given the co-expression in thalamic nuclei, we are unable to conclude the exact significance of this pattern of neuropil density.

2.4.2 Gene expression pattern within the SP:

A recent study revealed a unique pattern of gene expression among the SPN. They observed that genes that are specific to the SP are rarely specific at all ages (Hoerder-Suabedissen, Oeschger et al. 2013). They show a unique pattern of co-expression where genes expressed in the subplate are also expressed in the upper cortical plate especially in Layer 5. An example of such a gene is Cplx3, which is enriched in the subplate and also expressed in a small population of cells in layer 5. Hence while there are several possibilities for Cre lines with targeted expression in the subplate, there is likely to be Cre expression in different cortical areas and extra cortical areas in all these lines. In other words, it might not be entirely possible to have a SP driver with very high spatio-temporal specificity.

Given this caveat, in this study we have identified and characterized two driver lines that are available and that faithfully target SPN. These lines offer different levels of specificity and might be useful to manipulate and study this population. Nonetheless, extra-SP expression in cortical layers and subcortical expression is seen in both these lines. However, there are no other existing means to genetically target this population, and further targeting strategies might also have the same issues of non-specific expression. We have also provided some insights into the CTGF gene locus as a potential site for transgenesis for future studies.

2.5 Conclusions:

a) We have identified and thoroughly characterized one transgenic line expressing Cre recombinase in the SPN and another line expressing eGFP in SPN. Although there are technical limitations, these lines will facilitate studying this population at the molecular level.

b) We have also identified transgenic driver lines that could potentially be useful to target SPN.

c) While CTGF might be a SP specific gene, it might not be an ideal promoter with which to generate transgenic lines. The genomic context probably has some cryptic regulatory elements that either make the expression very sparse but SP specific or make it robust in SP but with extra-cortical expression that renders the line non specific.

d) The unique gene expression pattern in SPN points to a lack of spatiotemporal specificity of SP markers throughout development.

e) Genes specific to the SP also have a high level of co expression in upper cortical layers at different developmental time points.

f) The above two points indicate that a 'golden' SP specific driver line is highly unlikely and as such an additional level of specificity, either using functional tools or triple transgenics might be required to exclusively study this population.

2.6 Future directions:

1. **Targeted manipulation of activity:**

   The Cre lines characterized here could be useful where additional specificity is conferred by targeted imaging (GCaMP) or targeted activation/inactivation with the help of a laser. Targeted crosses with transgenic lines expressing calcium indicators (GCaMP6) in a Cre-dependent manner might facilitate targeted imaging of SPN activity during development. Alternatively, targeted activation and inactivation with ChR2/NpHR will permit the manipulation of a subpopulation of SPN.

2. **Promoter driven expression:**

   Expressing a single reporter or multiple reporters from promoters of the three genes identified here as SP specific with regulatory elements short enough to be used with viral payload.

2.7 Material and Methods

All procedures followed the University of Maryland College Park animal use regulations. In this study, we use mice (C57BL/6) of either sex from The Jackson Laboratory (jax.org).

Perfusion and sectioning: Brains were perfused transcardially with 4% PFA, post-fixed for 2 hours in 4% PFA at room temperature or overnight at 4C. Fixed brains were rinsed in cold PBS and cut coronally at 50μm thickness and collected in cold PBS and stored at 4C. Horizontal sections were made as described in (Tolner et al.).

Immunohistochemistry: Free floating sections were blocked in 3% BSA and 0.3% Triton for one hour at room temperature followed by incubation in primary antibody overnight at 4C. Sections were rinsed in 0.3% Triton 3 times (15' each) to remove non specifically bound primary antibodies followed by incubation in secondary antibodies. Sections were finally rinsed in 0.3% Triton to remove non-specific secondary antibodies and mounted onto glass slides. Sections were air dried at room temperature, rehydrated in PBS and coverslipped with Vectashield (Vector Labs). Antibodies and concentrations are shown in table 2.4.

Imaging:

Fluorescent sections were imaged with Pannoramic 250 Flash Whole Slide Digital Scanner to analyze cell and projection distribution. Quantification of cells and projections was done on images taken on a confocal microscope (Zeiss 510 or 710 meta). Filter sets were chosen to minimize any bleedthrough between fluorophores.

Analysis:

Images acquires as above were adjusted for contrast and brightness in Image J. Cell quantification was done in Image J using Cell counter plugin. Projection analysis was done in Image J and plotted using custom Matlab scripts.

Table 2. 4

Name	Vendor	Cat.No	Dilution	Species
Cplx3	Synaptic Systems	122 302	1:1000	Rb
VGLUT2	Synaptic Systems	135 404	1:5000-10,000	Gp
NeuN	Chemicon	MAB377	1:100	Ms

Name	Vendor	Cat.No	Dilution	Conjugate
Gt anti Rb	Invitrogen	A-11008	1:500	AF 488
Gt anti Gp	Invitrogen	A-21435	1:500	AF 568
NeuN	Invitrogen	A-21435	1:500	AF 647

Rb:rabbit, Gt: goat, Ms: mouse, Gp: guinea pig, AF: Alexa Flour

CHAPTER 3: DESIGN AND CHARACTERIZATION OF MULTIPLE TRACING TOOLS

ABSTRACT

We describe an engineered family of highly antigenic molecules based on GFP-like fluorescent proteins. These molecules contain numerous copies of peptide epitopes and are shown to simultaneously bind IgG antibodies at each location with high affinity. These 'spaghetti monster' fluorescent proteins (smFPs) distribute well in neurons, particularly into small dendrites, spines and axons. smFP immunolabeling reveals fine sub-cellular structures and permits the localization of weakly expressed proteins that are not well resolved with traditional epitope tags. By varying the epitope and scaffold, we generated a diverse family of mutually orthogonal antigens for cell tracing and protein tagging. When deployed in neurons and in mouse and fly brains, smFP probes allow robust, multi-color visualization of cell populations and neuropil with distinct epitopes. The antigens perform well in advanced preparations such as array tomography, super-resolution fluorescence imaging, and electron microscopy. Stochastic expression allows Brainbow-like discrimination of neuronal arborizations. These probes will facilitate experiments in connectomics, protein localization and the assembly of high-resolution brain atlases.

3.0 INTRODUCTION:

SPN comprise a diverse neuronal population, and the connectivity of multiple cell types within and beyond the SP is presently unknown. While the Cre driver lines characterized in the previous chapter will enable labeling of SPN in general, labeling multiple sub-populations of neurons calls for the development of high-quality labels ('probes') to distinguish them. In this chapter, I'll describe the efforts to engineer, characterize and optimize a class of high performance probes for light and electron microscopy that will, given the availability of a faithful Cre line, enable the integration of multiple subtypes of SPN in cortical and sub-cortical connectivity. In addition to the SP study, these probes can be immensely useful in several areas of biology including high-resolution microscopy including Array Tomography, STORM and immunoEM.

Most labels used for the purpose of discriminating cell populations fall under the general class of protein tags. Protein tags are ubiquitous tools in all areas of biology, where they greatly facilitate the detection and isolation of target proteins and cells from intact tissues and purified samples in a wide variety of applications (Waugh 2005). Although many types of molecular tags exist, the two most commonly used are peptide antigens ('epitopes') (Terpe 2003) and fluorescent proteins (FPs).

Epitope tags (Munro and Pelham 1984)are short antigenic peptide sequences that facilitate immunolabeling with tag-specific antibodies when attached to a protein of interest (POI). The principal advantage of epitope tags is the availability of reliable primary monoclonal and polyclonal antibodies, particularly in cases where antibodies to the POI are non-specific, raised in the same species as other targets, or unavailable entirely. Almost all epitope tagging experiments draw upon a small set of validated

peptide antigens (typically mapped from an immunizing antibody), including influenza hemagglutinin (HA)(Field, Nikawa et al. 1988), myelocytomatosis viral oncogene (myc)(Evan, Lewis et al. 1985), simian virus 5-derived epitope (V5)(Southern, Young et al. 1991), the synthetic peptide FLAG (Hopp, Prickett et al. 1988), the synthetic streptavidin-binding strep-tag (Schmidt, Koepke et al. 1996) and more recently OLLAS (*Escherichia coli* OmpF linker and mouse langerin)(Park, Cheong et al. 2008). Because epitope tags are small (typically 8-12 amino acids), they can usually be attached to POIs, even in multiple copies, without overtly affecting protein folding, targeting or protein-protein interactions. Secondary antibodies (anti-Fc antibodies raised in a distinct species) conjugated to a number of detection moieties, including fluorescent dyes and gold particles, allow signal amplification in most sample preparations. However, there are practical limitations to the use of peptide antigens for detection. Most importantly, the affinity of antibodies for small tags can be low; single or even multimeric tags are frequently insufficient for detection when the POI is weakly expressed. Furthermore, peptide epitopes, being weakly structured by themselves, are unable to be stably expressed in cells without fusion to a scaffold protein.

Alternatively, FP tags (Giepmans, Adams et al. 2006) may be used in fusions to visualize POI localization, or expressed alone as cell-filling tracers. *Aequorea victoria* green fluorescent protein (GFP), for example, is soluble, bright, highly stable, and generally well tolerated by cells. As a result, it has been used extensively for imaging experiments in both live and fixed preparations for both protein localization and cell tracing. The existing FP toolkit includes variants across the visible spectrum (Chudakov, Matz et al. 2010). Despite their widespread use, however, native FP tags are not optimal

for many applications. First, the excitation and emission spectra of FPs are broad, making them difficult to use in combinations of more than 2 or 3. Second, low levels of FP expression are often insufficient for high-resolution reconstruction of cellular morphology or protein localization without amplification. As such, FP tags are typically antibody-amplified, despite their intrinsic fluorescence.

Compared to peptide antigens, FPs can offer higher affinity for their corresponding antibodies and live fluorescence before immuno-amplification. However, the use of FPs as antigens has limitations. Over-expression of most coral-derived FPs can result in aggregation and cytotoxicity, while failing to label neurites and other small compartments uniformly. More importantly, many anti-FP antibodies cross-react with related FP probes, severely limiting options for the simultaneous use of multiple FP channels. Also, given the relatively large size of FPs, tagging a POI with multiple FP copies often disrupts the native expression and trafficking of the POI (although there are examples where such tagging is successful, *e.g.* (Yang, Marcello et al. 2006)).

Tracing studies are typically performed *ex vivo* to enhance the field of view, optical access and imaging resolution. However, tissue fixation (*e.g.* chemical cross-linking with paraformaldehyde or glutaraldehyde) often compromises FPs, resulting in the reduction or loss of fluorescence or antigenicity. The recognition of epitopes by antibodies can be similarly damaged by tissue preservation protocols. Preparations for high-resolution microscopy, such as electron microscopy and array tomography (Micheva and Smith 2007), place even greater demands on proteins, often employing secondary fixation with osmium tetroxide (OsO_4), dehydration, resin infiltration and embedding, all of which can greatly reduce the availability and antigenicity of labels. Historically, robust

immunolabeling has come at the expense of poor ultrastructure preservation. Very few studies have demonstrated adequate immunolabeling following fixation with osmium tetroxide (OsO_4) in electron microscopy. Approaches omitting OsO_4 have been developed (Skepper and Powell 2008), but ultrastructure preservation in these preparations is suboptimal.

To overcome the limitations of existing FP and fusion-probe labeling techniques, we sought to develop new molecular tags that combine the advantages of FPs and peptide epitopes. Specifically, an ideal probe should combine the solubility, cell tolerance and optional endogenous fluorescence of FPs (FPs can easily be rendered dark, while retaining their 3-dimensional structure), together with orthogonal antibody recognition and tagging of POIs with multiple epitope copies. Compatibility with heavy fixation protocols was also a key design goal. Here, we describe a new family of extremely antigenic protein tags called 'spaghetti monster' fluorescent proteins (smFPs). smFPs have 10-15 copies of single epitope tags inserted into an FP scaffold with either an intact or darkened chromophore. Engineering peptide epitopes into stable scaffolds resulted in accessible, high-affinity antibody binding. smFP expression is non-toxic and enables visualization of sparsely expressed proteins and sub-cellular structures poorly labeled by conventional FPs. smFPs permit robust, multi-color tracing of neurons, axons and dendrites in multiple independent channels that are easily separated by conventional epifluorescence filter sets. Our modular construct design strategy facilitates further expansion of this toolkit, and a common scaffold helps to normalize tag/tracer expression level, sub-cellular localization and half-life. The smFPs have direct applications in high-resolution light and electron microscopy, including array tomography (AT)(Micheva and

Smith 2007), super-resolution fluorescence imaging (Huang, Bates et al. 2009), immunoEM (Yi, Leunissen et al. 2001), and correlative light and electron microscopy (CLEM)(Sjollema, Schnell et al. 2012). These smFP reagents enable new experiments in neuroscience and other biological fields.

3.1 Specific Aim: Design and validate a set of probes that will complement the existing fluorescent protein-based labels and permit robust multiple labeling of cellular populations.

3.2 RESULTS

3.2.1 Molecular design and in vitro characterization

To Create hyperantigenic tags, we sought protein scaffolds that would accommodate the insertion of numerous peptide tags while retaining their proper folding and cellular trafficking. Tags were designed into the selected scaffolds to optimize their antigenicity and permit simultaneous binding of multiple antibodies. As scaffolds we selected members of the GFP superfamily. GFP is soluble, stable and well tolerated by cells. It has also been shown to accommodate the addition of peptide epitopes to its N- and C-termini or into internal loops (Abedi, Caponigro et al. 1998). 'Superfolder' GFP (sfGFP) is an engineered hyperstable GFP variant (Pedelacq, Cabantous et al. 2006) that accepts large insertions into its loops while retaining folding and fluorescence (Kiss, Fisher et al. 2006). Thus, we reasoned that sfGFP would be an ideal scaffold for antigen engineering.

We chose six epitope tags (HA, myc, V5, FLAG, strep II, OLLAS) primarily based on the commercial availability of high-affinity antibodies and widespread previous use in epitope-tagging applications. Epitopes were inserted in sets of 4 into the internal 172-173 loop of sfGFP (Kiss, Fisher et al. 2006). In addition, 3-4 epitopes were added to each terminus of the sfGFP protein (**Figure 3.1a,b**). For most epitopes, a protein structure of either an antigen/antibody complex or the epitope in its parental immunogenic protein was available. These were used to design linker sequences that would stabilize all inserted epitopes in the antibody-bound conformation and allow simultaneous steric access of antibodies to each (**Appendix. Fig. 3.1**). (We did not test alternative linker sequences for the smFP designs.) Following our initial characterization of the sfGFP-based designs, additional proteins were engineered using the stable red FP mRuby2 (Lam, St-Pierre et al. 2012) and the green FP mWasabi (Ai, Olenych et al. 2008). Insertion sites were designed to be homologous to the 172-173 loop of sfGFP, based on crystal structures of mRuby (Akerboom, Carreras Calderon et al. 2013) and mTFP1 (Ai, Henderson et al. 2006) (**Appendix. Figure3.1**). The sequences of all constructs tested are shown in **Table 3.1**.

Table 3.1 : Summarizes the sequences of all spaghetti monster variants

smFP_FLAG:

MDYKDDDDKGDYKDDDDKGDYKDDDDKGGVSKGEELFTGVVPILVELDGDVNGHKFSVR
GEGEGDATNGKLTLKFICTTGKLPVPWPTLVTTL**GGG**VQCFSRYPDHMKQHDFFKSAMP
EGYVQERTISFKDDGTYKTRAEVKFEGDTLVNRIELKGIDFKEDGNILGHKLEYNFNSH
N
VYITADKQKNGIKANFKIRHNVEGGDYKDDDDKQQDYKDDDDKGQQGDYKDDDDKQQDY
KDDDDKGGDGSVQLADHYQQNTPIGDGPVLLPDNHYLSTQSVLSKDPNEKRDHMVLLEF
VTAAGITLGMDELYKGGDYKDDDDKGDYKDDDDKGDYKDDDDK.

smFP_myc:

MEQKLISEEDLAEQKLISEEDLAEQKLISEEDLAGVSKGEELFTGVVPILVELDGDVNG
HKFSVRGEGEGDATNGKLTLKFICTTGKLPVPWPTLVTTL**GGG**VQCFSRYPDHMKQHDF
FKSAMPEGYVQERTISFKDDGTYKTRAEVKFEGDTLVNRIELKGIDFKEDGNILGHKLE
YNFNSHNVYITADKQKNGIKANFKIRHNVEGGAEQKLISEEDLAAEQKLISEEDLGGGG
EQKLISEEDLAAEQKLISEEDLAGGDGSVQLADHYQQNTPIGDGPVLLPDNHYLSTQSV
LSKDPNEKRDHMVLLEFVTAAGITLGMDELYKGAEQKLISEEDLAEQKLISEEDLAEQK
LISEEDL.

smFP_HA:

MYPYDVPDYAGYPYDVPDYAGYPYDVPDYAGGVSKGEELFTGVVPILVELDGDVNGHKF
SVRGEGEGDATNGKLTLKFICTTGKLPVPWPTLVTTL**GGG**VQCFSRYPDHMKQHDFFKS
AMPEGYVQERTISFKDDGTYKTRAEVKFEGDTLVNRIELKGIDFKEDGNILGHKLEYNF
NSHNVYITADKQKNGIKANFKIRHNVEGGYPYDVPDYAGGYPYDVPDYAGGGGYPYDVP
DYAGGYPYDVPDYAGGDGSVQLADHYQQNTPIGDGPVLLPDNHYLSTQSVLSKDPNEKR
DHMVLLEFVTAAGITLGMDELYKGGYPYDVPDYAGYPYDVPDYAGYPYDVPDYA.

smFP_V5:

MGKPIPNPLLGLDSTQQQGKPIPNPLLGLDSTQQQGKPIPNPLLGLDSTGQGVSKGEEL
FTGVVPILVELDGDVNGHKFSVRGEGEGDATNGKLTLKFICTTGKLPVPWPTLVTTL**GG**
GVQCFSRYPDHMKQHDFFKSAMPEGYVQERTISFKDDGTYKTRAEVKFEGDTLVNRIEL
KGIDFKEDGNILGHKLEYNFNSHNVYITADKQKNGIKANFKIRHNVEGGGKPIPNPLLG
LDSTQQQGKPIPNPLLGLDSTGGQQGGGKPIPNPLLGLDSTQQQGKPIPNPLLGLDSTG
GDGSVQLADHYQQNTPIGDGPVLLPDNHYLSTQSVLSKDPNEKRDHMVLLEFVTAAGIT
LGMDELYKGQGGKPIPNPLLGLDSTQQQGKPIPNPLLGLDSTQQQGKPIPNPLLGLDST
.

smFP_strep:

MWSHPQFEKQGQWSHPQFEKQGQWSHPQFEKQGQWSHPQFEKGQGSVSKGEELFTGVVP
ILVELDGDVNGHKFSVRGEGEGDATNGKLTLKFICTTGKLPVPWPTLVTTL**GGG**VQCFS
RYPDHMKQHDFFKSAMPEGYVQERTISFKDDGTYKTRAEVKFEGDTLVNRIELKGIDFK
EDGNILGHKLEYNFNSHNVYITADKQKNGIKANFKIRHNVEGGSWSHPQFEKGGGWSHP
QFEKGGQQGGWSHPQFEKGGGWSHPQFEKSGGDGSVQLADHYQQNTPIGDGPVLLPDNH
YLSTQSVLSKDPNEKRDHMVLLEFVTAAGITLGMDELYKSGQGWSHPQFEKQGQWSHPQ
FEKQGQWSHPQFEKQGQWSHPQFEK.

smFP_OLLAS

MSGFANELGPRLMGKQQQSGFANELGPRLMGKQQQSGFANELGPRLMGKGQGVSKGEEL
FTGVVPILVELDGDVNGHKFSVRGEGEGDATNGKLTLKFICTTGKLPVPWPTLVTTL**GG**
GVQCFSRYPDHMKQHDFFKSAMPEGYVQERTISFKDDGTYKTRAEVKFEGDTLVNRIEL
KGIDFKEDGNILGHKLEYNFNSHNVYITADKQKNGIKANFKIRHNVEGGSGFANELGPR
LMGKQQQSGFANELGPRLMGKGGQQGGSGFANELGPRLMGKQQQSGFANELGPRLMGKG
GDGSVQLADHYQQNTPIGDGPVLLPDNHYLSTQSVLSKDPNEKRDHMVLLEFVTAAGIT
LGMDELYKGQGSGFANELGPRLMGKQQQSGFANELGPRLMGKQQQSGFANELGPRLMGK
.

mRuby2_FLAG:

MDYKDDDDKGDYKDDDDKGDYKDDDDKGGNSLIKENMRMKVVMEGSVNGHQFKCTGEGE
GNPYMGTQTMRIKVIEGGPLPFAFDILATSF**GGG**SRTFIKYPKGIPDFFKQSFPEGFTW
ERVTRYEDGGVVTVMQDTSLEDGCLVYHVQVRGVNFPSNGPVMQKKTKGWEPNTEMMYP
ADGGLRGYTHMALKVDGGDYKDDDDKQQDYKDDDDKGQQGDYKDDDDKQQDYKDDDDKG
GGHLSCSFVTTYRSKKTVGNIKMPGIHAVDHRLERLEESDNEMFVVQREHAVAKFAGLG
GGGGDYKDDDDKGDYKDDDDKGDYKDDDDK.

mRuby2_OLLAS:

MGSGFANELGPRLMGKQQQSGFANELGPRLMGKQQQSGFANELGPRLMGKGQGNSLIKE
NMRMKVVMEGSVNGHQFKCTGEGEGNPYMGTQTMRIKVIEGGPLPFAFDILATSF**GGG**S
RTFIKYPKGIPDFFKQSFPEGFTWERVTRYEDGGVVTVMQDTSLEDGCLVYHVQVRGVN
FPSNGPVMQKKTKGWEPNTEMMYPADGGLRGYTHMALKVDGGSGFANELGPRLMGKQQQ
SGFANELGPRLMGKQQQSGFANELGPRLMGKGGQQGGSGFANELGPRLMGKQQQSGFAN
ELGPRLMGKQQQSGFANELGPRLMGKGGGHLSCSFVTTYRSKKTVGNIKMPGIHAVDHR
LERLEESDNEMFVVQREHAVAKFAGLGGGGQGSGFANELGPRLMGKQQQSGFANELGPRL
MGKQQQSGFANELGPRLMGK.

mWasabi_FLAG

MDYKDDDDKGDYKDDDDKGDYKDDDDKGGDYKDDDDKGGVSKGEETTMGVIKPDMKIKL
KMEGNVNGHAFVIEGEGEGKPYDGTNTINLEVKEGAPLPFSYDILTTAF**GGG**NRAFTKY
PDDIPNYFKQSFPEGYSWERTMTFEDKGIVKVKSDISMEEDSFIYEIHLKGENFPPNGP
VMQKETTGWDASTERMYVRDGVLKGDVKMKLLLEGGDYKDDDDKQQDYKDDDDKGQQGD
YKDDDDKQQDYKDDDDKGGGHHRVDFKTIYRAKKAVKLPDYHFVDHRIEILNHDKDYNK
VTVYEIAVARNSTDGMDELYKGGDYKDDDDKGDYKDDDDKGDYKDDDDK.

Sequences shown are for the ‘dark’ (chromophore mutated to Gly-Gly-Gly; bold) smFP versions. To preserve FP fluorescence, chromophores are left intact: **TYG for sfGFP**, **MYG for mRuby2**, and **SYG for mWasabi**.

Initial tests in *Drosophila* showed that all six FPs were recognized by their corresponding antibodies, and five (HA, V5, FLAG, myc, OLLAS) were selected for further use based on robust labeling of neuronal processes and absence of apparent toxicity to cells. To extend these results to mammalian cells, for each antigen, we tested up to 5 commercially available primary antibodies for specific binding in cultured cells using immunocytochemistry. Those with the highest labeling and lowest background were selected for further experiments (**Table 3.2**).

Fluorescence correlation spectroscopy was used to quantify the number of antibodies bound to smFPs in solution, based on the change in diffusion properties with increasing molecular weight of the smFP-antibody complex. In this experiment, the FLAG epitope-based smFP containing 10 FLAG peptides and an intact, fluorescent GFP chromophore ('smFP_FLAG_bright') was expressed in bacteria, purified, and titrated with either monoclonal IgG anti-GFP or monoclonal IgG anti-FLAG primary antibody. Then, the diffusion time (τ_D) of the GFP chromophore of smFP_FLAG_bright was determined (**Figure3. 1c,d**). Titration with the monoclonal anti-GFP antibody yielded a τ_D of 0.57 ± 0.02 msec (std. dev., n = 5), consistent with a single binding event with a K_d < 10 nM. (K_d accuracy is limited to the smFP concentration, which was 10 nM in these experiments. See **Methods** for details.) Titration with the anti-FLAG antibody M2 against 10 nM smFP_FLAG_bright yielded a τ_D of 1.31 ± 0.04 msec (n = 5), with saturation occurring at 100 nM antibody, consistent with the 100 nM concentration of epitopes (**Fig. figure3.1d**). This measured value of τ_D corresponds to a molecular weight of 1700 kD, consistent with 11.3 ± 1 bound anti-FLAG antibodies, based on a calibration series (**Figure 3.1c**), where τ_D scales as (complex MW)$^{0.39}$ and assuming an individual

antibody MW of 150 kD. A similar conclusion about the number of bound antibodies was found when the 10xFLAG smFP was replaced by the 3xFLAG version (**Figure 3. 1d**), where the bound antibody number was determined to be 3.4 ± 0.3. Thus, the smFP format displays FLAG epitopes with full M2 antibody accessibility and high affinity. We suggest that similar simultaneous binding of multiple antibodies also underlies the excellent performance of other smFP/antibody combinations (see below).

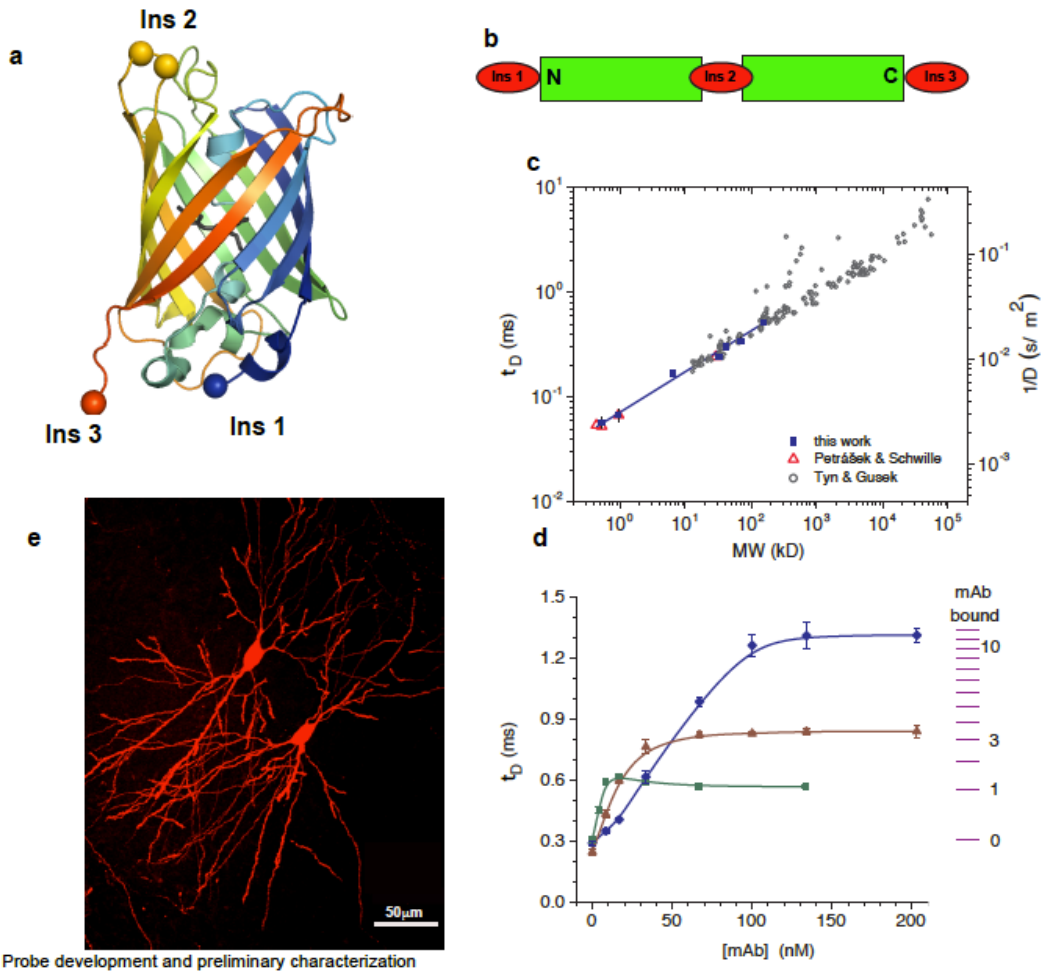

Figure 3.1: Probe development and preliminary characterization

a) Schematic of modular smFP construction. sfGFP shown in cartoon; chromophore either left intact or rendered invisible (grey). Epitope tags are inserted at the N (blue sphere) and C (red) termini and into a loop (yellow). b) Schematic of the primary structure with epitope insertion sites shown. c-e) Fluorescence correlation spectroscopy (FCS) measurements to quantify antibody binding to FLAG epitopes of smFP, based on changes in diffusion with molecular weight. c) Calibration of solution-phase diffusion time⊠⊠D and diffusion coefficient D versus molecular weight (MW) measured by FCS. Molecular weight markers ( ) were: hydrolyzed Alexa 488, 534 D; hydrolyzed Alexa 546, 963 D; epidermal growth factor (EGF)-FITC, 6.5 kD; eGFP, 32.7 kD; smFP_FLAG_bright, 42.3 kD; bovine serum albumin (BSA)-Alexa 488, 69 kD; anti-FLAG M2-FITC, 153 kD. n = 5 experimental replicates; mean ± SD shown.

Data was fit ( ) to a power-law:⊠⊠D = (0.0718 ± 0.0058) × MW(0.389±0.019) (± SEM, R2 = 0.99) with⊠⊠D in msec and MW in kD.

Diffusion time⊠ and diffusion coefficient (plotted as 1/D on right-hand scale) are related by D = wo2 / 8⊠⊠D, where wo is the e-2 laser-beam radiu here wo = 430 nm at 940 nm excitation. Also shown are literature values of protein diffusion coefficients compiled by Tyn & Gusek (1990) ( ), and dyes and proteins measured using scanning FCS by Petrášek & Schwille (2008) ( ). d) FCS-determined diffusion times of 10 nM smFP_FLAG_bright (with 10 FLAG copies per protein yielding 100 nM of FLAG epitopes) titrated with monoclonal antibodies against GFP (; Invitrogen rabbit monoclonal) or FLAG (; Sigma M2), which shows saturated binding above 100 nM antibody; and 10 nM smFP_3xFLAG_bright (30 nM epitopes) with anti-FLAG antibody (; Sigma M2), which shows saturated binding above 30 nM antibody. n = 5 experimental replicates for titrations; mean ± SD shown. Ladder at right is the calculated number of antibodies (assuming a MW of 150 kD per antibody) bound to smFP (42.3 kD) for the corresponding ⊠D, based on the calibration obtained in c). e) Expression of smFPs in mouse brain slice. Mouse embryos were electroporated with smFP_myc, harvested at P14 and stained for myc and detected with a secondary antibody conjugated to Alexa 568. Image was acquired on a Zeiss 510 confocal microscope and contrast adjusted in Image J.

3.2.2 Robust visualization of cells, neurons, and sub-cellular structures

To determine if smFPs express well in mammalian cells, HeLa cells were transfected with individual smFP constructs. After 24-48 hours, the cells were fixed and visualized by immunocytochemistry. All constructs expressed well with no obvious signs of cytotoxicity or aggregation (**Appendix. Figure. 3.2**). To investigate neuronal expression, smFPs were first transfected into primary rat hippocampal neurons in various combinations, where they were robustly expressed. Subsequently, the probes were delivered to cortical and hippocampal pyramidal cells by *in utero* electroporation (IUE) or adeno-associated virus (AAV) infection in mouse brain (**Figure. 3.3a, Appendix Figure 3.3a,b**). Both smFP_FLAG (red) and smFP_myc (green) labeled axons, dendrites, and spines in the mouse brain (**Figure 3.3a, Appendix Figure 3.3a,b**), providing excellent filling and traceability. Label density and sub-cellular localization were essentially identical for all smFP probes tested.

Given that smFPs contain multiple, high affinity binding sites for common primary antibodies, it is possible that smFPs will label fine neuronal structures at lower concentrations than GFP. To test this idea, limiting concentrations of plasmids (~0.5 µl of 0.25 µg/µl = 0.125 µg per brain) encoding either eGFP or smFP_FLAG were electroporated into hippocampi of E15.5 mouse embryos. 3 weeks later, at postnatal day 14, mice were perfused and 100 µm vibratome sections were immunostained with primary monoclonal antibodies against GFP or FLAG. Then, all sections were treated with secondary antibodies conjugated with Alexa 488 and imaged under identical conditions. In area CA1, although GFP appeared similar or slightly brighter in somata, neuronal processes were brighter and more completely labeled with smFP_FLAG as

compared to GFP (**Figure 3.3b,c,e,f**). In particular, basal dendrites in the *stratum oriens*, the most distal dendrites in the *stratum lacunosum moleculare* and spines were better resolved with smFP_FLAG than GFP (**Figure 3.3d,g**).

Among the dendritic arborizations of hippocampal CA3 pyramidal neurons are 'thorny excrescence' (TE) spines, the post-synaptic target structures of dentate gyrus mossy fiber axons. These multi-headed spines were first observed by Cajal from sparse Golgi silver staining (Ramon y Cajal 1952), and later by electron microscopy (Amaral and Dent 1981, Chicurel and Harris 1992). These spines are unique in that they posses multiple spine heads called 'thorns' in various shapes and sizes, all arising from a single dendritic site (Amaral and Dent 1981, Chicurel and Harris 1992). Fluorescent visualization of individual thorns has historically proven problematic, typically requiring the injection of a fixable small molecule dye (*e.g.* Lucifer Yellow) through a patch pipette, with subsequent immunohistochemical amplification (Williams, Wilke et al. 2011). In cases of strong FP over-expression, such as in the YFP-H mouse line, excrescences have sometimes been resolved (McAuliffe, Bronson et al. 2011). However, long-term, high-level FP expression from a very strong mouse line was required, precluding many experiments, including developmental analysis of thorns. Here we demonstrate that even the notoriously difficult-to-label CA3 thorns can be visualized with low levels of genetically encoded smFPs. As before, limiting amounts of DNA (0.125 μg) driving either eGFP or smFP_FLAG were expressed in hippocampal CA3 neurons by *in utero* electroporation and at P14 mice were perfused and brains were immunostained. The complex, multi-headed thorns were much more clearly resolved with smFP_FLAG than GFP (**Figure 3.3h,i**). For comparison, Lucifer Yellow-filled neurons had labeling

density similar to that of smFP_FLAG (**Figure 3.3h-j).** Together, our results suggest that smFP constructs label fine neuronal processes at much lower expression levels than conventional FPs.

3.2.3 Protein labeling

For proteins lacking suitable antibodies, epitope tagging provides a way to reveal sub-cellular distributions. Low-affinity tags are often adequate for detection of highly expressed proteins, but such tags are typically insufficient for proteins expressed in low abundance. In addition, strong exogenous over-expression of tagged proteins can cause mislocalization. Thus, high-affinity tags that provide specific labeling upon low exogenous expression, or from chromosomal knock-in, would be ideal for investigating proteins for which good primary antibodies do not exist. For example, cadherins are a large family of cell adhesion proteins, expressed in many cell types, including neurons (Redies 1995). Due to the high sequence similarity between cadherin family members, anti-cadherin antibodies often recognize multiple species in tissue, precluding unambiguous assignment of localization. N-cadherin (cadherin-2) plays a critical role in gastrulation, axon guidance (Ranscht 2000), synaptogenesis, synaptic plasticity (Bozdagi, Shan et al. 2000), and learning and memory (Arikkath and Reichardt 2008). N-cadherin, which has been shown to localize to post-synaptic structures (Fannon and Colman 1996), is a good candidate for evaluating whether smFP fusion proteins localize correctly and for comparing detection efficiency between smFPs and single-epitope tag fusion proteins. N-cadherin was fused to a standard HA tag or to smFP_HA, and transfected into primary hippocampal neurons. Neurons were also transfected with smFP_myc to label cell bodies

and neurites and to assess transfection efficiency. Neurons were stained with anti-HA (N-cadherin), anti-myc (transfected neurons) and anti-MAP2 (all cells). Cell density, transfection efficiency and smFP_myc labeling were equivalent between the two experiments (**Figure 3.3k,m**), as were all imaging parameters. However, the single HA tag labeled only the most strongly expressing regions (*i.e.* somata) (**Figure 3.3n**), whereas the smFP_HA tag had strong signal throughout somata, axons and dendrites and was overall much brighter than HA (**Figure 3.3l**). Moreover, with smFP_HA labeling, bright punctae of N-cadherin were observed in dendritic spines (**Figure 3.3o,q**), consistent with previous reports. In contrast, much weaker labeling was seen with the single HA tag (**Figure 3.3p,r**).

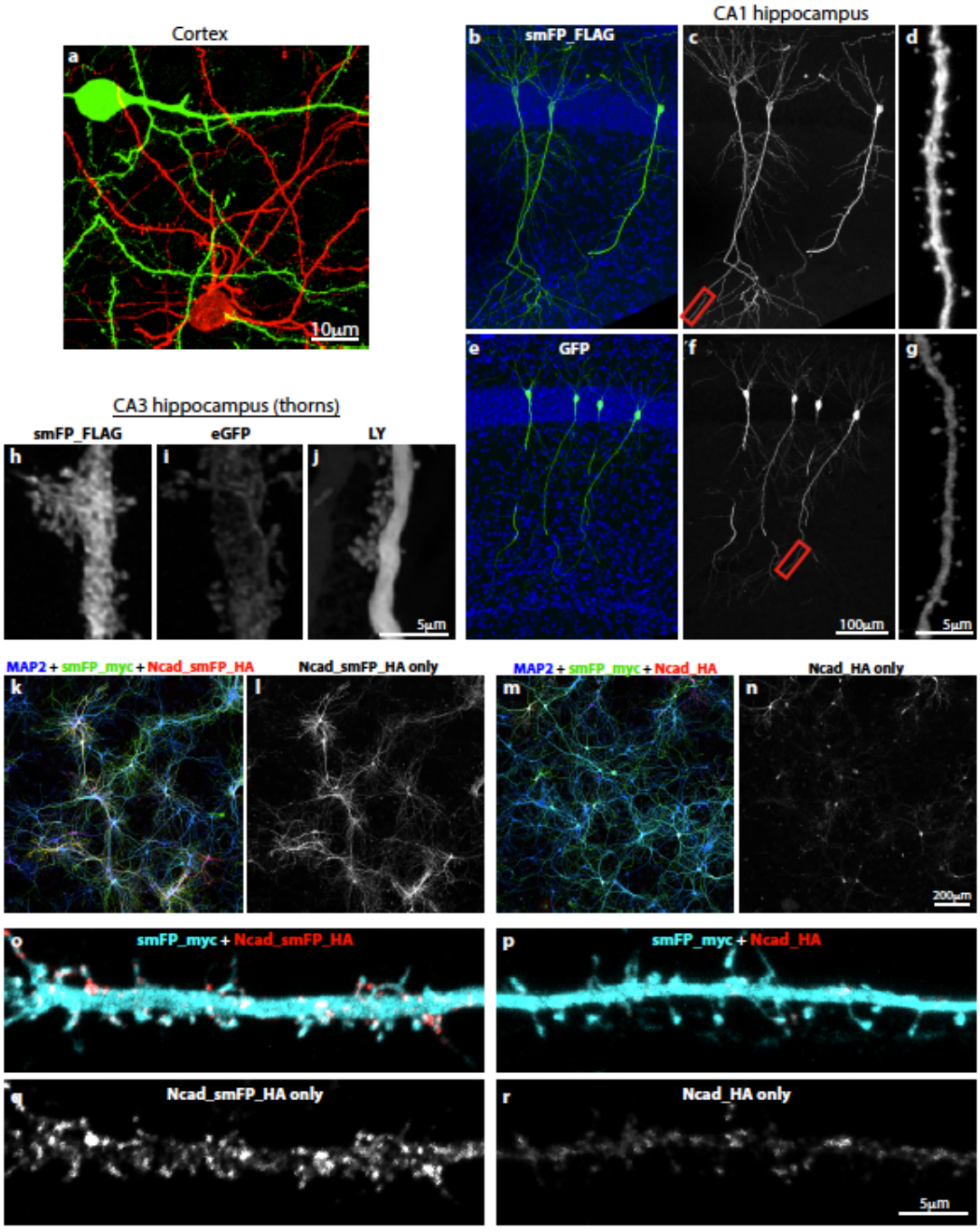

Figure 3.3: Improved labeling efficiency of cells and proteins
a) Brain slice of layer 2/3 cortical neurons co-electroporated with smFP_myc (green) and smFP_FLAG (red) and immunostained at P14. b and e) Fields of view showing sparsely labeled CA1 hippocampal pyramidal cells, from apical dendrites through soma to distal dendrites. c) and f) show the same fields in gray scale. d and g) Zoom of distal dendrite in boxed areas shown in c) and f). All images were taken under identical confocal settings. Blue shows Hoechst nuclear counterstain. h – j) Fills of CA3 "thorns" in P15 mouse brain slice, expressing either smFP_FLAG (h), eGFP (i) or filled with Lucifer Yellow (LY) (j). Samples were amplified with anti-FLAG, anti-GFP or anti-LY primary antibodies and detected with secondary-Alexa 488. k-r) Cultured rat hippocampal neurons (division 14) co-electroporated with smFP_myc and either N-cadherin-smFP_HA (k,l,o,q) or N-cadherin-HA (m,n,p,r). The smFP_myc serves to fill cells and to normalize for expression levels. Neurons were immunostained for microtubule-associated protein 2 (MAP2) to l abel all cells in the field of view. Blue: anti-MAP2 primary + secondary-Alexa 647 (pseudocolored in blue to increase contrast). Green: anti-myc primary + secondary-Alexa 488. Red: anti-HA primary + secondary-Alexa 555. o-r) High-magnification images of single dendrites. o,p: combined imaging channels; q-r: N-cadherin channel alone.

3.2.4 Use as connectomic tracers

The ability to trace fine neuronal processes through the brain is critical to mapping cellular and circuit connectivity. Electron microscopy is considered the 'gold standard' for conclusive identification of synaptic contacts and fluorescence microscopy, in both living and fixed samples, is an important tool for connectomics (Livet, Weissman et al. 2007) (Bohland, Wu et al. 2009, Ragan, Kadiri et al. 2012, Osten and Margrie 2013, Sunkin, Ng et al. 2013). Gaps in label density, however, frequently plague efforts to reconstruct neuronal morphology and even complicate the simpler task of assigning cell bodies to corresponding axons and dendrites. Automated algorithms for light-level reconstruction are particularly affected by such data quality issues (Gillette, Brown et al. 2011, He and Cline 2011, Liu 2011) and attempts to increase fluorescent labeling frequently result in significant background staining that also confounds morphological reconstruction.

GFP is widely used in most tracing studies but provides only a single channel of fluorescence labeling. Red fluorescent proteins (RFPs), which are sufficiently divergent from GFP to facilitate antibody labeling with low cross-reactivity, are typically used as a second color channel. However, RFPs suffer many shortcomings as anatomical tracers. Most notably, many RFP variants, including mCherry (Shaner, Campbell et al. 2004), are cytotoxic, prone to aggregation and do not diffuse readily into fine processes. Furthermore, existing anti-RFP antibodies typically result in both weak enhancement of signal and significant increase in background fluorescence. Other FP superfamily members, such as cyan and blue proteins, suffer similar defects. In short, the current fluorescent protein-based labels pose substantial practical limitations to performing

multiple-labeling experiments. smFPs, with strong label efficacy, robust cell filling, and highly-specific antibodies, could fill this gap and serve as ideal connectomic tracers for tracing experiments requiring several color channels.

We performed a set of experiments to demonstrate the use of smFPs as connectomic tracers, in comparison with published results with the conventional tracer GFP. smFPs were delivered by AAV2/1 into primary mouse vibrissal somatosensory cortex (S1). Opposite hemispheres of adult mice were infected with AAV expressing smFP_myc or smFP_FLAG (**Figure 3.4a,b**). Two weeks later, mice were perfused; brain slices were cut, antibody-stained, and imaged on a high-resolution scanner (Perkin-Elmer Pannoramic 250; **Methods**). Intense cytoplasmic staining was observed at the injection sites, and both smFP channels showed labeling of processes clearly visible in many brain regions. No signs of label aggregation or axonal blebbing were observed. Axonal projections were traced to several cortical and subcortical regions (**Figure 3. 4c-f**; **Appendix figure 3.4**), including secondary somatosensory cortex, whisker motor cortex, striatum, various thalamic nuclei including Vpm, Po and reticular nuclei, entorhinal cortex, ectorhinal cortex and piriform cortex. The projection patterns observed here are consistent with previous tracing studies (Mao, Kusefoglu et al. 2011) and demonstrate that, like GFP, smFPs are excellent long-distance neural tracers. However, unlike GFP, smFPs present the opportunity for multi-color labeling.

To demonstrate the applicability of smFPs for multi-channel tracing, three distinct smFP probes were delivered by AAV to various cortical areas (same hemisphere): smFP_myc to primary vibrissal motor cortex (M1), and smFP_FLAG and smFP_HA to two sites in S1, separated by 800 μm (**Figure3. 4g**). All three probes showed strong

labeling at and near the sites of injection (**Figure 3.4h,i**). Long-distance projections were clearly observed, including to the contralateral cortical hemisphere and to the thalamic nuclei Vpm (from S1; red) and Po (from M1; cyan) (**Figure 3.4j**). Axons individually expressing one of the three colors could be observed converging at the Vpm/Po boundary (**Figure 3.4k-o**).

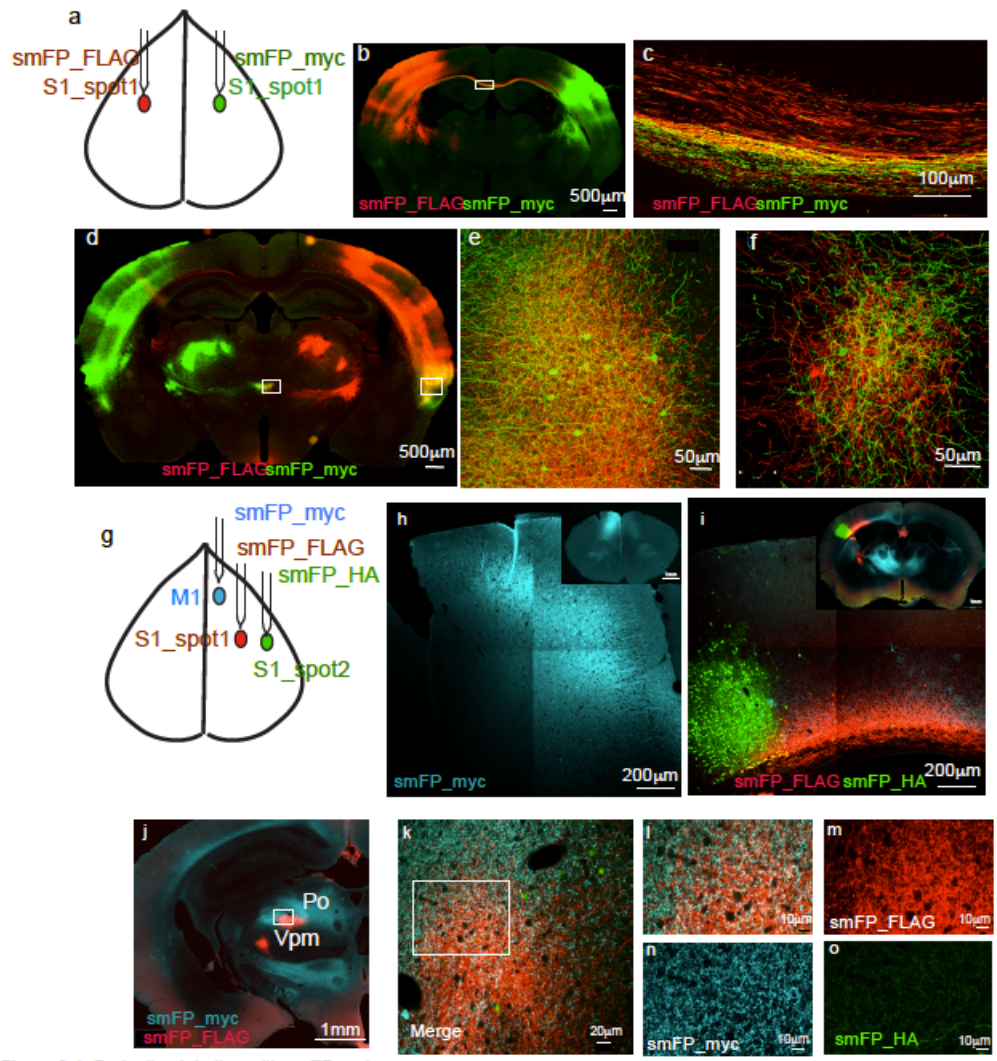

Figure 3.4: Projection labeling with smFP probes
a) Injection schematic. Right hemisphere injected with smFP_FLAG and left hemisphere injected with smFP_myc. smFP_FLAG and smFP_myc are detected with tag specific primary antibodies and corresponding secondary antibodies conjugated with Alexa 488 (myc) and Alexa 594 (FLAG). b) Representative injection site image. c) Confocal image showing a zoomed view of boxed area in panel (b); long-range axonal projections from S1 in both hemispheres crossing the corpus callosum. d) Representative image of the projections from S1 detected by smFPs. Dense axonal projections are seen in S1, S2, entorhinal cortex (e), and reticular thalamus (f). e) High-magnification confocal image of convergent axons in entorhinal cortex (right box in d). Red and green terminals show projections ipsilateral to the smFP_FLAG and contralateral to the smFP_myc injections, respectively. Some somata are marked with smFP_myc, as well. f) High-magnification confocal image of axons in right-hemisphere reticular thalamus (left box in d). Red and green terminals show projections ipsilateral to the smFP_FLAG and contralateral to the smFP_myc injections, respectively. g) Schematic of triple injection. h) Representative image of the injection site in M1; inset shows a representative image of the entire section. i) Representative image of the two injection sites in S1; inset shows a representative image of the entire section. j) Representative image showing thalamic nuclei labeled with all three probes: cyan (smFP_myc), green (smFP_HA), red (smFP_FLAG). k) High-magnification confocal image of boxed region in (j) showing intense label in thalamic nuclei Vpm and Po. l-o) Zoomed confocal images of the boxed region in (k) as composite (l) and in single channel (m,n,o) showing abundant projections from cortical areas. Images were contrast-adjusted in ImageJ.

3.2.5 Variant smFP scaffolds

As discussed above, despite its endogenous fluorescence, GFP is typically antibody-amplified for tracing experiments. The smFPs made on the sfGFP scaffold cross-react with all tested anti-GFP antibodies (**Appendix Figure 3. 5c**), precluding immunostaining for these smFPs alongside GFP. Therefore, we also developed a distinct set of smFPs based on mRuby2 (Lam, St-Pierre et al. 2012) and mWasabi (Ai, Olenych et al. 2008) scaffolds (**Table 3.1**). These classes of smFPs are not detected with anti-GFP antibodies (**Appendix Figure 3. 5 e,h**). When AAVs expressing mRuby2-based smFPs were delivered to hippocampi of mice expressing eGFP, high-efficiency labeling was observed with no cross-reactivity with anti-GFP antibodies (**Appendix Figure. 3.7**). Taken together, the smFP toolbox currently provides up to 6 independent channels for multiple labeling and is expandable through the modular design strategy.

3.2.6 Utility in high-resolution microscopy

The previous results highlight the utility of hyper-antigenic probes for traditional confocal and wide-field microscopy. A number of techniques offer dramatic improvements in imaging resolution, including array tomography (AT) (Micheva and Smith 2007), super-resolution fluorescence imaging such as stochastic optical reconstruction microscopy (STORM) (Huang, Bates et al. 2009), and electron microscopy (EM). To achieve this high resolution, however, these methods require very high label density, which can dramatically limit applications. Furthermore, harsh sample preparation conditions can weaken or destroy antigenicity. To examine the efficacy of smFPs for these higher-resolution imaging applications we tested the smFP antigens

under each of these imaging modalities including Array Tomography, STORM and ImmunoEM (Appendix).

3.3 DISCUSSION:

3.3.1 Utility for the general scientific community:

We describe and validate a set of strongly antigenic labels and demonstrate their utility in immunohistochemistry, protein tagging, and light- and electron microscopy-level anatomy experiments. The tags are well tolerated by cells and sufficiently antigenic to facilitate robust labeling at low expression levels with or without secondary antibody amplification. These reagents significantly expand the toolkit of cell-filling anatomical tracers, which is most commonly limited to a single reliable channel (*i.e.* GFP). The smFPs are fully compatible with GFP, tdTomato, and other existing probes in multi-channel labeling and offer superior performance to single-copy epitope fusions.

Multi-channel anatomical tracing is an important approach for understanding function in the context of cellular diversity. Cell type-specific expression of fluorescent labels facilitates assembly of large-scale anatomical atlases of model organism brains and other tissues (*e.g.* the fly brain (Geschwind 2004, Heintz 2004, Heintz 2004, Jenett, Rubin et al. 2012)). Expression from anterograde or retrograde viral tracers enables long-range circuit mapping, critical for understanding the 'meso-scale' connectome (Bohland, Wu et al. 2009, Ragan, Kadiri et al. 2012, Osten and Margrie 2013, Sunkin, Ng et al. 2013). The enhanced staining provided by the smFP labels will be useful for the reconstruction of fine axons, which are typically quite difficult to faithfully follow using

current labeling approaches. Trans-synaptic delivery of the hyper-antigens *via* rabies virus (Wickersham, Lyon et al. 2007, Wall, Wickersham et al. 2010) should permit robust labeling of functional synaptic connectivity. Most importantly, the existence of 6 (or more) viable, orthogonal labels provided by the smFP platform greatly increases the capabilities of all such methods.

Stochastic expression of the probes within neuronal populations *via* microbial recombinases Creates 'Brainbow'-like (Livet, Weissman et al. 2007) labeling with several important advantages. First, the large number of distinct smFP antigens, each with strong labeling from primary antibodies, provides combinatorial complexity. Second, as the antigen/antibody binding profiles are orthogonal and small molecule dye excitation/emission spectra are narrow, the smFP label channels are easily separable; this is a significant advantage over the conventional FPs used in Brainbow, which give rise to notorious difficulties in differentiating spectral mixtures (Livet, Weissman et al. 2007). Additionally, the AutoBow system (Cai, Cohen et al. 2013) leaves endogenous fluorescence of Cerulean and mKate2 intact, which may pollute immunofluorescence channels. Lastly, smFP variants based on a single FP scaffold exhibit similar sub-cellular distribution within individual neurons, a critical point for proper segmentation of co-expressing cells.

smFP staining revealed the complex sub-cellular morphology of multi-headed thorny excrescence spines, with quality superior to GFP and equivalent to the pipette-loaded small molecule dye Lucifer Yellow. At limiting probe expression levels, as often occurs following an internal ribosome entry site (IRES) sequence or in multi-cistronic cassettes, the smFP labels may prove better than GFP for the visualization of small

structures such as these. Furthermore, the smFP labels enable visualization of fused proteins with greater fidelity and sensitivity than that provided by existing tags. Fusion of the antigens to POIs, expressed as transgenes or driven from virus, and especially proteins expressed at their endogenous levels, are often at too low a level to be observed from GFP fusions. Robust multi-channel tagging facilitates experiments to visualize protein co-localization.

The strong performance of the smFP labels in high-resolution microscopy such as array tomography, super-resolution fluorescence imaging, and immunoEM is significant for experiments relying on these imaging modalities. Few antigens perform well in resin-embedded conditions and most samples exhibit significant decreases in antigenicity following aldehyde cross-linking. Moreover, until development of smFPs, very few existing labels survived osmium fixation. The high thermodynamic stability and epitope avidity of the smFP labels appear to promote resistance to such harsh fixatives and resins, providing a wide array of cell tracers and protein tags for these advanced preparations. Some smFP labels survive 1% OsO_4 fixation, allowing immunoEM with strong ultrastructure preservation. The immunoEM staining observed with the smFPs shows high label density that fills fine neuronal processes in their entirety with low background, facilitating the tracing of thin neurites through serial TEM image stacks. High-affinity commercial anti-epitope antibodies resulted in high signal-to-noise ratio, and their high specificity to individual tags allowed specific labeling of multiple targets with different gold particle sizes. The availability of at least six different types of probes with optimized commercial antibodies will enable mapping of cell type-specific connectivity in different preparations. The option of leaving the smFP fluorescence intact

will facilitate correlative light and electron microscopic (CLEM) studies. At the light level, labeling efficiency from three distinct smFPs, with all color channels tested, was sufficient to trace fine axonal processes across multiple physical sections. Such versatility is particularly useful for AT, where weakly expressed synaptic proteins generally require the brightest fluorophores for adequate detection. Furthermore, combinatorial super-epitope labeling could make it possible to trace connectivity of many cells simultaneously at high resolution.

The success of the smFPs in the experiments shown here validates the design strategy. Strikingly, biophysical characterization showed that smFP_FLAG bound the maximum possible number of IgG antibodies with no evidence of steric occlusion. Similar avidity would not be expected from very long linear epitope repeats, which are susceptible to hydrolytic cleavage and aggregation. The fluorescent protein backbone renders the antigens readily expressed and diffusible in cells, as evidenced by their penetration into long, thin structures like axons and spines. The modular nature of the design strategy and the compatibility with diverse FP scaffolds implies that the toolkit may be systematically expanded. Several FP scaffolds make the super-antigens orthogonal to anti-GFP antibodies, adding an additional imaging channel. Rendering FP chromophores invisible, while preserving folding and stability, preserves spectral bandwidth for small molecule dyes. Alternatively, keeping FP chromophores intact permits the use of the labels in live imaging followed by *post hoc* immunohistochemistry as is needed to locate small, labeled regions for EM reconstruction.

3.3.2 Utility for SP study and further experiments: The study of SPN neuroanatomy would greatly benefit from these probes in the following ways:

a) *Brainbow*

The 'Brainbow' technique involves the stochastic expression of 3-4 FPs to generate cytoplasmic color hues for tracing neurons and their processes (Livet, Weissman et al. 2007) (Cai, Cohen et al. 2013). Following its initial development in mouse, versions have been deployed in fly (Hampel, Chung et al. 2011) (Hadjieconomou, Rotkopf et al. 2011) and fish (Pan, Livet et al. 2011). In theory, the method could discriminate >10 different colors of neurons based on expression levels of each FP (Livet, Weissman et al. 2007). However, the method has limitations that have hindered its widespread use. Endogenous FP fluorescence shows broad excitation and emission spectra that result in cross-contamination of color channels when imaging complex FP mixtures. Additionally, many FPs do not traffic well in neuronal processes and the unamplified FP signal is typically insufficient for neurite tracing, as discussed above. For these reasons, recent Brainbow versions have incorporated antibody amplification (Hampel, Chung et al. 2011, Cai, Cohen et al. 2013), which effectively restricts imaging to fixed samples (although endogenous expression of fluorescent affinity reagents is possible (Gross, Junge et al. 2013)) but greatly increases signal and cuts down bleed-through owing to the sharper fluorescence spectra of small molecule dyes compared to FPs. Accordingly, this extensive set of reagents will be ideal for multi-color stochastic labeling of SPN and tracing out fine projections to different cortical and sub-cortical areas.

b) Tracing fine projections from multiple subtypes of active and remnant SPN. We have already shown that smFPs perform under conditions of limiting protein

concentrations. During development SPN form an active component of connectivity, while not much is known about remnant SPN. In Chapter 2, we identified at least 2-3 promoters (Cplx3, Nxph4, Abdh4) as short regulatory elements capable of driving expression in the SP. Expressing three different smFPs off these promoters using AAV viral vectors *in utero* or post-natally might label multiple subtypes. While these experiments can theoretically be performed using traditional FPs (such as tdTomato or BFP), the smFP probes show superior performance. More sensitive detection with spectral separation might allow unambiguous tracing of fine projections to different cell types.

c) High resolution microscopy: As a follow up to the light microscopic studies above, high-resolution microscopy will unambiguously validate the connections and might also help quantifying connections (Array Tomography, ImmunoEM). An example of this would be quantifying the connections made by Cplx3 positive SPN.

3.4 MATERIALS & METHODS:

Molecular Biology

DNA encoding smFPs were ordered from DNA2.0. Genes encoding smFPs were sub-cloned into pRSETa (Life Technologies) for protein expression and purification in *Escherichia coli* BL21 (this adds an N-terminal His tag for purification, and increases the MW by 4 kD). Genes encoding smFP variants were sub-cloned into the pCAGGS vector with a *CAG* promoter (*CMV* enhancer, b-actin promoter and regulatory element from the woodchuck hepatitis virus (WPRE)(Gray, Weimer et al. 2006) for expression in HeLa cells and *in utero* electroporation (Saito and Nakatsuji 2001, Tabata and Nakajima 2001).

For expression in flies, *R59A05*-GAL4 (Pfeiffer, Jenett et al. 2008)was used to drive expression of UAS-smFP reporter constructs. Detailed fly constructs will be described elsewhere (Nern *et al.*, in preparation). For expression in mice, GFP and smFP variants were expressed using an adeno-associated virus 2/1 (AAV2/1) driving the probe under control of the human *synapsin-1* promoter or a Cre-dependent (FLEX) version of the *CAG* promoter; live virus was produced (JFRC Viral Vector Core). All constructs were verified by sequencing.

Cell and neuronal cultures

Cells were obtained from the American Type Culture Collection (ATCC) and cultured according to their protocol. smFP variants were transfected using an Amaxa (Lonza) Nucleofector 96w shuttle device. 7e05 live HeLa cells were transfected with 1 μg DNA per shuttle well and plated onto two 35mm MatTek plates. Cells were immunostained 24 – 48 hrs post transfection. Primary hippocampal neurons were obtained from P0 rat pups by dissection, dissociated with papain and plated onto coverslips coated with Poly – D-Lysine (PDL) at a density of 80-100,000 per coverslip and cultured in NBActiv4 medium (BrainBits LLC).

Fluorescence correlation spectroscopy (FCS)

The number of antibodies bound to smFP was found from solution measurements of diffusion time of antibody-bound smFP_FLAG_bright using two-photon FCS. Calibration of diffusion time versus molecular weight was obtained using the following markers: hydrolyzed Alexa 488, 534 D (A-20000, Invitrogen); hydrolyzed Alexa 546,

963 D (A-20002, Invitrogen); epidermal growth factor (EGF)-FITC, 6.5 kD (E-3478, Invitrogen); RSET-eGFP, 32.7 kD (4999-100 Biovision); RSET-smFP_FLAG_bright, 42.3 kD; bovine serum albumin (BSA)-Alexa488, 69 kD (A13100, Invitrogen); anti-FLAG mAb-FITC, 153 kD. Protein solutions were prepared in PBS buffer containing 0.2 mg/ml BSA. For antibody titrations, unlabeled anti-FLAG and anti-GFP antibodies were purchased (**Table 3.1**), and their concentrations were based on manufacturers' mg/ml specifications. Both smFP_FLAG_bright (10 FLAG epitopes) and smFP_FLAG_bright_3x (3 FLAG epitopes at the C-terminus) were used at 10 nM protein concentration for the titration, yielding 100 nM and 30 nM of FLAG binding sites, respectively. Antibody-antigen solutions were incubated 30 minutes before measurements, then pipetted into coverslip-bottom dishes (MatTech) that had been pre-treated with 0.2 mg/ml BSA in PBS for 5 min, rinsed and dried, to block the surface. All measurements were taken at 25 ^{o}C on an inverted microscope (IX-81; Olympus) with a 1.2 NA water-immersion objective. Focused laser excitation at the sample was 2 mW of 940 nm light from a Ti:sapphire laser (Chameleon Ultra II; Coherent), characterized by a beam radius w_o of 430 nm at the focus. Details of the experimental setup and methods are described elsewhere (Mutze, Iyer et al. 2012). The diffusion time was found by fitting the fluorescence autocorrelation data to a diffusion model using a custom fitting program (Vijay Iyer, Janelia Farm) running on Matlab (Mathworks). The calibration of diffusion time versus molecular weight was obtained from fitting performed in OriginPro 8 (OriginLab Corp.; Northampton, MA). Diffusion coefficients D were related to diffusion times τ_D by $D = w_o^2/8\tau_D$, where the beam radius w_o is given above.

In utero electroporation

All procedures were performed according to the guidelines set by the Institutional Animal Care and Use Committees and Institutional Biosafety Committees of the University of Utah and HHMI Janelia Farm. Pregnant mothers (pups E14-E18) were deeply anesthetized with isoflurane (2%). The uterine horns were exposed and plasmid DNA (0.5 μl of ~5 μg/μl for most experiments; 0.5 μl of ~0.25 μg/μl for limiting expression) (EndoQ-prepped DNA mixed with 0.03% Fast Green dye in phosphate buffer), injected into the ventricle of 3-4 embryos through a micropipette (~0.1 μl per embryo) and electroporated using custom forceps electrodes (5 pulses, 100 ms, 40 V each).

Immunohistochemistry

Mice were perfused with 4% PFA and post fixed for 2 hours at room temperature. Brains were rinsed in 1X PBS (3x 15 mins) and 50 μm thick coronal sections were cut on a vibratome. Sections were blocked in 3% BSA + 0.3% Triton in PBS for 1- 2 hrs and incubated with primary antibody diluted in block overnight at 4 ^{o}C. Sections were rinsed in 0.3% triton (3x 15 mins) and incubated in secondary antibody diluted in blocking buffer for 2 hrs at room temperature. Sections were rinsed as before, mounted on glass slides and cover-slipped with Vectashield (Vectashield).

Table 3.2 Primary antibodies used in this study:

Epitope	Vendor	Cat. no.	Species	Type	Dilution
V5	ABD Serotech	MCA1360	Ms (mono)	IgG2a	1:250
Myc	Sigma	C3956	Rb	IgG	1:1000
Myc	Sigma	M4439	Ms	IgG1	1:1000
Myc	Novus	NB 600 335	Gt		1:500
HA	Roche	11 867 423 001	Rat (mono) 3F10	IgG1	1:100
FLAG	Sigma	F1804	Ms	IgG1	1:1000

Ms: Mouse, Rb: rabbit, Gt: Goat, Rt: Rat

Intracranial injections

All procedures were performed according to the guidelines set by the Janelia Farm Research Campus Institutional Animal Care and Use Committee and Institutional Biosafety Committee. Animals (adult C57/BL6; either sex) mice were anesthetized under isoflurane and AAV virus encoding smFPs, serotype 2/1 (prepared at JFRC Viral Vector core) was injected with a custom-made volumetric injection system (based on a Narishige MO-10 manipulator). Glass pipettes (Drummond) were pulled and beveled to a sharp tip (30 μm outer diameter), back-filled with mineral oil and front-loaded with viral suspension immediately before injection.

Injection coordinates

Double labeling experiment:

Target	**A-P**	**M-L**	**D-V**	**Construct**
S1 (LH)	-0.59	3	-0.6 and -0.4	AAV_CAG_smFP_myc
S1 (RH)	-0.59	3	-0.6 and -0.4	AAV_CAG_Ruby_FLAG

Triple labeling experiment:

Target	**A-P**	**M-L**	**D-V**	**Construct**
M1	1.1	0.9	0.5-0.8	smFP_myc
S1 a	-0.6	2.8	0.5-0.8	smFP_FLAG
S1 b	-0.6	3.6	0.5-0.8	smFP_HA

All measurements in mm relative to Bregma suture. A-P = anterior-posterior. M-L = medial-lateral. D-V=dorsal-ventral.

ACKNOWLEDGEMENTS:

Data in Figure 3.2 is from Dr. Megan E Williams, University of Utah.

SUPPLEMENTARY INFORMATION

Supplemental information is available in an Appendix.

Chapter 4:

A class of molecularly defined subplate neurons are involved in intra-cortical, thalamo-cortical, and cortico-thalamic circuits

4.0 Introduction:

Subplate neurons (SPNs) are a heterogeneous population of neurons present transiently in the future cortical white matter. They are one of the earliest generated neuronal populations in the cerebral cortex (Kostovic and Rakic 1980) and play critical, distinct roles in the embryonic and postnatal stages of development. SPNs play an instrumental role in the establishment and refinement of early cortical circuits (Kanold and Luhmann 2010). They pioneer the corticofugal (*i.e.* originating in the cortex) (McConnell, Ghosh et al. 1989, McConnell, Ghosh et al. 1994) and corticopetal (*i.e.* terminating in the cortex) (Ghosh, Antonini et al. 1990) pathways and play an essential role in the establishment (Ghosh, Antonini et al. 1990, Ghosh and Shatz 1992) and functional maturation (Kanold and Shatz 2006) of thalamo-cortical connections and intra-cortical inhibitory connections (Kanold, Kara et al. 2003, Kanold and Shatz 2006, Tolner, Sheikh et al. 2012). Large numbers of SPNs undergo programmed cell death (*i.e.* apoptosis) and disappear over development while a certain percentage survives into adulthood to form Layer 6b, subgriseal neurons (Clancy, Silva-Filho et al. 2001, Kanold and Luhmann 2010).

Recent advances in molecular profiling (Hoerder-Suabedissen, Wang et al. 2009, Wang, Oeschger et al. 2011, Hoerder-Suabedissen and Molnar 2013) have revealed a number of subtypes of SPNs with diverse expression patterns. This raises the possibility that different SPN cell types form different sub-circuits, making it very important to

understand the spatio-temporal integration of different SPN subtypes into the circuitry of the developing cortex.

In this study we examined selected SPN cell types based on molecular markers that were spatiotemporally restricted to the subplate and followed their spatial pattern of expression in cortical and subcortical targets. Complexin 3 (Cplx3), a part of the SNARE machinery (Bracher, Kadlec et al. 2002, Chen, Tomchick et al. 2002), was revealed in a genetic screen (Hoerder-Suabedissen, Wang et al. 2009, Hoerder-Suabedissen, Oeschger et al. 2013) as one of the few genes that had a tight spatio-temporal regulation of expression in murine SP over development. Using specific antibodies against Cplx3 we investigated how molecularly defined subpopulations of SPNs are incorporated into intra-cortical and thalamo-cortical circuits (Figure 4.1a). SPNs provide excitatory inputs to L4 (Kanold, Kara et al. 2003, Zhao, Kao et al. 2009). We also wanted to investigate if these projections to layer 4 are oriented in a specific pattern with respect to the thalamic afferents in L4 (Figure 4.1b).

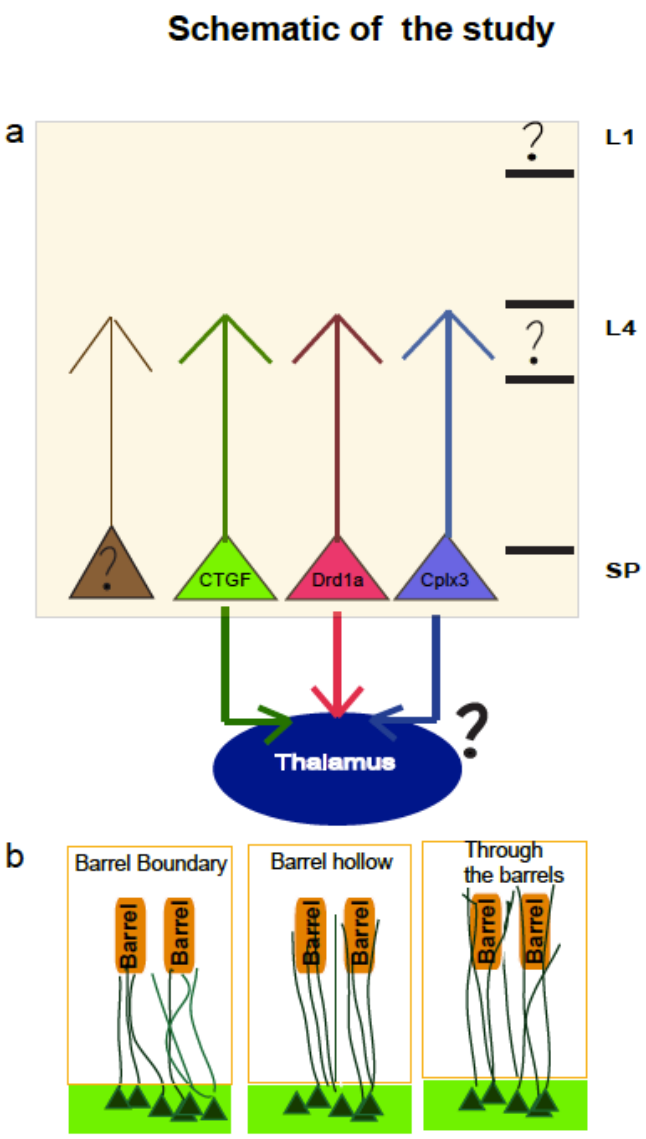

Figure 4.1: Schematic of this study. (a) The goal of this study is to see if different subpopulation subserve different functions in intra cortical and subcortical connectivity. Scematic shows three subtypes analyzed in this study Cplx3, CTGF, Drd1a. We wanted to investigate these subtypes extend projections into the cortical plate. Within the cortical plate, what are the different layers innervated by them. Finally we wanted to investigate if these neurons project locally or extend projections to subcortical targets.
(b) Neurons projecting to layer 4 can have different patterns of projection with respect to the barrel cytoarchitecture. We wanted to study how the axon terminals of the Cplx3 positive Spn project to the cortical with respect to the thalamic afferents.

4.1 Specific Aim:

Different classes of SPNs could serve different functions. Here we investigate the connectivity of molecularly defined classes of SPNs in mouse somatosensory cortex during development.

In our study, we find that Cplx3-expressing SPNs extend projections into cortical layers 1 and 4 in different cortical areas. Moreover, in the barrel field of primary somatosensory cortex (S1), terminals from a particular cell type have a spatial pattern related to the barrel cyto-architecture, reflecting the organization of thalamo-cortical projections. We observe that Cplx3-positive neurons project long distances and extend axon terminals to different thalamic nuclei. This subpopulation is thus engaged in intra-cortical as well as cortico-thalamic circuitry and thus could subserve the instructive feed-forward role (Kanold and Luhmann 2010) as well as a role in feed-back circuits (Viswanathan, Bandyopadhyay et al. 2012). Together our results show that a particular subtype of SPNs engages in different aspects of cortical and subcortical circuitry.

4.2 Results:

To study the integration of the different subpopulations of SPNs into the cortico-cortical and intra-cortical connectivity, we used antibody-mediated protein labeling in wild type mice at postnatal day 9 (P9). We used confocal microscopy to image the integration of neuropil from labeled SP subpopulations into different thalamo-recipient layers.

4.2.1 Cplx3 specifically labels a population of excitatory SPNs in multiple cortical areas:

Cplx3 belongs to a family of proteins that facilitate neurotransmitter release by promoting synaptic vesicle exocytosis (Hu, Carroll et al. 2002, Xue, Stradomska et al. 2008). Recent studies have demonstrated that Cplx3 is highly localized within the subplate, across the entire anterior-posterior extent of the cortex (Hoerder-Suabedissen, Wang et al. 2009, Viswanathan, Bandyopadhyay et al. 2012). We localized the Cplx3 protein using specific antibodies and analyzed the somatic and projection profiles in different cortical areas: primary vibrissal somatosensory (S1), primary vibrissal motor (M1) and primary auditory (A1). Since SPNs play an essential role in the establishment of thalamo-cortical circuitry during the critical period (Kanold and Luhmann 2010), we studied SPNs at a young age (P7 – P9), which corresponds to the critical period in S1. In all cortical areas, Cplx3 localized to axon terminals (likely functional protein) (Figure 4.2e – yellow arrow) and to cell bodies (likely precursor protein in the endoplasmic reticulum) (Figure 4.2e – white arrow). Cplx3 expression was consistently restricted to a subset of subplate neurons in all sensory and motor areas.

The heterogeneity of SPNs extends beyond areal differences. Neurons in the upper and lower SP laminas are differently connected with the cortical plate, presumably due to differences in dendritic morphology (Viswanathan, Bandyopadhyay et al. 2012). Here we find that in A1 and S1, Cplx3-positive SPNs reside both superficially and in deep SP laminas (Figure 4.2a panel a- white and yellow arrowheads), implying this molecularly defined population can have different dendritic morphologies and connectivity. Although we did not carry out a systematic morphological analysis in this

study, we observed that Cplx3 positive neurons exhibited a variety of morphologies such as horizontal and pyramidal (Figure 4.2a b). Being a presynaptic protein, the Cplx3 antibody labeling did not fill the entire neuronal morphology and hence we restricted the study to a qualitative classification. Firstly, we observed significant differences in morphologies between different cortical areas. While Cplx3-positive neurons in rostral areas like vibrissal motor cortex (M1) exhibited a range of morphologies like pyramidal, horizontal and a few neurons that resembled bipolar, neurons residing in caudal areas like primary somatosensory cortex (S1) had a rather uniform horizontal and pyramidal morphology (Figures 4.2c,d). The white arrow in Figure 4.2c points to a bipolar neuron that in our preparations was not observed in caudal areas. Further systematic morphometric studies will be required to validate this, but these observations point to an areal difference in SPN morphology, which might correlate with areal differences in SPN function.

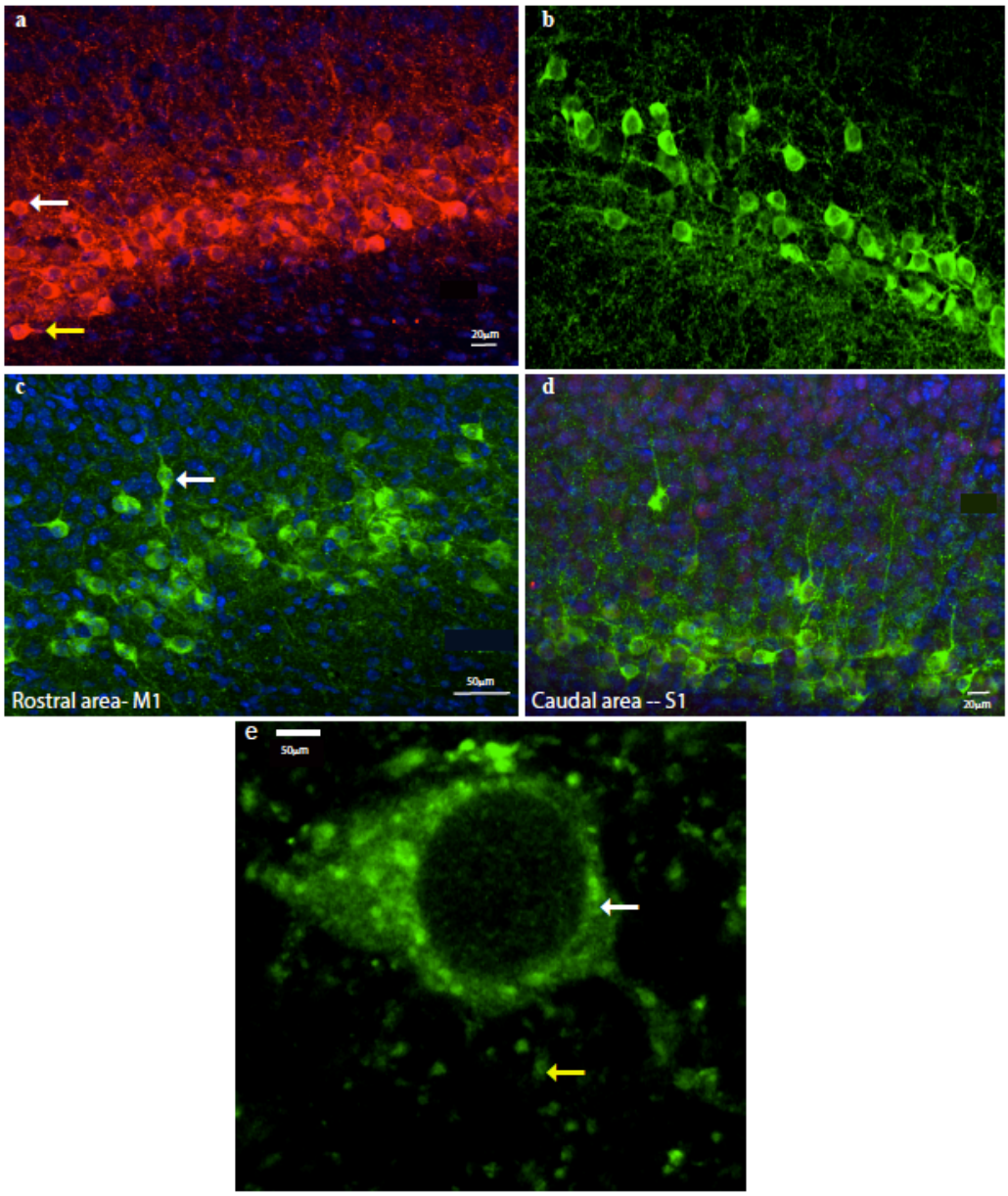

Fig 4.2a Cplx3 positive Spn are a heterogeneous population.
Figure shows images from coronal sections of mouse brain immunolabeled for Cplx3 (green).Panel A shows an example of Cplx3 positive Spn occupying different SP lamina. White arrow points to a neuron residing in upper/superficial SP while yellow arrow shows a neuron in the lower SP lamina. Panel B shows Cplx3 positive Spn in different morphologies. Panel C shows an image of Cplx3 positive neuron in M1 showing diverse morphologies. White arrow shows a bipolar neuron. Panel E shows Cplx3 precursor protein in the cytoplasmic compartment (white arrow), functional protein and terminals (yellow arrow). Panel D shows Cplx3 positive neuron in S1 showing less diversity in morphology than M1. Panel E High magnification image of a cplx3 positive neuron showing the cytosolic and synaptic proteins.

Co-labeling with the neuronal nuclear antigen NeuN shows that the majority of neurons in the subplate are Cplx3-positive (Figure 4.3a,b (M1), d,e (S1), g,h (A1)). Taken together, Cplx3 labels a dense band of neurons above the white matter corresponding to the SP (Hoerder-Suabedissen and Molnar 2013). Moreover our areal comparison shows a

rostral-caudal gradient in the extent of Cplx3 labeling. Labeled neurons form a more compact band in caudal areas like S1 and A1, while expression in M1 is less compact and SP-restricted.

By P7, we find a few Cplx3-expressing neurons in the cortical plate in S1 but not A1 (Figure 4.3f vs 4.3i). This non-specificity, however, is reduced in S1 by adolescence (P14/15) and stabilizes through adulthood (P21). These results indicate that either a small subpopulation of cortical neurons in rostral areas is Cplx3-positive, or that a subpopulation of Cplx3 SPNs is heterotopic and is later eliminated by programmed cell death. Nevertheless, the vast majority of Cplx3-positive somata at any age reside within the subplate lamina.

SPNs are reported to undergo apoptosis at the end of the critical period and a large fraction gets eliminated (Kanold and Luhmann 2010). However we did observe Cplx3-positive SPNs neurons in several cortical areas across the age different groups studied (Figure 3), suggesting that this cell type might represent a distinct population of 'surviving' SPNs (Kanold and Luhmann 2010).

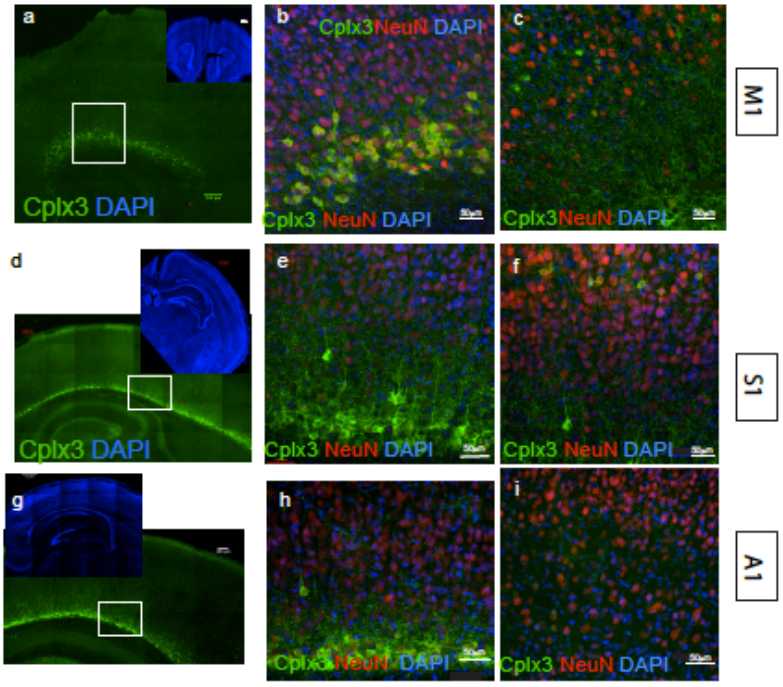

Cplx3 expression in different cortical areas. Figures show the expression of Cplx3 (green) labeled neurons with respect to NeuN (red) and DAPI(Blue) in coronal section from Wild type Mice at P7. In all the images,the left most pannels a,d and g show low power images of the area imaged. Insets in these pannels show a representative image of the entire section imaged. The mid panels b,e and f show expression of Cplx3 (green) positive neurons in the subplate and the right most panels c,f and i show expression in the cortical plate. Panels a-c show expression pattern in primary motor cortex M1. Cplx3 positive neurons form a thick/wide band above the white matter.Diffuse expression in upper cortical plate also seen (c) Panels d-f show expression in primary somatosensoty cortexS1. Similar to M1, Cplx3 positive neurons in S1 show expression in a majority of Sp neurons with some extra SP expression. Panels g-i show expression pattern in primary Auditory cortex A1. SP specific expression in the SP is more compact in A1 when compared to M1 and S1. Expression in upper cortical neurons is also much lower in A1.

4.2.2 Thalamo-recipient layers receive projections from different subclasses of SPNs:

Cplx3 is involved in synaptic vesicle release (Hu, Carroll et al. 2002, Xue, Stradomska et al. 2008) and as such localizes to axons and synaptic terminals. Thus Cplx3 offers a unique tool for the study of axonal projections of Cplx3-positive SPNs. We carried out a systematic analysis of intra-cortical projections of defined SPNs wild type (WT) mice by localizing Cplx3 with specific antibodies in S1. In order to determine the layers to which SPNs project, we localized SPNs projections with respect to thalamic afferents. Thalamic afferents are localized primarily in three different cortical layers- L1, L4 and L6 (Frost and Caviness 1980) and utilize Vesicular Glutamate Transporter 2 (VGLUT2) (Nahmani and Erisir 2005) as the primary vesicular neurotransmitter transporter for thalamo-cortical signaling. As such VGLUT2 serves as a reliable marker to identify thalamic afferents (Nahmani and Erisir 2005) and hence the different cortical layers. In this study, we localized projections from SPNs with respect to the VGLUT2 label from thalamic terminals to determine the cortical layers receiving projections from SPNs.

Upon localizing with respect to VGLUT2 immunoreactivity, we observed a distinct pattern of projections from Cplx3-expressing SPNs throughout the cortical plate. Projections mainly extended to the thalamo-recipient layers L1 and L4. (Figure 4.4a,b,c) in the different cortical areas studied. High-magnification images revealed punctate Cplx3-positive axon terminals and varicosities along with VGLUT2 terminals in L1 (Figure 4.4c). These results are consistent with prior physiological and anatomical studies showing SPN projections to layer 1 (Clancy and Cauller 1999). Since this is one of the

main feedback layers in the neocortex, presence of axon terminals in this layer suggests a role of SPNs in the feed-forward cortical circuit.

L4 is one of the main thalamo-recipient layers in the neocortex (Bannister 2005) and SPNs are essential for the maturation of thalamo-cortical projections to L4 (Kanold, Kara et al. 2003). However the role of the different subclasses in this function remains unknown. Consistent with earlier physiological studies (Zhao, Kao et al. 2009) we observed projections from Cplx3-positive SPNs in L4 at ages corresponding to the critical period. Upon co-localizing with VGLUT2, we observed that most of the projections from Cplx3-positive SPNs were concentrated not within, but rather above and below, the barrels, thus forming a scaffold around the barrel hollow (Figure 4.4d,e,f). Taken together, these results suggest that a molecularly distinct population of SPNs has a spatially distinct pattern of projections with respect to the thalamic afferents and is possibly engaged in different microcircuits than other populations.

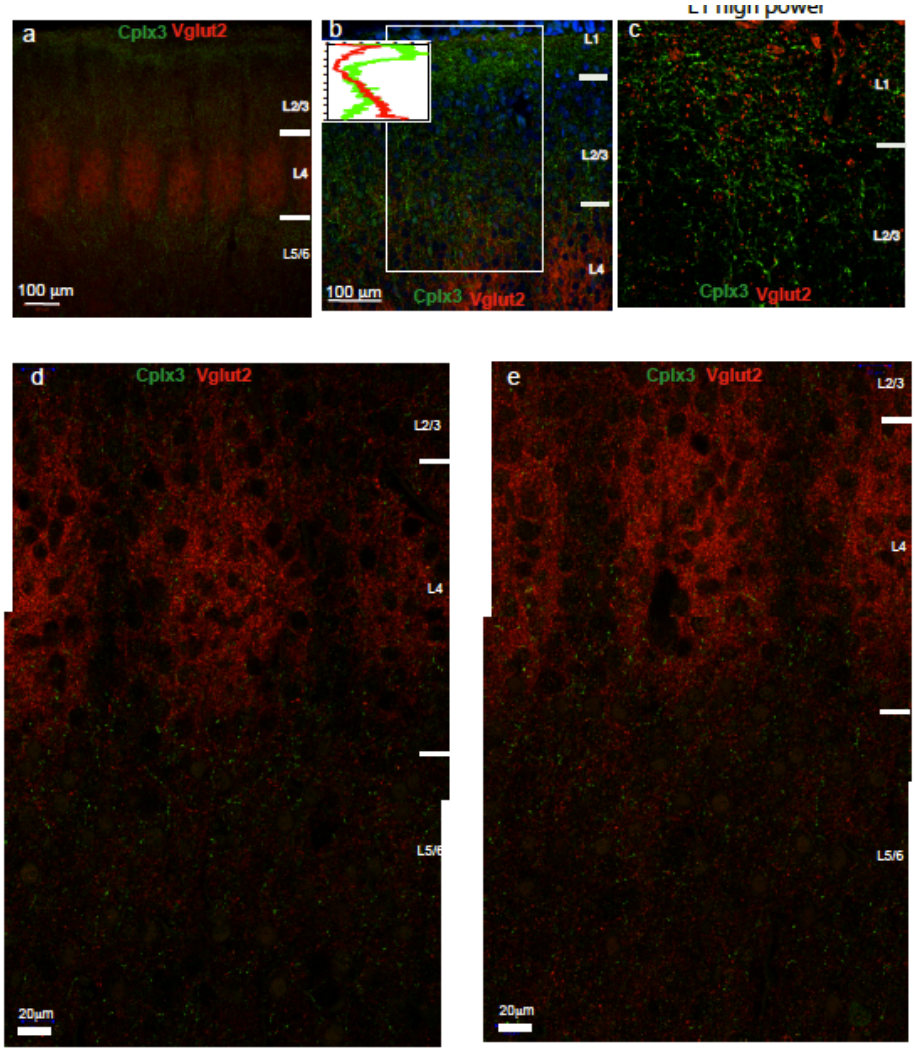

Figure shows the projections of Cplx3 positive Spn in the cortical plate.Figures reprsent coronal sections of wild type mice (P8-9), stained for Vglut 2 (red) and Cplx3 (Green).Panel a shoes a tiled view of the barel field showing barrels (red) and Clx3 projections from the Spn (green). Note the projections in the cortical plate around the barrel field. Panel b shows a zoomed in view of the area above the barrels. Note the Cplx3 positive terminals in the pia and barrel boundaries. The graph in the inset is a quantification of the pixel intensities in the boxed region. Panel C shows a high power image of the region around L1. Panels d and e show two examples of tiled images at and below the barrels.Note the Cplx3 positive punctate green signal below the barrel field.

4.2.3 The spatial pattern of SPN projections to L4 is related to the spatial pattern of thalamo-cortical projections

SPNs play an instructive role during the critical period of thalamo-cortical development (Kanold and Luhmann 2010). Thus SPNs could guide or associate with thalamic axons and thereby sculpt future thalamo-cortical connectivity. Thalamic afferents within L4 of S1 are clustered into a patterned arrangement called barrels (Agmon, Yang et al. 1995) that are separated by inter-barrel spaces called septa. Since Cplx3 projects to L4, we sought to study the spatial distribution of SPN axons with respect to thalamic afferents clustered as barrels and septa to see if axons from a particular cell type had a particular pattern of arrangement in L4 or if the projections were uniformly distributed.

Axons in L4 could have several possible patterns of projections with respect to the thalamic afferents: they could be randomly distributed throughout the cortical plate, they could be enriched in L4 within the barrel field or they could be enriched at the boundaries. In order to determine the location of axons from SPNs with respect to the whisker barrels, we labeled thalamic afferents by localizing Vglut2 and SPNs neurites by localizing Cplx3 protein. We analyzed the axon pattern in coronal sections and observed that at P9, Cplx3-positive axon terminals had a laminar preference in the cortical plate with respect to the barrel cyto-architecture. In the cortical plate, the terminals were enriched below the barrel. We observed this laminar enrichment in ~10 barrels from 4 animals. Figures 4.5 shows coronal sections from mice aged P7-9, stained for Cplx3 (green) and Vglut2 (red). We quantified the mean pixel intensity from Cplx3 terminals in the barrel field and observed an increase in intensity in the horizontal axis (Figure 4.5)

Since barrels and septa serve different functions in information processing (Agmon, Yang et al. 1995), we wanted to see if the Cplx3 terminals at the barrel boundary had a preference for the barrel hollow or the septal compartment. We quantified the terminals in coronal sections and while individual section showed preferences, as a population we found no preference for either the barrel or septa (Note the absence of peaks in Cplx3 intensity along the horizontal axis in horizontal sections, Figure 4.5) However, we did observe a septal preference in the flattened horizontal sections 4.5f. Further studies are required to validate this observation.

Figures 4.5: Laminar enrichment of Cplx3 terminals:

Figure 4.5 a

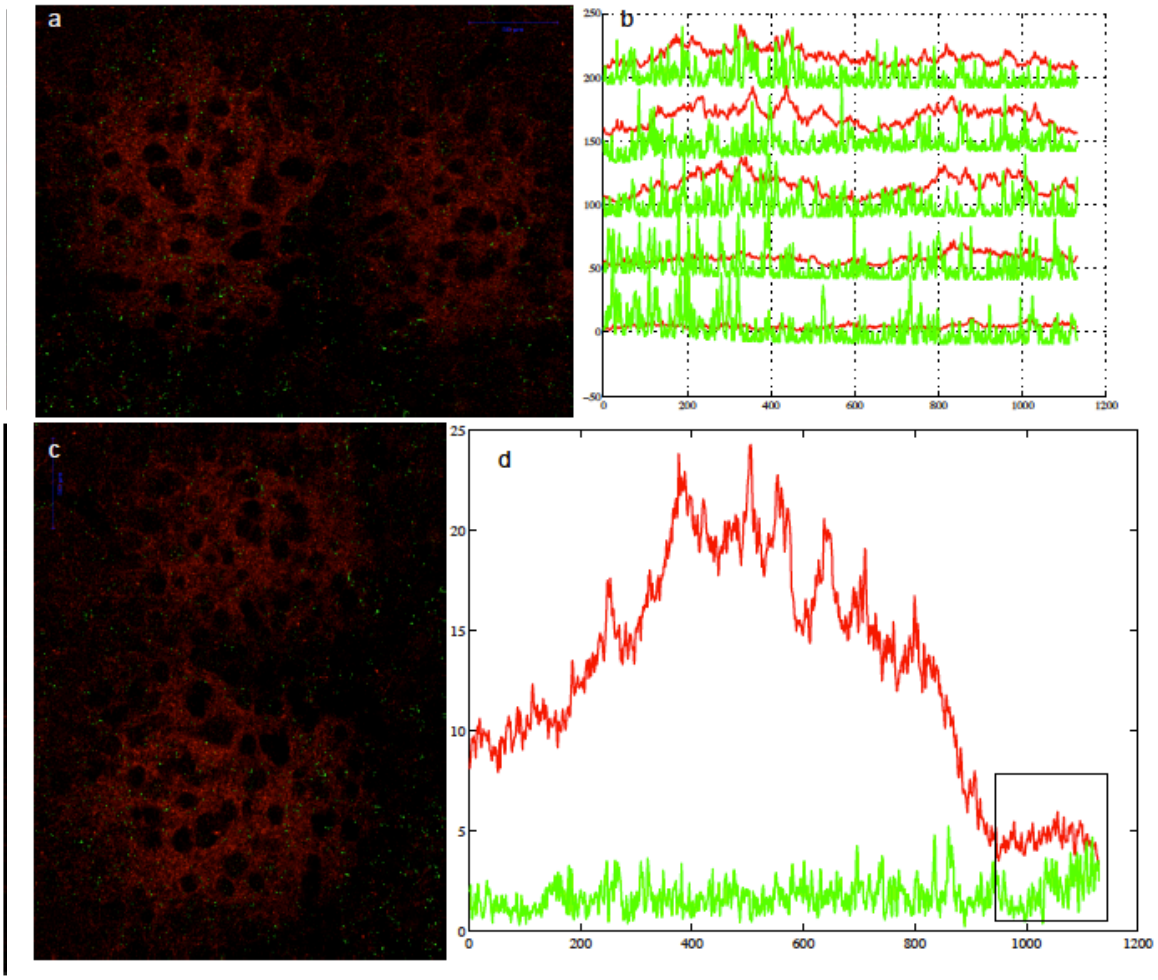

Figure shows images from coronal brain sections at P8 stained for Cplx3 (Spn terminals) and Vglut 2 (thalamixc afferents). Panel b shows the quantification of the cplx3 intensity along the horizontal axes.Note that the Cplx3 intensity increases along the horizontal axis. Panel c shows a rotated view of the same image such that the bottom of the barrels is to the right. Panel d shows the quantification of Cplx3 pixel intensity along the vertical axis. Note that teh Cplx3 intensity shows an increase in the vertical axis (box).

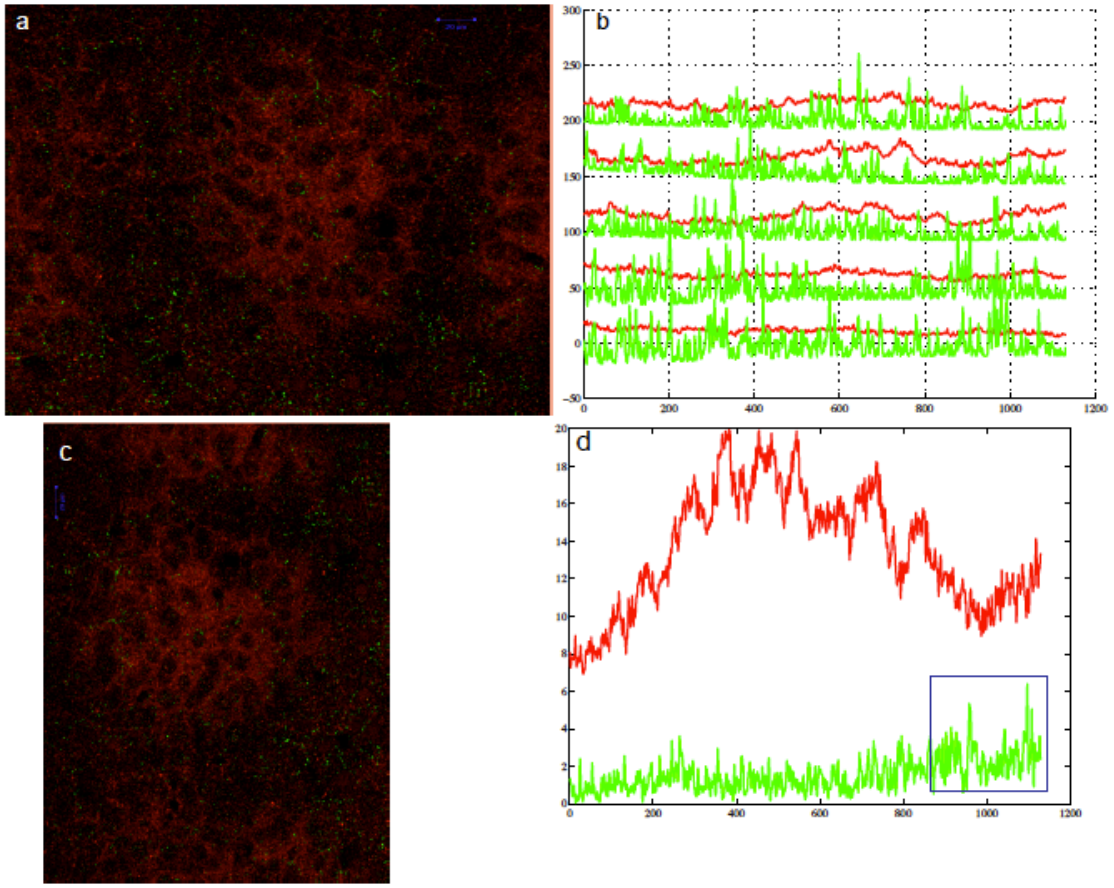

Figure shows images from coronal brain sections at P8 stained for Cplx3 (Spn terminals) and Vglut 2 (thalamixc afferents). Panel b shows the quantification of the cplx3 intensity along the horizontal axes.Note that the Cplx3 intensity increases along the horizontal axis. Panel c shows a rotated view of the same image such that the bottom of the barrels is to the right. Panel d shows the quantification of Cplx3 pixel intensity along the vertical axis. Note that the Cplx3 intensity shows an increase in the vertical axis (box).

Figure 4.5 b

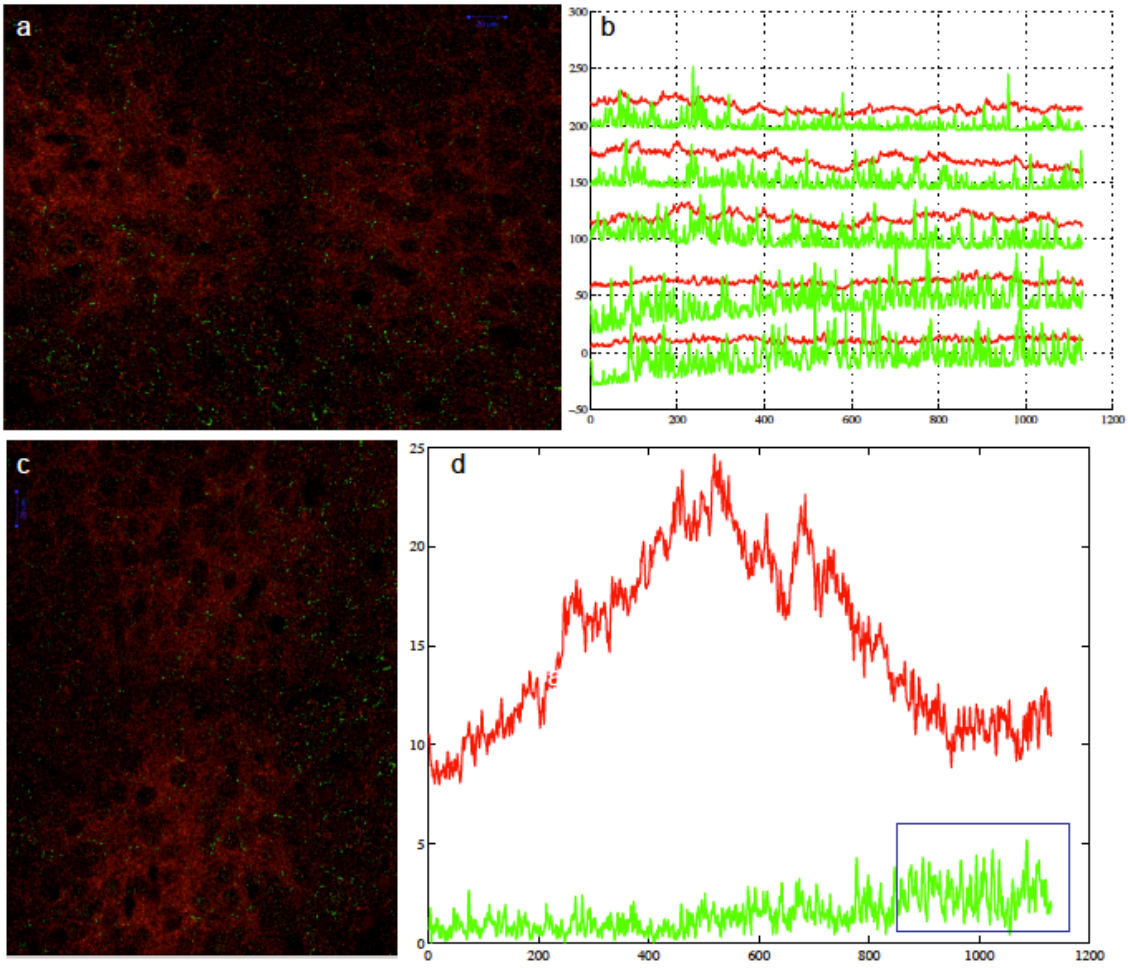

Figure shows images from coronal brain sections at P8 stained for Cplx3 (Spn terminals) and Vglut 2 (thalamixc afferents). Panel b shows the quantification of the cplx3 intensity along the horizontal axes.Note that the Cplx3 intensity increases along the horizontal axis. Panel c shows a rotated view of the same image such that the bottom of the barrels is to the right. Panel d shows the quantification of Cplx3 pixel intensity along the vertical axis. Note that teh Cplx3 intensity shows an increase (box) in the vertical axis.

Figure 4.5 c

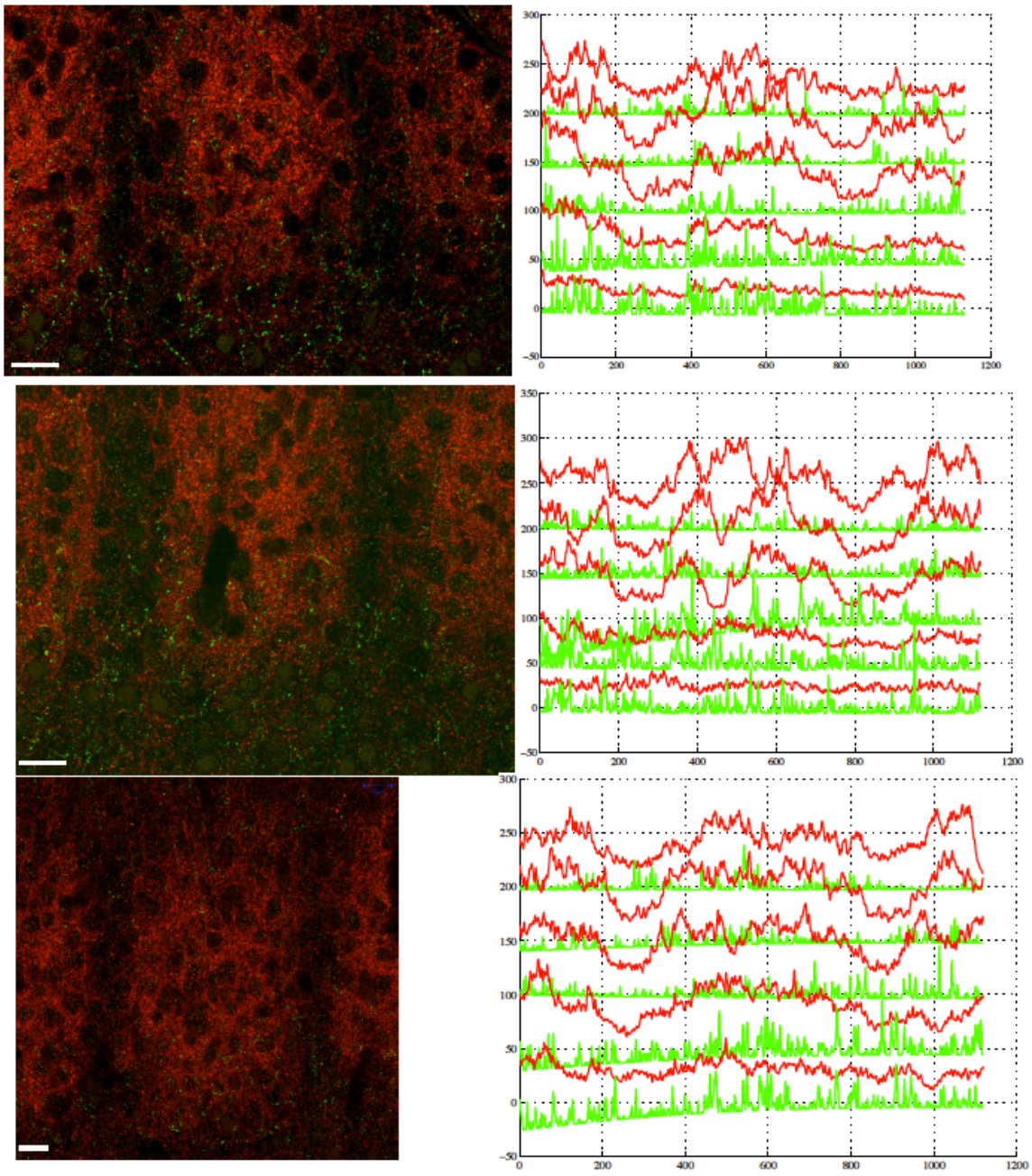

Figure shows additional examples from three different hemispheres from 2 animals showing the quantiication of Cplx3 in the lower layers of the barrel field. All scale bars - 20microns

Figure 4.5d

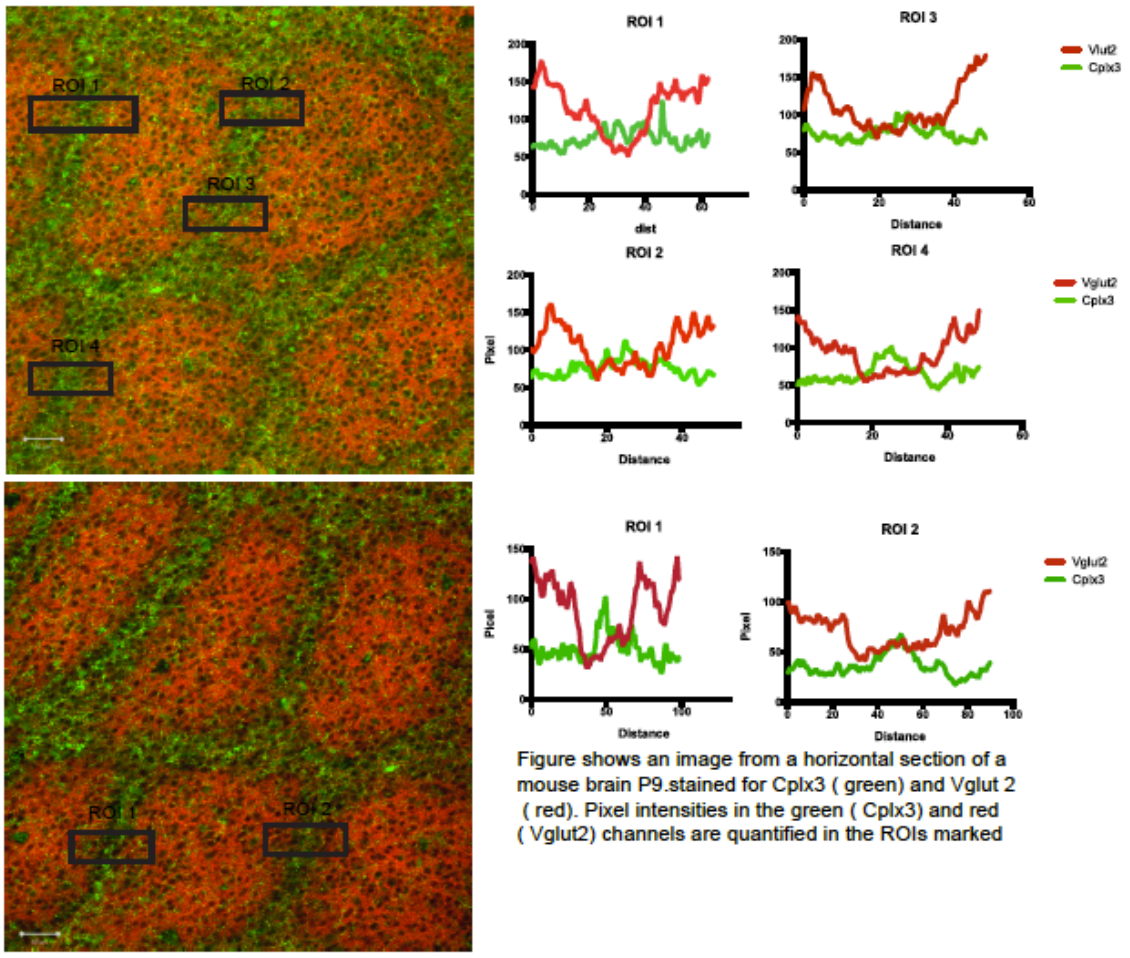

Figure 4.5e

4.2.4 Cplx3 positive SPNs project to the thalamus

SPNs have been implicated in pioneering the cortico-thalamic pathway (McConnell, Ghosh et al. 1989, McConnell, Ghosh et al. 1994, Grant, Hoerder-Suabedissen et al. 2012). Timed ablation of SPNs in cats resulted in cortico-thalamic axons failing to segregate into appropriate thalamic nuclei (McConnell, Ghosh et al. 1994). What is the molecular identity of the SPNs that extend long-range projections into subcortical targets? Molnar et al. (Grant, Hoerder-Suabedissen et al. 2012) have shown through DiI (a hydrophobic small molecule dye) tracing studies from the ventrobasal complex (VB) and corpus callosum (CC) that CTGF-positive

SPNs do not project to the thalamus. Here we investigated if Cplx3 positive SPNs project to the thalamus. We also wanted to see if the other subpopulations studied here project long range. We observed extensive axonal projections through the internal capsule and punctate Cplx3-positive terminals in the thalamus (Figure 4.6). Punctate signals from Cplx3 are seen scattered in thalamic nuclei roughly corresponding to Vpm. We also observe a small cluster of punctae (white box in 4.5c) above the scattered signals.

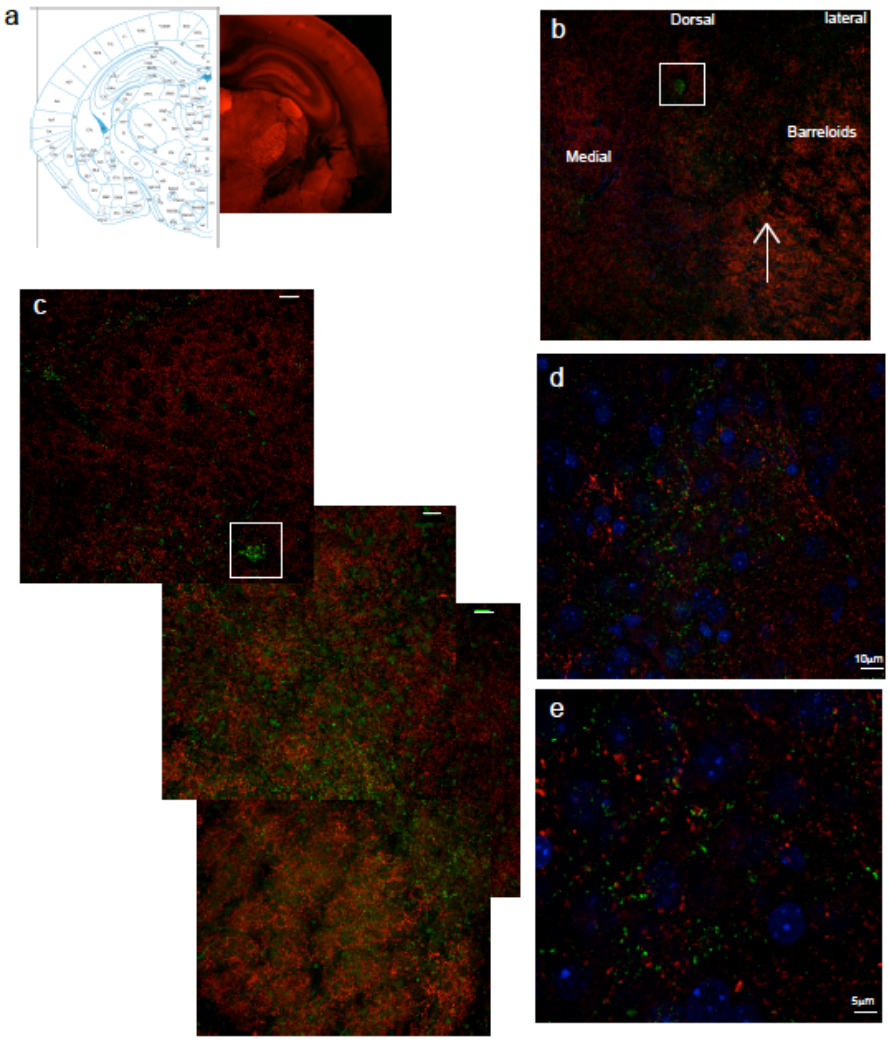

Cplx3 terminals in thalamus. Images show coronal brain slices at P9, CPLX3 (green) and Vglut 2 (red).Panel a:shows a low power image of the region imaged along with an atlas image.Panel b shows a low power image showing the thalamic region with terminals highlighted (white box).Tiled sections showing the terminals. Scale bars - 20µm.Panels d and e high power images showing the Cplx3 terminals in the thalamic nuclei shown in c.

4.3 Discussion:

Neuronal cell types are perhaps most commonly classified according to their epigenetic/ transcriptomic identity. But a more functional classification would be their role in connectivity. SPNs are a heterogeneous population of different cell types. In this study, for the first time, using an anatomical approach, we try to understand the role of a particular cell type in connectivity and observe that a particular molecular class of SPNs engages in different sub-circuits. We chose a marker that had high spatiotemporal specificity to the SPNs during different developmental time points.

Cplx3, first identified as an SP-specific marker by Molnar et al. (Hoerder-Suabedissen, Wang et al. 2009), localizes in the same lamina as CTGF, which is another molecular marker having SP specific restricted expression in rodents (Figure 2.8) (Hoerder-Suabedissen, Wang et al. 2009, Viswanathan, Bandyopadhyay et al. 2012) and other species (Wang, Oeschger et al. 2011). Cplx3 belongs to a family of four closely related proteins involved in vesicle release (Hu, Carroll et al. 2002, Xue, Stradomska et al. 2008), thus allowing us to specifically study axonal projections of this subset of SPNs. Cplx3 expression is postnatally up-regulated and reaches a peak at P8 (Hoerder-Suabedissen, Wang et al. 2009).

While Cplx3 transcripts, as seen by *in situ* hybridization (Allen Brain Atlas and Hoerder-Suabedissen, Wang et al. 2009), shows a largely subplate-specific expression in all sensory areas (most RNA transcripts are retained in the nucleus/cell body), the protein (which is transported to the axon terminal) labels additional neurons in upper cortical

layers during development (Hoerder-Suabedissen, Wang et al. 2009). At P2, neurons in the upper cortical layers resemble bipolar migratory neurons (data not shown). However, by P7, the morphology of these neurons undergoes a change and they appear as mature neurons and extra-SP expression is reduced to fewer neurons. The role of these neurons in the developing cortex is unclear. It is likely that some subplate neurons get displaced during cortical migration and are heterotopic in the upper cortical layers and are later eliminated by apoptosis. It is also possible that some migratory neurons express Cplx3 and at later stages in development, either Cplx3 expression is down regulated or these cells are eliminated by apoptosis. The expression in upper cortical layers undergoes a dramatic reduction at stages past the critical period. It is interesting to note that the number of neurons expressing Cplx3 in the upper cortical layers shows large inter-areal differences. At P7, the Cplx3 positive neurons in the upper cortical layers are more in number in S1 than in A1, for instance. These differences could indicate differing roles of SPNs in different cortical areas or different maturational stages between areas. Moreover our results show that the particular subset of SPNs labeled depends on the cortical area, pointing to a functional specialization of SPNs.

Layer 1, a cell-sparse, neuropil-rich zone (Ma, Yao et al. 2013, Hestrin and Armstrong 1996), is the layer of converging connections between cortical and subcortical regions. In addition to apical dendrites from different cortical layers, this layer receives intra-areal cortico-cortical projections (Cauller, Clancy et al. 1998) and inputs from subcortical areas like thalamus (Herkenham 1986). This zone thus plays an important role in synaptic integration (Ma, Yao et al. 2013) between different cortical layers and subcortical regions (Chu, Galarreta et al. 2003). The projections from SPNs to layer 1

imply a role in synaptic integration and intra-cortical connectivity. Further physiological studies are required to elucidate the precise mechanism of this connection.. Since SPNs are actively engaged in circuitry immediately from the embryonic stage (Ghosh and Shatz 1992, Ghosh and Shatz 1993), it will be interesting to see the temporal integration of this cell type into the connectivity. However the postnatal up-regulation of the markers studied here precludes the study / analysis of connectivity at the embryonic stage.

4.3.1 Laminar enrichment:

SPNs play a very important role in establishing thalamo-cortical connections over development (Kanold and Luhmann 2010). They establish a transient circuit and relay incoming thalamic inputs to developing layer 4. Our results demonstrate a distinct laminar pattern of projections from Cplx3-positive SPNs with respect to the thalamic afferents in L4. We observe that Cplx3 neurites are enriched in deep layer 4 at the boundary of the barrel cyto-architecture in layer 4 formed by the thalamic afferents.

Barrels and septa subserve distinct cortical circuits and receive inputs from parallel subcortical pathways. Distribution of neurites with respect to the barrel hollow is indicative of a particular pattern of integration in the thalamo-cortical connectivity. While we did not observe a statistically significant differential arrangement of terminals with respect to the barrel hollow and septal compartments in coronal sections, we did observe a septal preference in flattened sections cut in the horizontal plane. This difference could be due to the angle of sectioning. Since the terminals have a laminar preference, sectioning in the horizontal plane and imaging at different layers might represent the

localization of the terminals differently from the coronal sections. As Cplx3 terminals are also observed in L1, Cplx3-positive SPNs would appear to form a scaffold around the barrel hollow, similar to the 'barrel nets' formed by L2/3 axons (Sehara, Toda et al. 2010). However, further studies are required to validate this observation.

A study using the *golli*-tau-EGFP mouse, which expresses GFP in SPNs (and some L6 neurons), showed that S1 barrel cortex has a characteristic periphery-related arrangement in L4, in that SPNs neurites in L4 seem to associate with thalamic projections (Pinon, Jethwa et al. 2009). Further studies to investigate if Cplx3 terminals had a barrel /septal preference will help us better understand the role of this subtype in SP connectivity.

While Cplx3 antibody-mediated staining is informative, there are certain limitations to this technique. The signal-to-noise ratio is very low (due to weak protein expression), making statistical evaluation extremely difficult. Transgenic lines expressing a reporter encoded by the Cplx3 promoter will be an invaluable tool to further investigate the projection patterns and hence their role in connectivity.

Pinon et al. observed a dynamic remodeling of neurites from SPNs in Layer 4. The Cplx3 gene studied here has a postnatal up-regulation of expression in the SP reaching a peak around P8 (Hoerder-Suabedissen, Wang et al. 2009). While it will be interesting to see if these cell types undergo similar remodeling, the developmental up-regulation precludes such studies. Similar studies on SP-specific genes with an embryonic onset will enable us to study any possible developmental up-regulation.

SPNs receive thalamic inputs over development that are relayed to the developing cortex (Kanold and Luhmann 2010). Here we show that a particular class of SPNs relays

this input to Layer 4 and thus fulfills a feed-forward function. Further anatomical and physiological studies to identify the post-synaptic targets and to characterize their synaptic connectivity within the barrel field will help us understand their role in cortical processing.

SPNs are strategically located to pioneer cortico-thalamic projections. Our data show that Cplx3-positive SPNs extend axons through the internal capsule and project to different thalamic nuclei while one subpopulation (CTGF) has been shown to be local. This clearly shows that molecular subtypes are segregating into functional cell types. It is quite likely that SPNs that are generated at different gestation times have different roles in connectivity. Further analysis of cell types that have an embryonic onset of expression might answer this question.

We studied a single marker that is expressed throughout the SP at all stages. There are other subtypes – CTGF, Nurr1, Drd1a – of SPNs that are known to have a specific spatio-temporal gradient of expression (Hoerder-Suabedissen, Oeschger et al. 2013). Analysis of their integration into the connectivity might help us further understand the role of SPNs during specific developmental time points. Different SP markers have considerable overlap in their expression pattern (Hoerder-Suabedissen, Wang et al. 2009). Nurr1 and Cplx3 have a partly overlapping expression (Hoerder-Suabedissen, Wang et al. 2009), so a subpopulation of Nurr1 positive Spn is likely also to be long-range projecting.

While we did observe interesting patterns of intra-cortical projections in a transgenic line expressing eGFP in CTGF positive cells and Cre in Drd1a positive SP

cells (data not shown), technical limitations of the transgenic lines prevent us from drawing many rigorous conclusions from those observations.

We also observe projections in thalamic nuclei from Drd1a positive cells but the caveat is that Drd1a also has expression in upper cortical layers and some projections could be from L6. Importantly, we do observe neurites in the internal capsule from Drd1a positive neurons in the subplate and hence at least a fraction of these projections are likely to be from SPNs. CTGF-GFP has a very sparse expression pattern. It is likely that the population that is labeled by this BAC transgenic selectively extends local projections. Transgenic lines with a more pan-SP expression and with more spatiotemporal specificity might be able to address these limitations. Targeted ablation of specific cell types will reveal the exact role played by each cell type in connectivity.

To conclude, we provide anatomical evidence for integration of a particular cell type of Spn in cortical circuitry. Transgenic lines that allow genetic labeling of other cell types can help us to better understand the molecular basis of this connectivity. Physiological recordings show that SPNs are tightly embedded in intra-cortical connectivity (Zhao, Kao et al. 2009, Tolner, Sheikh et al. 2012, Viswanathan, Bandyopadhyay et al. 2012). However, given the diversity of this population, it is important to understand the connectivity in the context of different cell types. Our results show that Cplx3 positive SPNs extend projections throughout the cortical plate during development. Interestingly, a large fraction of SPNs projections were in Layers 1 and 4, which are also the main thalamo-recipient layers (Bannister 2005). Since SPNs play an important role in the establishment of thalamo-cortical connectivity, this is indicative of

an instructive role of SPNs in the establishment and/or strengthening of thalamic projections in these layers.

4.4 Material And Methods:

All procedures followed the University of Maryland College Park animal use regulations. In this study, we use mice (C57BL/6) of either sex from The Jackson Laboratory (jax.org).

Perfusion and sectioning: Brains were perfused transcardially with 4% PFA, post-fixed for 2 hours in 4% PFA at room temperature or overnight at 4°C. Fixed brains were rinsed in cold PBS and cut coronally at 50 μm thickness and collected in cold PBS and stored at 4°C. Horizontal sections were made as described in (Tolner, Sheikh et al. 2012).

Immunohistochemistry: Free floating sections were blocked in 3% BSA and 0.3% Triton for one hour at room temperature followed by incubation in primary antibody overnight at 4°C. Sections were rinsed in 0.3% Triton 3 times (15' each) to remove non-specifically bound primary antibody followed by incubation in secondary antibody. Sections were finally rinsed in 0.3% Triton to remove non-specific secondary antibody and mounted onto glass slides.

Sections were air dried at room temperature, rehydrated in PBS and coverslipped with Vectashield (Vector Labs). Antibodies and concentrations are mentioned in Table 4.2.

Imaging:

Fluorescent sections were imaged with a Pannoramic 250 Flash Whole Slide Digital Scanner to analyze cell and projection distribution. Quantification of cells and projections were done on images taken on a confocal microscope (Zeiss 510 or 710 meta). Filter sets were chosen to minimize any bleed-through between fluorophores.

Analysis:

Images acquired as above were adjusted for contrast and brightness in ImageJ. Cell quantification was done in ImageJ using the Cell Counter plugin. Projection analysis was done in ImageJ and plotted using custom MATLAB scripts.

Table: 4.1: Antibodies and concentrations used in Chapter 4

Name	**Vendor**	**Cat. #**	**Dilution**	**Species**
Cplx3	Synaptic Systems	122 302	1:1000	Rb
Vglut2	Synaptic Systems	135 404	1:5000-10,000	Gp
NeuN	Chemicon	MAB377	1:100	Ms

Name	Vendor	Cat. #	Dilution	Conjugate
Gt anti Rb	Invitrogen	A-11008	1:500	AF 488
Gt anti Gp	Invitrogen	A-11075	1:500	AF 568
Gt anti Ms	Invitrogen	A-21235	1:500	AF 647

Rb: rabbit, Gt: goat, Ms: mouse, Gp: guinea pig, AF: Alexa Fluor

References:

Introduction:

Aboitiz, F. and J. Montiel (2007). 'Origin and evolution of the vertebrate telencephalon, with special reference to the mammalian neocortex.' Adv Anat Embryol Cell Biol **193**: 1-112.

Arimatsu, Y., M. Ishida, T. Kaneko, S. Ichinose and A. Omori (2003). 'Organization and development of corticocortical associative neurons expressing the orphan nuclear receptor Nurr1.' J Comp Neurol **466**(2): 180-196.

Avino, T. A. and J. J. Hutsler (2010). 'Abnormal cell patterning at the cortical gray-white matter boundary in autism spectrum disorders.' Brain Res **1360**: 138-146.

Bunney, W. E. and B. G. Bunney (2000). 'Evidence for a compromised dorsolateral prefrontal cortical parallel circuit in schizophrenia.' Brain Res Brain Res Rev **31**(2-3): 138-146.

Bystron, I., C. Blakemore and P. Rakic (2008). 'Development of the human cerebral cortex: Boulder Committee revisited.' Nat Rev Neurosci **9**(2): 110-122.

Chen, L., C. Yang and G. D. Mower (2001). 'Developmental changes in the expression of GABA(A) receptor subunits (alpha(1), alpha(2), alpha(3)) in the cat visual cortex and the effects of dark rearing.' Brain Res Mol Brain Res **88**(1-2): 135-143.

Chun, J. J., M. J. Nakamura and C. J. Shatz (1987). 'Transient cells of the developing mammalian telencephalon are peptide-immunoreactive neurons.' Nature **325**(6105): 617-620.

Chun, J. J. and C. J. Shatz (1988). 'A fibronectin-like molecule is present in the developing cat cerebral cortex and is correlated with subplate neurons.' J Cell Biol **106**(3): 857-872.

Chun, J. J. and C. J. Shatz (1989). 'The earliest-generated neurons of the cat cerebral cortex: characterization by MAP2 and neurotransmitter immunohistochemistry during fetal life.' J Neurosci **9**(5): 1648-1667.

Chun, J. J. and C. J. Shatz (1989). 'Interstitial cells of the adult neocortical white matter are the remnant of the early generated subplate neuron population.' J Comp Neurol **282**(4): 555-569.

Craddock, R. C., S. Jbabdi, C.-G. Yan, J. T. Vogelstein, F. X. Castellanos, A. Di Martino, C. Kelly, K. Heberlein, S. Colcombe and M. P. Milham (2013). 'Imaging human connectomes at the macroscale.' Nat Meth **10**(6): 524-539.

Druga, R. (2009). 'Neocortical inhibitory system.' Folia Biol (Praha) **55**(6): 201-217.

Dupont, E., I. L. Hanganu, W. Kilb, S. Hirsch and H. J. Luhmann (2006). 'Rapid developmental switch in the mechanisms driving early cortical columnar networks.' Nature **439**(7072): 79-83.

Ferriero, D. M. and S. P. Miller (2010). 'Imaging selective vulnerability in the developing nervous system.' J Anat **217**(4): 429-435.

Finney, E. M. and C. J. Shatz (1998). 'Establishment of patterned thalamocortical connections does not require nitric oxide synthase.' J Neurosci **18**(21): 8826-8838.

Freeman, J. M. and K. B. Nelson (1988). 'Intrapartum asphyxia and cerebral palsy.' Pediatrics **82**(2): 240-249.

Friauf, E., S. K. McConnell and C. J. Shatz (1990). 'Functional synaptic circuits in the subplate during fetal and early postnatal development of cat visual cortex.' J Neurosci **10**(8): 2601-2613.

Friston, K. J. and C. D. Frith (1995). 'Schizophrenia: a disconnection syndrome?' Clin Neurosci **3**(2): 89-97.

Ganguly, K., A. F. Schinder, S. T. Wong and M. Poo (2001). 'GABA itself promotes the developmental switch of neuronal GABAergic responses from excitation to inhibition.' Cell **105**(4): 521-532.

Ghosh, A., A. Antonini, S. K. McConnell and C. J. Shatz (1990). 'Requirement for subplate neurons in the formation of thalamocortical connections.' Nature **347**(6289): 179-181.

Ghosh, A. and C. J. Shatz (1993). 'A role for subplate neurons in the patterning of connections from thalamus to neocortex.' Development **117**(3): 1031-1047.

Golshani, P., H. Truong and E. G. Jones (1997). 'Developmental expression of GABA(A) receptor subunit and GAD genes in mouse somatosensory barrel cortex.' J Comp Neurol **383**(2): 199-219.

Hanganu, I. L., W. Kilb and H. J. Luhmann (2002). 'Functional synaptic projections onto subplate neurons in neonatal rat somatosensory cortex.' J Neurosci **22**(16): 7165-7176.

Hankins, G. D. V. and M. Speer (2003). 'Defining the Pathogenesis and Pathophysiology of Neonatal Encephalopathy and Cerebral Palsy.' Obstetrics & Gynecology **102**(3): 628-636.

Harman, A. M., N. J. Eastough and L. D. Beazley (1995). 'Development of the visual cortex in a wallaby--phylogenetic implications.' Brain Behav Evol **45**(3): 138-152.
Hensch, T. K. (2004). 'Critical period regulation.' Annu Rev Neurosci **27**: 549-579.
Herrmann, K., A. Antonini and C. J. Shatz (1994). 'Ultrastructural Evidence for Synaptic-Interactions between Thalamocortical Axons and Subplate Neurons.' European Journal of Neuroscience **6**(11): 1729-1742.

Heuer, H., S. Christ, S. Friedrichsen, D. Brauer, M. Winckler, K. Bauer and G. Raivich (2003). 'Connective tissue growth factor: a novel marker of layer VII neurons in the rat cerebral cortex.' Neuroscience **119**(1): 43-52.

Hevner, R. and N. Zecevic (2006). Pioneer Neurons and Interneurons in the Developing Subplate: Molecular Markers, Cell Birthdays, and Neurotransmitters. Development and Plasticity in Sensory Thalamus and Cortex. R. Erzurumlu, W. Guido and Z. Molnár, Springer US**:** 1-18.

Hoerder-Suabedissen, A. and Z. Molnar (2012). 'Morphology of mouse subplate cells with identified projection targets changes with age.' J Comp Neurol **520**(1): 174-185.

Hoerder-Suabedissen, A. and Z. Molnar (2013). 'Molecular diversity of early-born subplate neurons.' Cereb Cortex **23**(6): 1473-1483.

Hoerder-Suabedissen, A., F. M. Oeschger, M. L. Krishnan, T. G. Belgard, W. Z. Wang, S. Lee, C. Webber, E. Petretto, A. D. Edwards and Z. Molnar (2013). 'Expression profiling of mouse subplate reveals a dynamic gene network and disease association with autism and schizophrenia.' Proc Natl Acad Sci U S A **110**(9): 3555-3560.

Hoerder-Suabedissen, A., W. Z. Wang, S. Lee, K. E. Davies, A. M. Goffinet, S. Rakic, J. Parnavelas, K. Reim, M. Nicolic, O. Paulsen and Z. Molnar (2009). 'Novel markers reveal subpopulations of subplate neurons in the murine cerebral cortex.' Cereb Cortex **19**(8): 1738-1750.

Hubel, D. H. and T. N. Wiesel (1970). 'The period of susceptibility to the physiological effects of unilateral eye closure in kittens.' The Journal of Physiology **206**(2): 419-436.

Hubel, D. H. and T. N. Wiesel (1977). 'Ferrier lecture. Functional architecture of macaque monkey visual cortex.' Proc R Soc Lond B Biol Sci **198**(1130): 1-59.

Hutsler, J. J. and T. A. Avino (2013). 'Sigmoid fits to locate and characterize cortical boundaries in human cerebral cortex.' J Neurosci Methods **212**(2): 242-246.

Judas, M., G. Sedmak and M. Pletikos (2010). 'Early history of subplate and interstitial neurons: from Theodor Meynert (1867) to the discovery of the subplate zone (1974).' J Anat **217**(4): 344-367.

Kanold, P. O. and H. J. Luhmann (2010). 'The subplate and early cortical circuits.' Annu Rev Neurosci **33**: 23-48.

Kanold, P. O. and C. J. Shatz (2006). 'Subplate neurons regulate maturation of cortical inhibition and outcome of ocular dominance plasticity.' Neuron **51**(5): 627-638.

Kostovic, I. and P. S. Goldman-Rakic (1983). 'Transient cholinesterase staining in the mediodorsal nucleus of the thalamus and its connections in the developing human and monkey brain.' J Comp Neurol **219**(4): 431-447.

Kostovic, I. and N. Jovanov-Milosevic (2008). 'Subplate zone of the human brain: historical perspective and new concepts.' Coll Antropol **32 Suppl 1**: 3-8.

Kostovic, I., M. Judas and G. Sedmak (2011). 'Developmental history of the subplate zone, subplate neurons and interstitial white matter neurons: relevance for schizophrenia.' Int J Dev Neurosci **29**(3): 193-205.

Kostovic, I. and P. Rakic (1980). 'Cytology and time of origin of interstitial neurons in the white matter in infant and adult human and monkey telencephalon.' J Neurocytol **9**(2): 219-242.

Kostovic, I. and P. Rakic (1990). 'Developmental history of the transient subplate zone in the visual and somatosensory cortex of the macaque monkey and human brain.' J Comp Neurol **297**(3): 441-470.

Lein, E. S., A. Hohn and C. J. Shatz (2000). 'Dynamic regulation of BDNF and NT-3 expression during visual system development.' J Comp Neurol **420**(1): 1-18.

Lewis, D. A. and P. Levitt (2002). 'Schizophrenia as a disorder of neurodevelopment.' Annu Rev Neurosci **25**: 409-432.

Lichtman, J. W. and W. Denk (2011). 'The big and the small: challenges of imaging the brain's circuits.' Science **334**(6056): 618-623.

Lopez, V. and C. K. Wagner (2009). 'Progestin Receptor Is Transiently Expressed Perinatally in Neurons of the Rat Isocortex.' Journal of Comparative Neurology **512**(1): 124-139.

Luhmann, H. J., W. Kilb and I. L. Hanganu-Opatz (2009). 'Subplate cells: amplifiers of neuronal activity in the developing cerebral cortex.' Front Neuroanat **3**: 19.

Luskin, M. B. and C. J. Shatz (1985). 'Studies of the earliest generated cells of the cat's visual cortex: cogeneration of subplate and marginal zones.' J Neurosci **5**(4): 1062-1075.

Macchi, G., M. Bentivoglio, D. Minciacchi and M. Molinari (1996). 'Trends in the anatomical organization and functional significance of the mammalian thalamus.' Ital J Neurol Sci **17**(2): 105-129.

Marin-Padilla, M. (1971). 'Early prenatal ontogenesis of the cerebral cortex (neocortex) of the cat (Felis domestica). A Golgi study. I. The primordial neocortical organization.' Z Anat Entwicklungsgesch **134**(2): 117-145.

McFadden, K. and N. J. Minshew (2013). 'Evidence for dysregulation of axonal growth and guidance in the etiology of ASD.' Front Hum Neurosci **7**: 671.

McQuillen, P. S., M. F. DeFreitas, G. Zada and C. J. Shatz (2002). 'A novel role for p75NTR in subplate growth cone complexity and visual thalamocortical innervation.' J Neurosci **22**(9): 3580-3593.

McQuillen, P. S., R. A. Sheldon, C. J. Shatz and D. M. Ferriero (2003). 'Selective vulnerability of subplate neurons after early neonatal hypoxia-ischemia.' J Neurosci **23**(8): 3308-3315.

Miller, J. A., S. L. Ding, S. M. Sunkin, K. A. Smith, L. Ng, A. Szafer, A. Ebbert, Z. L. Riley, J. J. Royall, K. Aiona, J. M. Arnold, C. Bennet, D. Bertagnolli, K. Brouner, S. Butler, S. Caldejon, A. Carey, C. Cuhaciyan, R. A. Dalley, N. Dee, T. A. Dolbeare, B. A. Facer, D. Feng, T. P. Fliss, G. Gee, J. Goldy, L. Gourley, B. W. Gregor, G. Gu, R. E. Howard, J. M. Jochim, C. L. Kuan, C. Lau, C. K. Lee, F. Lee, T. A. Lemon, P. Lesnar, B. McMurray, N. Mastan, N. Mosqueda, T. Naluai-Cecchini, N. K. Ngo, J. Nyhus, A. Oldre, E. Olson, J. Parente, P. D. Parker, S. E. Parry, A. Stevens, M. Pletikos, M. Reding, K. Roll, D. Sandman, M. Sarreal, S. Shapouri, N. V. Shapovalova, E. H. Shen, N. Sjoquist, C. R. Slaughterbeck, M. Smith, A. J. Sodt, D. Williams, L. Zollei, B. Fischl, M. B. Gerstein, D. H. Geschwind, I. A. Glass, M. J. Hawrylycz, R. F. Hevner, H. Huang, A. R. Jones, J. A. Knowles, P. Levitt, J. W. Phillips, N. Sestan, P. Wohnoutka, C. Dang, A. Bernard, J. G. Hohmann and E. S. Lein (2014). 'Transcriptional landscape of the prenatal human brain.' Nature.

Molliver, M. E., I. Kostovic and H. van der Loos (1973). 'The development of synapses in cerebral cortex of the human fetus.' Brain Res **50**(2): 403-407.

Molnar, Z., C. Metin, A. Stoykova, V. Tarabykin, D. J. Price, F. Francis, G. Meyer, C. Dehay and H. Kennedy (2006). 'Comparative aspects of cerebral cortical development.' Eur J Neurosci **23**(4): 921-934.

Mountcastle, V. B. (1997). 'The columnar organization of the neocortex.' Brain **120 (Pt 4)**: 701-722.

Osheroff, H. and M. E. Hatten (2009). 'Gene expression profiling of preplate neurons destined for the subplate: genes involved in transcription, axon extension, neurotransmitter regulation, steroid hormone signaling, and neuronal survival.' Cereb Cortex **19 Suppl 1**: i126-134.

Piven, J., M. L. Berthier, S. E. Starkstein, E. Nehme, G. Pearlson and S. Folstein (1990). 'Magnetic resonance imaging evidence for a defect of cerebral cortical development in autism.' Am J Psychiatry **147**(6): 734-739.

Raizada, R. D. and S. Grossberg (2003). 'Towards a theory of the laminar architecture of cerebral cortex: computational clues from the visual system.' Cereb Cortex **13**(1): 100-113.

Rakhade, S. N. and F. E. Jensen (2009). 'Epileptogenesis in the immature brain: emerging mechanisms.' Nat Rev Neurol **5**(7): 380-391.

Rakic, P. (1976). 'Prenatal genesis of connections subserving ocular dominance in the rhesus monkey.' Nature **261**(5560): 467-471.

Reep, R. L. and G. S. Goodwin (1988). 'Layer VII of rodent cerebral cortex.' Neurosci Lett **90**(1-2): 15-20.

Rickmann, M., B. M. Chronwall and J. R. Wolff (1977). 'On the development of non-pyramidal neurons and axons outside the cortical plate: The early marginal zone as a pallial anlage.' Anatomy and Embryology **151**(3): 285-307.

Sheppard, A. M., S. K. Hamilton and A. L. Pearlman (1991). 'Changes in the distribution of extracellular matrix components accompany early morphogenetic events of mammalian cortical development.' J Neurosci **11**(12): 3928-3942.

Smart, I. H., C. Dehay, P. Giroud, M. Berland and H. Kennedy (2002). 'Unique morphological features of the proliferative zones and postmitotic compartments of the neural epithelium giving rise to striate and extrastriate cortex in the monkey.' Cereb Cortex **12**(1): 37-53.

Sporns, O., G. Tononi and R. Kotter (2005). 'The human connectome: A structural description of the human brain.' PLoS Comput Biol **1**(4): e42.

Suarez-Sola, M. L., F. J. Gonzalez-Delgado, M. Pueyo-Morlans, O. C. Medina-Bolivar, N. C. Hernandez-Acosta, M. Gonzalez-Gomez and G. Meyer (2009). 'Neurons in the white matter of the adult human neocortex.' Front Neuroanat **3**: 7.

Tolner, E. A., A. Sheikh, A. Y. Yukin, K. Kaila and P. O. Kanold (2012). 'Subplate neurons promote spindle bursts and thalamocortical patterning in the neonatal rat somatosensory cortex.' J Neurosci **32**(2): 692-702.

Torres-Reveron, J. and M. J. Friedlander (2007). 'Properties of persistent postnatal cortical subplate neurons.' J Neurosci **27**(37): 9962-9974.

Valverde, F., L. Lopez-Mascaraque, M. Santacana and J. A. De Carlos (1995). 'Persistence of early-generated neurons in the rodent subplate: assessment of cell death in neocortex during the early postnatal period.' J Neurosci **15**(7 Pt 1): 5014-5024.

Volpe, J. J. (2009). 'Brain injury in premature infants: a complex amalgam of destructive and developmental disturbances.' Lancet Neurol **8**(1): 110-124.

Wahle, P. and G. Meyer (1987). 'Morphology and quantitative changes of transient NPY-ir neuronal populations during early postnatal development of the cat visual cortex.' J Comp Neurol **261**(2): 165-192.

Xu, G., A. K. Knutsen, K. Dikranian, C. D. Kroenke, P. V. Bayly and L. A. Taber (2010). 'Axons pull on the brain, but tension does not drive cortical folding.' J Biomech Eng **132**(7): 071013.

Yuste, R., D. A. Nelson, W. W. Rubin and L. C. Katz (1995). 'Neuronal domains in developing neocortex: mechanisms of coactivation.' Neuron **14**(1): 7-17.

Chapter 2:

Agmon, A. and B. W. Connors (1991). 'Thalamocortical responses of mouse somatosensory (barrel) cortex in vitro.' Neuroscience **41**(2-3): 365-379.

Agmon, A., L. T. Yang, E. G. Jones and D. K. O'Dowd (1995). 'Topological precision in the thalamic projection to neonatal mouse barrel cortex.' J Neurosci **15**(1 Pt 2): 549-561.

Allendoerfer, K. L. and C. J. Shatz (1994). 'The subplate, a transient neocortical structure: its role in the development of connections between thalamus and cortex.' Annu Rev Neurosci **17**: 185-218.

Alloway, K. D. (2008). 'Information processing streams in rodent barrel cortex: the differential functions of barrel and septal circuits.' Cereb Cortex **18**(5): 979-989.
Bannister, A. P. (2005). 'Inter- and intra-laminar connections of pyramidal cells in the neocortex.' Neurosci Res **53**(2): 95-103.

Beaulieu, J. M., T. Del'guidice, T. D. Sotnikova, M. Lemasson and R. R. Gainetdinov (2011). 'Beyond cAMP: The Regulation of Akt and GSK3 by Dopamine Receptors.' Front Mol Neurosci **4**: 38.

Chen, T. W., T. J. Wardill, Y. Sun, S. R. Pulver, S. L. Renninger, A. Baohan, E. R. Schreiter, R. A. Kerr, M. B. Orger, V. Jayaraman, L. L. Looger, K. Svoboda and D. S. Kim (2013). 'Ultrasensitive fluorescent proteins for imaging neuronal activity.' Nature **499**(7458): 295-300.

Chhatwal, J. P., S. E. Hammack, A. M. Jasnow, D. G. Rainnie and K. J. Ressler (2007). 'Identification of cell-type-specific promoters within the brain using lentiviral vectors.' Gene Ther **14**(7): 575-583.

Chow, B. Y., X. Han, A. S. Dobry, X. Qian, A. S. Chuong, M. Li, M. A. Henninger, G. M. Belfort, Y. Lin, P. E. Monahan and E. S. Boyden (2010). 'High-performance genetically targetable optical neural silencing by light-driven proton pumps.' Nature **463**(7277): 98-102.

Clancy, B. and L. J. Cauller (1999). 'Widespread projections from subgriseal neurons (layer VII) to layer I in adult rat cortex.' J Comp Neurol **407**(2): 275-286.

Eberling, J. L., C. Wu, R. Tong-Turnbeaugh and W. J. Jagust (2004). 'Estrogen- and tamoxifen-associated effects on brain structure and function.' Neuroimage **21**(1): 364-371.

Fernstrom, J. D. and M. H. Fernstrom (2007). 'Tyrosine, phenylalanine, and catecholamine synthesis and function in the brain.' J Nutr **137**(6 Suppl 1): 1539S-1547S; discussion 1548S.
Gerfen, C. R., R. Paletzki and N. Heintz (2013). 'GENSAT BAC cre-recombinase driver lines to study the functional organization of cerebral cortical and basal ganglia circuits.' Neuron **80**(6): 1368-1383.

Goldman-Rakic, P. S., S. A. Castner, T. H. Svensson, L. J. Siever and G. V. Williams (2004). 'Targeting the dopamine D1 receptor in schizophrenia: insights for cognitive dysfunction.' Psychopharmacology (Berl) **174**(1): 3-16.

Gong, S., M. Doughty, C. R. Harbaugh, A. Cummins, M. E. Hatten, N. Heintz and C. R. Gerfen (2007). 'Targeting Cre recombinase to specific neuron populations with bacterial artificial chromosome constructs.' J Neurosci **27**(37): 9817-9823.

Gradinaru, V., K. R. Thompson and K. Deisseroth (2008). 'eNpHR: a Natronomonas halorhodopsin enhanced for optogenetic applications.' Brain Cell Biol **36**(1-4): 129-139.

Hasbi, A., B. F. O'Dowd and S. R. George (2011). 'Dopamine D1-D2 receptor heteromer signaling pathway in the brain: emerging physiological relevance.' Mol Brain **4**: 26.

Heuer, H., S. Christ, S. Friedrichsen, D. Brauer, M. Winckler, K. Bauer and G. Raivich (2003). 'Connective tissue growth factor: a novel marker of layer VII neurons in the rat cerebral cortex.' Neuroscience **119**(1): 43-52.

Hilakivi-Clarke, L., E. Cho, I. Onojafe, D. J. Liao and R. Clarke (2000). 'Maternal exposure to tamoxifen during pregnancy increases carcinogen-induced mammary tumorigenesis among female rat offspring.' Clinical Cancer Research **6**(1): 305-308.

Hirsch, M. L., M. Agbandje-McKenna and R. J. Samulski (2010). 'Little vector, big gene transduction: fragmented genome reassembly of adeno-associated virus.' Mol Ther **18**(1): 6-8.

Hoerder-Suabedissen, A. and Z. Molnar (2013). 'Molecular diversity of early-born subplate neurons.' Cereb Cortex **23**(6): 1473-1483.

Hoerder-Suabedissen, A., F. M. Oeschger, M. L. Krishnan, T. G. Belgard, W. Z. Wang, S. Lee, C. Webber, E. Petretto, A. D. Edwards and Z. Molnar (2013). 'Expression profiling of mouse subplate reveals a dynamic gene network and disease association with autism and schizophrenia.' Proc Natl Acad Sci U S A **110**(9): 3555-3560.
Hoerder-Suabedissen, A., W. Z. Wang, S. Lee, K. E. Davies, A. M. Goffinet, S. Rakic, J. Parnavelas, K. Reim, M. Nicolic, O. Paulsen and Z. Molnar (2009). 'Novel markers reveal subpopulations of subplate neurons in the murine cerebral cortex.' Cereb Cortex **19**(8): 1738-1750.

Kanold, P. O., P. Kara, R. C. Reid and C. J. Shatz (2003). 'Role of subplate neurons in functional maturation of visual cortical columns.' Science **301**(5632): 521-525.
Kanold, P. O. and H. J. Luhmann (2010). 'The subplate and early cortical circuits.' Annu Rev Neurosci **33**: 23-48.

Kaspar, B. K., B. Vissel, T. Bengoechea, S. Crone, L. Randolph-Moore, R. Muller, E. P. Brandon, D. Schaffer, I. M. Verma, K. F. Lee, S. F. Heinemann and F. H. Gage (2002). 'Adeno-associated virus effectively mediates conditional gene modification in the brain.' Proc Natl Acad Sci U S A **99**(4): 2320-2325.

Klemm, W. R. (1989). 'Drug effects on active immobility responses: what they tell us about neurotransmitter systems and motor functions.' Prog Neurobiol **32**(5): 403-422.

Kuhlman, S. J. and Z. J. Huang (2008). 'High-resolution labeling and functional manipulation of specific neuron types in mouse brain by Cre-activated viral gene expression.' PLoS One **3**(4): e2005.

Lee, C. H., B. Shah, E. K. Moioli and J. J. Mao (2010). 'CTGF directs fibroblast differentiation from human mesenchymal stem/stromal cells and defines connective tissue healing in a rodent injury model.' J Clin Invest **120**(9): 3340-3349.

Ma, J., X. H. Yao, Y. Fu and Y. C. Yu (2013). 'Development of Layer 1 Neurons in the Mouse Neocortex.' Cereb Cortex.

Madisen, L., T. A. Zwingman, S. M. Sunkin, S. W. Oh, H. A. Zariwala, H. Gu, L. L. Ng, R. D. Palmiter, M. J. Hawrylycz, A. R. Jones, E. S. Lein and H. Zeng (2010). 'A robust and high-throughput Cre reporting and characterization system for the whole mouse brain.' Nat Neurosci **13**(1): 133-140.

Marvin, J. S., B. G. Borghuis, L. Tian, J. Cichon, M. T. Harnett, J. Akerboom, A. Gordus, S. L. Renninger, T. W. Chen, C. I. Bargmann, M. B. Orger, E. R. Schreiter, J. B. Demb, W. B. Gan, S. A. Hires and L. L. Looger (2013). 'An optimized fluorescent probe for visualizing glutamate neurotransmission.' Nat Methods **10**(2): 162-170.

Miller, J. A., S. L. Ding, S. M. Sunkin, K. A. Smith, L. Ng, A. Szafer, A. Ebbert, Z. L. Riley, J. J. Royall, K. Aiona, J. M. Arnold, C. Bennet, D. Bertagnolli, K. Brouner, S. Butler, S. Caldejon, A. Carey, C. Cuhaciyan, R. A. Dalley, N. Dee, T. A. Dolbeare, B. A. Facer, D. Feng, T. P. Fliss, G. Gee, J. Goldy, L. Gourley, B. W. Gregor, G. Gu, R. E. Howard, J. M. Jochim, C. L. Kuan, C. Lau, C. K. Lee, F. Lee, T. A. Lemon, P. Lesnar, B. McMurray, N. Mastan, N. Mosqueda, T. Naluai-Cecchini, N. K. Ngo, J. Nyhus, A. Oldre, E. Olson, J. Parente, P. D. Parker, S. E. Parry, A. Stevens, M. Pletikos, M. Reding, K. Roll, D. Sandman, M. Sarreal, S. Shapouri, N. V. Shapovalova, E. H. Shen, N. Sjoquist, C. R. Slaughterbeck, M. Smith, A. J. Sodt, D. Williams, L. Zollei, B. Fischl, M. B. Gerstein, D. H. Geschwind, I. A. Glass, M. J. Hawrylycz, R. F. Hevner, H. Huang, A. R. Jones, J. A.

Knowles, P. Levitt, J. W. Phillips, N. Sestan, P. Wohnoutka, C. Dang, A. Bernard, J. G. Hohmann and E. S. Lein (2014). 'Transcriptional landscape of the prenatal human brain.' Nature.
Nahmani, M. and A. Erisir (2005). 'VGluT2 immunochemistry identifies thalamocortical terminals in layer 4 of adult and developing visual cortex.' J Comp Neurol **484**(4): 458-473.

Nathanson, J. L., R. Jappelli, E. D. Scheeff, G. Manning, K. Obata, S. Brenner and E. M. Callaway (2009). 'Short Promoters in Viral Vectors Drive Selective Expression in Mammalian Inhibitory Neurons, but do not Restrict Activity to Specific Inhibitory Cell-Types.' Front Neural Circuits **3**: 19.

Nieoullon, A. (2002). 'Dopamine and the regulation of cognition and attention.' Prog Neurobiol **67**(1): 53-83.

O'Leary, D. D., B. L. Schlaggar and R. Tuttle (1994). 'Specification of neocortical areas and thalamocortical connections.' Annu Rev Neurosci **17**: 419-439.

Petersen, C. C. (2007). 'The functional organization of the barrel cortex.' Neuron **56**(2): 339-355.

Petreanu, L., D. Huber, A. Sobczyk and K. Svoboda (2007). 'Channelrhodopsin-2-assisted circuit mapping of long-range callosal projections.' Nat Neurosci **10**(5): 663-668.

Pinon, M. C., A. Jethwa, E. Jacobs, A. Campagnoni and Z. Molnar (2009). 'Dynamic integration of subplate neurons into the cortical barrel field circuitry during postnatal development in the Golli-tau-eGFP (GTE) mouse.' J Physiol **587**(Pt 9): 1903-1915.

Rahim, A. A., A. M. Wong, S. Ahmadi, K. Hoefer, S. M. Buckley, D. A. Hughes, A. N. Nathwani, A. H. Baker, J. H. McVey, J. D. Cooper and S. N. Waddington (2012). 'In utero administration of Ad5 and AAV pseudotypes to the fetal brain leads to efficient, widespread and long-term gene expression.' Gene Ther **19**(9): 936-946.

Roy, S., P. Coffee, G. Smith, R. K. Liem, S. T. Brady and M. M. Black (2000). 'Neurofilaments are transported rapidly but intermittently in axons: implications for slow axonal transport.' J Neurosci **20**(18): 6849-6861.

Schultz, W. (2007). 'Multiple dopamine functions at different time courses.' Annu Rev Neurosci **30**: 259-288.

Seeman, P. and S. Kapur (2000). 'Schizophrenia: more dopamine, more D2 receptors.' Proc Natl Acad Sci U S A **97**(14): 7673-7675.

Shimo, T., T. Nakanishi, T. Nishida, M. Asano, M. Kanyama, T. Kuboki, T. Tamatani, K. Tezuka, M. Takemura, T. Matsumura and M. Takigawa (1999). 'Connective tissue growth factor induces the proliferation, migration, and tube formation of vascular endothelial cells in vitro, and angiogenesis in vivo.' J Biochem **126**(1): 137-145.
Shimo, T., T. Nakanishi, T. Nishida, M. Asano, A. Sasaki, M. Kanyama, T. Kuboki, T. Matsumura and M. Takigawa (2001). 'Involvement of CTGF, a hypertrophic chondrocyte-specific gene product, in tumor angiogenesis.' Oncology **61**(4): 315-322.

Shimogori, T. and M. Ogawa (2008). 'Gene application with in utero electroporation in mouse embryonic brain.' Dev Growth Differ **50**(6): 499-506.

Sun, Q. Q., J. R. Huguenard and D. A. Prince (2006). 'Barrel cortex microcircuits: thalamocortical feedforward inhibition in spiny stellate cells is mediated by a small number of fast-spiking interneurons.' J Neurosci **26**(4): 1219-1230.

Taymans, J. M., L. H. Vandenberghe, C. V. Haute, I. Thiry, C. M. Deroose, L. Mortelmans, J. M. Wilson, Z. Debyser and V. Baekelandt (2007). 'Comparative analysis of adeno-associated viral vector serotypes 1, 2, 5, 7, and 8 in mouse brain.' Hum Gene Ther **18**(3): 195-206.

Tian, L., S. A. Hires, T. Mao, D. Huber, M. E. Chiappe, S. H. Chalasani, L. Petreanu, J. Akerboom, S. A. McKinney, E. R. Schreiter, C. I. Bargmann, V. Jayaraman, K. Svoboda and L. L. Looger (2009). 'Imaging neural activity in worms, flies and mice with improved GCaMP calcium indicators.' Nat Methods **6**(12): 875-881.

Wise, R. A. and P. P. Rompre (1989). 'Brain dopamine and reward.' Annu Rev Psychol **40**: 191-225.

Wu, Z., H. Yang and P. Colosi (2010). 'Effect of genome size on AAV vector packaging.' Mol Ther **18**(1): 80-86.

Zanazzi, G. and G. Matthews (2010). 'Enrichment and differential targeting of complexins 3 and 4 in ribbon-containing sensory neurons during zebrafish development.' Neural Dev **5**: 24.

Zariwala, H. A., B. G. Borghuis, T. M. Hoogland, L. Madisen, L. Tian, C. I. De Zeeuw, H. Zeng, L. L. Looger, K. Svoboda and T. W. Chen (2012). 'A Cre-dependent GCaMP3 reporter mouse for neuronal imaging in vivo.' J Neurosci **32**(9): 3131-3141.

Zhang, F., L. P. Wang, M. Brauner, J. F. Liewald, K. Kay, N. Watzke, P. G. Wood, E. Bamberg, G. Nagel, A. Gottschalk and K. Deisseroth (2007). 'Multimodal fast optical interrogation of neural circuitry.' Nature **446**(7136): 633-639.

Chapter 3

Abedi, M. R., G. Caponigro and A. Kamb (1998). 'Green fluorescent protein as a scaffold for intracellular presentation of peptides.' Nucleic Acids Research **26**(2): 623-630.

Ai, H. W., J. N. Henderson, S. J. Remington and R. E. Campbell (2006). 'Directed evolution of a monomeric, bright and photostable version of Clavularia cyan fluorescent protein: structural characterization and applications in fluorescence imaging.' Biochem J **400**(3): 531-540.

Ai, H. W., S. G. Olenych, P. Wong, M. W. Davidson and R. E. Campbell (2008). 'Hue-shifted monomeric variants of Clavularia cyan fluorescent protein: identification of the molecular determinants of color and applications in fluorescence imaging.' BMC Biol **6**: 13.

Akerboom, J., N. Carreras Calderon, L. Tian, S. Wabnig, M. Prigge, J. Tolo, A. Gordus, M. B. Orger, K. E. Severi, J. J. Macklin, R. Patel, S. R. Pulver, T. J. Wardill, E. Fischer, C. Schuler, T. W. Chen, K. S. Sarkisyan, J. S. Marvin, C. I. Bargmann, D. S. Kim, S. Kugler, L. Lagnado, P. Hegemann, A. Gottschalk, E. R. Schreiter and L. L. Looger (2013). 'Genetically encoded calcium indicators for multi-color neural activity imaging and combination with optogenetics.' Front Mol Neurosci **6**: 2.

Amaral, D. G. and J. A. Dent (1981). 'Development of the mossy fibers of the dentate gyrus: I. A light and electron microscopic study of the mossy fibers and their expansions.' J Comp Neurol **195**(1): 51-86.

Arikkath, J. and L. F. Reichardt (2008). 'Cadherins and catenins at synapses: roles in synaptogenesis and synaptic plasticity.' Trends in Neurosciences **31**(9): 487-494.

Bohland, J. W., C. Wu, H. Barbas, H. Bokil, M. Bota, H. C. Breiter, H. T. Cline, J. C. Doyle, P. J. Freed, R. J. Greenspan, S. N. Haber, M. Hawrylycz, D. G. Herrera, C. C. Hilgetag, Z. J. Huang, A. Jones, E. G. Jones, H. J. Karten, D. Kleinfeld, R. Kotter, H. A. Lester, J. M. Lin, B. D. Mensh, S. Mikula, J. Panksepp, J. L. Price, J. Safdieh, C. B. Saper, N. D. Schiff, J. D. Schmahmann, B. W. Stillman, K. Svoboda, L. W. Swanson, A. W. Toga, D. C. Van Essen, J. D. Watson and P. P. Mitra (2009). 'A proposal for a coordinated effort for the determination of brainwide neuroanatomical connectivity in model organisms at a mesoscopic scale.' PLoS Comput Biol **5**(3): e1000334.

Bozdagi, O., W. Shan, H. Tanaka, D. L. Benson and G. W. Huntley (2000). 'Increasing Numbers of Synaptic Puncta during Late-Phase LTP: N-Cadherin Is Synthesized, Recruited to Synaptic Sites, and Required for Potentiation.' Neuron **28**(1): 245-259.

Cai, D., K. B. Cohen, T. Luo, J. W. Lichtman and J. R. Sanes (2013). 'Improved tools for the Brainbow toolbox.' Nat Methods **10**(6): 540-547.

Chicurel, M. E. and K. M. Harris (1992). 'Three-dimensional analysis of the structure and composition of CA3 branched dendritic spines and their synaptic relationships with mossy fiber boutons in the rat hippocampus.' J Comp Neurol **325**(2): 169-182.

Chudakov, D. M., M. V. Matz, S. Lukyanov and K. A. Lukyanov (2010). 'Fluorescent Proteins and Their Applications in Imaging Living Cells and Tissues.' Physiological Reviews **90**(3): 1103-1163.

Dahl, R. and L. A. Staehelin (1989). 'High-Pressure Freezing for the Preservation of Biological Structure - Theory and Practice.' Journal of Electron Microscopy Technique **13**(3): 165-174.

Evan, G. I., G. K. Lewis, G. Ramsay and J. M. Bishop (1985). 'Isolation of monoclonal antibodies specific for human c-myc proto-oncogene product.' Mol Cell Biol **5**(12): 3610-3616.

Fannon, A. M. and D. R. Colman (1996). 'A Model for Central Synaptic Junctional Complex Formation Based on the Differential Adhesive Specificities of the Cadherins.' Neuron **17**(3): 423-434.

Feng, G., R. H. Mellor, M. Bernstein, C. Keller-Peck, Q. T. Nguyen, M. Wallace, J. M. Nerbonne, J. W. Lichtman and J. R. Sanes (2000). 'Imaging neuronal subsets in transgenic mice expressing multiple spectral variants of GFP.' Neuron **28**(1): 41-51.
Field, J., J. Nikawa, D. Broek, B. MacDonald, L. Rodgers, I. A. Wilson, R. A. Lerner and M. Wigler (1988). 'Purification of a RAS-responsive adenylyl cyclase complex from Saccharomyces cerevisiae by use of an epitope addition method.' Mol Cell Biol **8**(5): 2159-2165.

Geschwind, D. (2004). 'GENSAT: a genomic resource for neuroscience research.' Lancet Neurol **3**(2): 82.

Giepmans, B. N. G., S. R. Adams, M. H. Ellisman and R. Y. Tsien (2006). 'The Fluorescent Toolbox for Assessing Protein Location and Function.' Science **312**(5771): 217-224.

Gillette, T. A., K. M. Brown and G. A. Ascoli (2011). 'The DIADEM metric: comparing multiple reconstructions of the same neuron.' Neuroinformatics **9**(2-3): 233-245.

Gray, N. W., R. M. Weimer, I. Bureau and K. Svoboda (2006). 'Rapid redistribution of synaptic PSD-95 in the neocortex in vivo.' PLoS Biol **4**(11): e370.

Gross, Garrett G., Jason A. Junge, Rudy J. Mora, H.-B. Kwon, C. A. Olson, Terry T. Takahashi, Emily R. Liman, Graham C. R. Ellis-Davies, Aaron W. McGee, Bernardo L. Sabatini, Richard W. Roberts and Don B. Arnold (2013). 'Recombinant Probes for Visualizing Endogenous Synaptic Proteins in Living Neurons.' Neuron **78**(6): 971-985.

Hadjieconomou, D., S. Rotkopf, C. Alexandre, D. M. Bell, B. J. Dickson and I. Salecker (2011). 'Flybow: genetic multicolor cell labeling for neural circuit analysis in Drosophila melanogaster.' Nat Methods **8**(3): 260-266.

Hampel, S., P. Chung, C. E. McKellar, D. Hall, L. L. Looger and J. H. Simpson (2011). 'Drosophila Brainbow: a recombinase-based fluorescence labeling technique to subdivide neural expression patterns.' Nat Methods **8**(3): 253-259.

He, H. Y. and H. T. Cline (2011). 'Diadem X: automated 4 dimensional analysis of morphological data.' Neuroinformatics **9**(2-3): 107-112.
Heintz, N. (2004). 'Gene expression nervous system atlas (GENSAT).' Nat Neurosci **7**(5): 483-483.
Heintz, N. (2004). 'Gene expression nervous system atlas (GENSAT).' Nat Neurosci **7**(5): 483.

Hopp, T. P., K. S. Prickett, V. L. Price, R. T. Libby, C. J. March, D. P. Cerretti, D. L. Urdal and P. J. Conlon (1988). 'A Short Polypeptide Marker Sequence Useful for Recombinant Protein Identification and Purification.' Bio-Technology **6**(10): 1204-1210.

Huang, B., M. Bates and X. Zhuang (2009). 'Super-resolution fluorescence microscopy.' Annu Rev Biochem **78**: 993-1016.

Huang, B., W. Wang, M. Bates and X. Zhuang (2008). 'Three-dimensional super-resolution imaging by stochastic optical reconstruction microscopy.' Science **319**(5864): 810-813.

Jenett, A., G. M. Rubin, T. T. Ngo, D. Shepherd, C. Murphy, H. Dionne, B. D. Pfeiffer, A. Cavallaro, D. Hall, J. Jeter, N. Iyer, D. Fetter, J. H. Hausenfluck, H. Peng, E. T. Trautman, R. R. Svirskas, E. W. Myers, Z. R. Iwinski, Y. Aso, G. M. DePasquale, A. Enos, P. Hulamm, S. C. Lam, H. H. Li, T. R. Laverty, F. Long, L. Qu, S. D. Murphy, K. Rokicki, T. Safford, K. Shaw, J. H. Simpson, A. Sowell, S. Tae, Y. Yu and C. T. Zugates (2012). 'A GAL4-driver line resource for Drosophila neurobiology.' Cell Rep **2**(4): 991-1001.

Kiss, C., H. Fisher, E. Pesavento, M. H. Dai, R. Valero, M. Ovecka, R. Nolan, M. L. Phipps, N. Velappan, L. Chasteen, J. S. Martinez, G. S. Waldo, P. Pavlik and A. R. M. Bradbury (2006). 'Antibody binding loop insertions as diversity elements.' Nucleic Acids Research **34**(19): E132-E132.

Lam, A. J., F. St-Pierre, Y. Gong, J. D. Marshall, P. J. Cranfill, M. A. Baird, M. R. McKeown, J. Wiedenmann, M. W. Davidson and M. J. Schnitzer (2012). 'Improving FRET dynamic range with bright green and red fluorescent proteins.' Nat Methods.

Liu, Y. (2011). 'The DIADEM and beyond.' Neuroinformatics **9**(2-3): 99-102.

Livet, J., T. A. Weissman, H. Kang, R. W. Draft, J. Lu, R. A. Bennis, J. R. Sanes and J. W. Lichtman (2007). 'Transgenic strategies for combinatorial expression of fluorescent proteins in the nervous system.' Nature **450**(7166): 56-62.

Lovett-Barron, M., G. F. Turi, P. Kaifosh, P. H. Lee, F. Bolze, X.-H. Sun, J.-F. Nicoud, B. V. Zemelman, S. M. Sternson and A. Losonczy (2012). 'Regulation of neuronal input transformations by tunable dendritic inhibition.' Nat Neurosci **15**(3): 423-430.

McAuliffe, J. J., S. L. Bronson, M. S. Hester, B. L. Murphy, R. Dahlquist-Topala, D. A. Richards and S. C. Danzer (2011). 'Altered patterning of dentate granule cell mossy fiber inputs onto CA3 pyramidal cells in limbic epilepsy.' Hippocampus **21**(1): 93-107.

Micheva, K. D. and S. J. Smith (2007). 'Array tomography: a new tool for imaging the molecular architecture and ultrastructure of neural circuits.' Neuron **55**(1): 25-36.
Munro, S. and H. R. B. Pelham (1984). 'Use of Peptide Tagging to Detect Proteins Expressed from Cloned Genes - Deletion Mapping Functional Domains of Drosophila Hsp70.' Embo Journal **3**(13): 3087-3093.

Mutze, J., V. Iyer, J. J. Macklin, J. Colonell, B. Karsh, Z. Petrasek, P. Schwille, L. L. Looger, L. D. Lavis and T. D. Harris (2012). 'Excitation spectra and brightness optimization of two-photon excited probes.' Biophys J **102**(4): 934-944.

Osten, P. and T. W. Margrie (2013). 'Mapping brain circuitry with a light microscope.' Nat Methods **10**(6): 515-523.

Pan, Y. A., J. Livet, J. R. Sanes, J. W. Lichtman and A. F. Schier (2011). 'Multicolor Brainbow imaging in zebrafish.' Cold Spring Harbor Protocols **2011**(1): pdb. prot5546.

Park, S. H., C. Cheong, J. Idoyaga, J. Y. Kim, J. H. Choi, Y. Do, H. Lee, J. H. Jo, Y. S. Oh, W. Im, R. M. Steinman and C. G. Park (2008). 'Generation and application of new

rat monoclonal antibodies against synthetic FLAG and OLLAS tags for improved immunodetection.' J Immunol Methods **331**(1-2): 27-38.

Pedelacq, J. D., S. Cabantous, T. Tran, T. C. Terwilliger and G. S. Waldo (2006). 'Engineering and characterization of a superfolder green fluorescent protein.' Nat Biotechnol **24**(1): 79-88.

Pfeiffer, B. D., A. Jenett, A. S. Hammonds, T. T. Ngo, S. Misra, C. Murphy, A. Scully, J. W. Carlson, K. H. Wan, T. R. Laverty, C. Mungall, R. Svirskas, J. T. Kadonaga, C. Q. Doe, M. B. Eisen, S. E. Celniker and G. M. Rubin (2008). 'Tools for neuroanatomy and neurogenetics in Drosophila.' Proc Natl Acad Sci U S A **105**(28): 9715-9720.

Ragan, T., L. R. Kadiri, K. U. Venkataraju, K. Bahlmann, J. Sutin, J. Taranda, I. Arganda-Carreras, Y. Kim, H. S. Seung and P. Osten (2012). 'Serial two-photon tomography for automated ex vivo mouse brain imaging.' Nat Methods **9**(3): 255-258.

Ramon y Cajal, S. (1952). 'Histologie du Systeme Nerveux de I'Homme et des Vertebres, Institutio Ramon y Cajal.' Madrid, Spain.(Translated from Spanish by L. Azoulay.).

Ranscht, B. (2000). 'Cadherins: molecular codes for axon guidance and synapse formation.' Int J Dev Neurosci **18**(7): 643-651.

Redies, C. (1995). 'Cadherin expression in the developing vertebrate CNS: from neuromeres to brain nuclei and neural circuits.' Exp Cell Res **220**(2): 243-256.

Rust, M. J., M. Bates and X. Zhuang (2006). 'Sub-diffraction-limit imaging by stochastic optical reconstruction microscopy (STORM).' Nat Methods **3**(10): 793-795.

Saito, T. and N. Nakatsuji (2001). 'Efficient gene transfer into the embryonic mouse brain using in vivo electroporation.' Developmental Biology **240**(1): 237-246.

Schmidt, T. G. M., J. Koepke, R. Frank and A. Skerra (1996). 'Molecular Interaction Between the Strep-tag Affinity Peptide and its Cognate Target, Streptavidin.' Journal of Molecular Biology **255**(5): 753-766.

Shaner, N. C., R. E. Campbell, P. A. Steinbach, B. N. Giepmans, A. E. Palmer and R. Y. Tsien (2004). 'Improved monomeric red, orange and yellow fluorescent proteins derived from Discosoma sp. red fluorescent protein.' Nat Biotechnol **22**(12): 1567-1572.

Sjollema, K. A., U. Schnell, J. Kuipers, R. Kalicharan and B. N. G. Giepmans (2012). 'Correlated Light Microscopy and Electron Microscopy.' Correlative Light and Electron Microscopy **111**: 157-173.

Skepper, J. N. and J. M. Powell (2008). 'Immunogold Staining of London Resin (LR) White Sections for Transmission Electron Microscopy (TEM).' CSH Protoc **2008**: pdb prot5016.

Southern, J. A., D. F. Young, F. Heaney, W. K. Baumgartner and R. E. Randall (1991). 'Identification of an Epitope on the P-Proteins and V-Proteins of Simian-Virus 5 That Distinguishes between 2 Isolates with Different Biological Characteristics.' Journal of General Virology **72**: 1551-1557.

Sunkin, S. M., L. Ng, C. Lau, T. Dolbeare, T. L. Gilbert, C. L. Thompson, M. Hawrylycz and C. Dang (2013). 'Allen Brain Atlas: an integrated spatio-temporal portal for exploring the central nervous system.' Nucleic Acids Research **41**(Database issue): D996-D1008.

Tabata, H. and K. Nakajima (2001). 'Efficient in utero gene transfer system to the developing mouse brain using electroporation: Visualization of neuronal migration in the developing cortex.' Neuroscience **103**(4): 865-872.

Terpe, K. (2003). 'Overview of tag protein fusions: from molecular and biochemical fundamentals to commercial systems.' Appl Microbiol Biotechnol **60**(5): 523-533.

Wall, N. R., I. R. Wickersham, A. Cetin, M. De La Parra and E. M. Callaway (2010). 'Monosynaptic circuit tracing in vivo through Cre-dependent targeting and complementation of modified rabies virus.' Proceedings of the National Academy of Sciences **107**(50): 21848-21853.

Waugh, D. S. (2005). 'Making the most of affinity tags.' Trends Biotechnol **23**(6): 316-320.

Wickersham, I. R., D. C. Lyon, R. J. Barnard, T. Mori, S. Finke, K.-K. Conzelmann, J. A. Young and E. M. Callaway (2007). 'Monosynaptic restriction of transsynaptic tracing from single, genetically targeted neurons.' Neuron **53**(5): 639-647.

Williams, M. E., S. A. Wilke, A. Daggett, E. Davis, S. Otto, D. Ravi, B. Ripley, E. A. Bushong, M. H. Ellisman, G. Klein and A. Ghosh (2011). 'Cadherin-9 regulates synapse-specific differentiation in the developing hippocampus.' Neuron **71**(4): 640-655.

Yang, Y., M. Marcello, V. Endris, R. Saffrich, R. Fischer, M. F. Trendelenburg, R. Sprengel and G. Rappold (2006). 'MEGAP impedes cell migration via regulating actin and microtubule dynamics and focal complex formation.' Experimental Cell Research **312**(12): 2379-2393.

Yi, H., J. L. Leunissen, G.-M. Shi, C.-A. Gutekunst and S. M. Hersch (2001). 'A novel procedure for pre-embedding double immunogold–silver labeling at the ultrastructural level.' Journal of Histochemistry & Cytochemistry **49**(3): 279-283.

Chapter 4:

Agmon, A., L. T. Yang, E. G. Jones and D. K. O'Dowd (1995). 'Topological precision in the thalamic projection to neonatal mouse barrel cortex.' J Neurosci **15**(1 Pt 2): 549-561.

Bannister, A. P. (2005). 'Inter- and intra-laminar connections of pyramidal cells in the neocortex.' Neurosci Res **53**(2): 95-103.

Bracher, A., J. Kadlec, H. Betz and W. Weissenhorn (2002). 'X-ray structure of a neuronal complexin-SNARE complex from squid.' J Biol Chem **277**(29): 26517-26523.

Cauller, L. J., B. Clancy and B. W. Connors (1998). 'Backward cortical projections to primary somatosensory cortex in rats extend long horizontal axons in layer I.' J Comp Neurol **390**(2): 297-310.

Chen, X., D. R. Tomchick, E. Kovrigin, D. Arac, M. Machius, T. C. Sudhof and J. Rizo (2002). 'Three-dimensional structure of the complexin/SNARE complex.' Neuron **33**(3): 397-409.

Chu, Z., M. Galarreta and S. Hestrin (2003). 'Synaptic interactions of late-spiking neocortical neurons in layer 1.' J Neurosci **23**(1): 96-102.

Clancy, B. and L. J. Cauller (1999). 'Widespread projections from subgriseal neurons (layer VII) to layer I in adult rat cortex.' J Comp Neurol **407**(2): 275-286.

Clancy, B., M. Silva-Filho and M. J. Friedlander (2001). 'Structure and projections of white matter neurons in the postnatal rat visual cortex.' J Comp Neurol **434**(2): 233-252.

Frost, D. O. and V. S. Caviness, Jr. (1980). 'Radial organization of thalamic projections to the neocortex in the mouse.' J Comp Neurol **194**(2): 369-393.

Ghosh, A., A. Antonini, S. K. McConnell and C. J. Shatz (1990). 'Requirement for subplate neurons in the formation of thalamocortical connections.' Nature **347**(6289): 179-181.

Ghosh, A. and C. J. Shatz (1992). 'Involvement of subplate neurons in the formation of ocular dominance columns.' Science **255**(5050): 1441-1443.

Ghosh, A. and C. J. Shatz (1992). 'Pathfinding and target selection by developing geniculocortical axons.' J Neurosci **12**(1): 39-55.

Ghosh, A. and C. J. Shatz (1993). 'A role for subplate neurons in the patterning of connections from thalamus to neocortex.' Development **117**(3): 1031-1047.

Grant, E., A. Hoerder-Suabedissen and Z. Molnar (2012). 'Development of the corticothalamic projections.' Front Neurosci **6**: 53.

Herkenham, M. (1986). New Perspectives on the Organization and Evolution of Nonspecific Thalamocortical Projections. Sensory-Motor Areas and Aspects of Cortical Connectivity. E. Jones and A. Peters, Springer US. **5:** 403-445.

Hestrin, S. and W. E. Armstrong (1996). 'Morphology and physiology of cortical neurons in layer I.' J Neurosci **16**(17): 5290-5300.

Hoerder-Suabedissen, A. and Z. Molnar (2013). 'Molecular diversity of early-born subplate neurons.' Cereb Cortex **23**(6): 1473-1483.

Hoerder-Suabedissen, A., F. M. Oeschger, M. L. Krishnan, T. G. Belgard, W. Z. Wang, S. Lee, C. Webber, E. Petretto, A. D. Edwards and Z. Molnar (2013). 'Expression profiling of mouse subplate reveals a dynamic gene network and disease association with autism and schizophrenia.' Proc Natl Acad Sci U S A **110**(9): 3555-3560.

Hoerder-Suabedissen, A., W. Z. Wang, S. Lee, K. E. Davies, A. M. Goffinet, S. Rakic, J. Parnavelas, K. Reim, M. Nicolic, O. Paulsen and Z. Molnar (2009). 'Novel markers reveal subpopulations of subplate neurons in the murine cerebral cortex.' Cereb Cortex **19**(8): 1738-1750.

Hu, K., J. Carroll, C. Rickman and B. Davletov (2002). 'Action of complexin on SNARE complex.' J Biol Chem **277**(44): 41652-41656.

Kanold, P. O., P. Kara, R. C. Reid and C. J. Shatz (2003). 'Role of subplate neurons in functional maturation of visual cortical columns.' Science **301**(5632): 521-525.
Kanold, P. O. and H. J. Luhmann (2010). 'The subplate and early cortical circuits.' Annu Rev Neurosci **33**: 23-48.

Kanold, P. O. and C. J. Shatz (2006). 'Subplate neurons regulate maturation of cortical inhibition and outcome of ocular dominance plasticity.' Neuron **51**(5): 627-638.

Kostovic, I. and P. Rakic (1980). 'Cytology and time of origin of interstitial neurons in the white matter in infant and adult human and monkey telencephalon.' J Neurocytol **9**(2): 219-242.

Ma, J., X. H. Yao, Y. Fu and Y. C. Yu (2013). 'Development of Layer 1 Neurons in the Mouse Neocortex.' Cereb Cortex.

McConnell, S. K., A. Ghosh and C. J. Shatz (1989). 'Subplate neurons pioneer the first axon pathway from the cerebral cortex.' Science **245**(4921): 978-982.

McConnell, S. K., A. Ghosh and C. J. Shatz (1994). 'Subplate pioneers and the formation of descending connections from cerebral cortex.' J Neurosci **14**(4): 1892-1907.

Nahmani, M. and A. Erisir (2005). 'VGluT2 immunochemistry identifies thalamocortical terminals in layer 4 of adult and developing visual cortex.' J Comp Neurol **484**(4): 458-473.

Pinon, M. C., A. Jethwa, E. Jacobs, A. Campagnoni and Z. Molnar (2009). 'Dynamic integration of subplate neurons into the cortical barrel field circuitry during postnatal development in the Golli-tau-eGFP (GTE) mouse.' J Physiol **587**(Pt 9): 1903-1915.

Sehara, K., T. Toda, L. Iwai, M. Wakimoto, K. Tanno, Y. Matsubayashi and H. Kawasaki (2010). 'Whisker-related axonal patterns and plasticity of layer 2/3 neurons in the mouse barrel cortex.' J Neurosci **30**(8): 3082-3092.

Tolner, E. A., A. Sheikh, A. Y. Yukin, K. Kaila and P. O. Kanold (2012). 'Subplate neurons promote spindle bursts and thalamocortical patterning in the neonatal rat somatosensory cortex.' J Neurosci **32**(2): 692-702.

Viswanathan, S., S. Bandyopadhyay, J. P. Kao and P. O. Kanold (2012). 'Changing microcircuits in the subplate of the developing cortex.' J Neurosci **32**(5): 1589-1601.

Wang, W. Z., F. M. Oeschger, J. F. Montiel, F. Garcia-Moreno, A. Hoerder-Suabedissen, L. Krubitzer, C. J. Ek, N. R. Saunders, K. Reim, A. Villalon and Z. Molnar (2011). 'Comparative Aspects of Subplate Zone Studied with Gene Expression in Sauropsids and Mammals.' Cereb Cortex.

Xue, M., A. Stradomska, H. Chen, N. Brose, W. Zhang, C. Rosenmund and K. Reim (2008). 'Complexins facilitate neurotransmitter release at excitatory and inhibitory synapses in mammalian central nervous system.' Proc Natl Acad Sci U S A **105**(22): 7875-7880.

Zhao, C., J. P. Kao and P. O. Kanold (2009). 'Functional excitatory microcircuits in neonatal cortex connect thalamus and layer 4.' J Neurosci **29**(49): 15479-15488.